Nonlinear Finite Element Analysis: Structures

C. J. Earls*

August 16, 2019

1 Introduction

In its broadest conception, the finite element method is a systematic and robust numerical method for solution of *partial differential equations, (PDEs)*. While precise agreement with closed-form (*weak*) solutions are possible (within the floating point precision of the given hardware in use), one important strength of the method comes from its ability to furnish approximate solutions, over complex domains, where closed-form solutions are either unknown, or impossible to obtain.

Another important strength of the finite element method relates to its firm foundation within the mathematical theories contained under the rubric of *Functional Analysis*. As a direct result of such foundations, it is often possible to guarantee the *existence* and *uniqueness* of finite element solutions. Functional analysis enables the study of convergence in finite element solutions to their exact hypothetical counterparts. The ability to analyze new finite element technics in terms of existence, uniqueness, and convergence motivate the study of functional analysis for the mechanician. Indeed, an inability to understand the convergence properties of any numerical solution method represents a serious drawback in terms of the reliable and proper use of the method.

This course takes as its point of departure continuum mechanics, elementary mathematics, numerical methods, computer programming, and introductory finite element analysis. The primary focus of the course is to introduce the solution of nonlinear PDEs with finite element method, with an emphasis on those problems arising within the application domain of structural mechanics. Solution methods, algorithms, and finite element formulations will be treated in a theoretical context, and implemented in computer software through a series

*Professor, School of Civil and Environmental Engineering, 220 Hollister Hall, Ithaca, NY 14853

of project assignments. The tools developed will subsequently be applied to problems related to structural stability and acoustic fluid-structure interaction.

1.1 Review of topics from Continuum Mechanics

As a beginning point to discussions concerning nonlinear finite element analysis, a review of the fundamentals of continuum mechanics is undertaken. An excellent, and more in-depth treatment of these topics may be found in the monograph by Malvern [10]. The current treatment of review topics is meant to refresh important ideas, introduce useful notation, and furnish a sense of continuity in concepts with this, and earlier, courses.

In many important themes in engineering and applied mathematics, where a physical system comprised of matter is under investigation, the idealization of a *continuum* is appropriate. Understanding the nature of matter, at length scales of hundreds of pico-meters (*i.e.* 100E-10 meters), to be discontinuous, the utility of the conceptual framework associated with the continuum is, nonetheless, useful in certain contexts. Meaning, if the length scale of the problem under investigation is much larger than atomic length scale, then the behavior of the medium comprising the domain of the problem may be considered as possessing the properties of the atoms, and molecules, of the material, as an aggregation.

With this perspective in mind, a *material point*, P, is defined as being an infinitesimally small volume of atoms / molecules possessing the aggregate properties of the material comprising a given body, $\mathcal{B}$. We then say:

$$P \in \mathcal{B} \tag{1}$$

with the assumption that there are an infinity of analogous material points in the neighborhood surrounding the point under discussion, P. This conception of a material point is useful in the so-called *referential description* of continuum mechanics (a description that is very important in nonlinear finite element method). Changes in space-time of the body, $\mathcal{B}$, comprised of the infinite collection of material points, P, may now be considered.

It is oftentimes convenient to conceive of the body, $\mathcal{B}$, as being notionally "embedded" in $\mathbb{R}^3$, in a manner to be made precise later. For simplicity a right-handed rectangular Cartesian reference frame with origin, O, is constructed. The orhthonormal bases defining such a reference system are given in indicial notation as: e_i, $i = 1, 2, 3$. At a specific point in time, each of the infinity of material points, P, in the body, $\mathcal{B}$, are assumed to posses an invertible mapping from the body into a subspace of $\mathbb{R}^3$ that represents the geometric outline of the body. This outline is referred to as the *configuration* of the body, $\mathcal{B}$, at a given point in time, t. Now each of the material points, P in the body, $\mathcal{B}$ correspond uniquely with the infinity of points contained within the configuration, Ω, defined at a particular time instant. Position vectors, $\mathbf{X}$, locating the individual

material points, mapped to a particular configuration of the body, may now be used to label the points under consideration within a particular configuration; as well as to facilitate the description of changes occurring when going from one configuration to another. This may be summarized as:

$$\mathcal{L}(P) = \mathbf{X}, \quad \forall P \in \mathcal{B},\, X \in \Omega_t \subset \mathbb{R}^3,\, t \geq 0 \tag{2}$$

where $\mathcal{L}$ is the bijective (*i.e.* *one-to-one* and *onto*) operator mapping material points, P, into distinct position vectors within $\mathbb{R}^3$. The subscript on the configuration, Ω, is used to specify which particular configuration is under consideration (*e.g.* perhaps body, $\mathcal{B}$, is acted upon by some time varying external agency leading to some rigid body motion and deformation).

A so-called *referential* (or *Lagrangian*) description is frequently adopted in the consideration of solids and structures, where the deformation history of the body is commonly of interest (*e.g.* consider plasticity). In such a case, an initial stress free conception of the body, as a configuration in the reference frame ($span(e_i)$), is identified by uniquely mapping all material points in the body to real numbers in the *reference configuration*; the unique triplet of real number locating the points are then the components of the position vectors of these same points, $\mathbf{X}$. We may then speak of the reference configuration as the collection of all such points $\mathbf{X}$ (notice that we are now labeling the points using only the position vectors). Any hypothetical motion taking the body, $\mathcal{B}$, from the reference configuration to some new configuration (we can now label the the material points, in the new configuration, using new position vectors, $\mathbf{x}$), can then be expressed using the following mapping:

$$\mathbf{x} = \phi(\mathbf{X}, t) \tag{3}$$

In such a description, the initial position of the material points in the reference configuration are used to describe any subsequent motion in the body, occurring at various solution times. Meaning, the future and fate of all points in the body are measured in reference to some starting position in the stress free state. Again, this makes perfect sense for the case of solids and structures where the various engineering theories are tied to overall deformation. The same is not true for fluids.

Consider now the case of a fluid medium that is incompressible and of negligible shear resistance (*invicid*). In such a situation, it is no longer as important to know the motion of a given material point, as it is to understand the nature of the flow within some *control volume*. In such a case, rather than a configuration of a body, we consider a region of space at some arbitrary time. We label the infinity of *stations* (locations) in the control volume, that various material points may pass through, using the same position vectors that we considered for use in an arbitrary configuration of body, $\mathcal{B}$. In other words, we monitor all points located in the control volume with position vectors, $\mathbf{x}$; and subsequently use these position vectors to label the material points that happen to occur at

these locations at a particular time instant. Such a description is termed as being *spatial* (or *Eulerian*)

Consideration of the motion in terms of the referential and spatial descriptions permits the introduction of the displacement field, as the difference in the position of two points. In the case of the referential description, the displacement field may be defined as:

$$\mathbf{u}(\mathbf{X},t) = \phi(\mathbf{X},t) - \phi(\mathbf{X},0) = \phi(\mathbf{X},t) - \mathbf{X} \tag{4}$$

whereas in the spatial case the following holds:

$$\mathbf{u}(\mathbf{x},t) = \mathbf{x} - \phi^{-1}(\mathbf{x},t) \tag{5}$$

where ϕ^{-1} is the inverse of the transformation introduced in Equation (3); a mapping that may be difficult to obtain in every practical case. However, it is pointed out that:

$$\mathbf{u}(\mathbf{x},t) = \mathbf{u}(\phi(\mathbf{X},t),t) = \mathbf{u}(\mathbf{X},t) \tag{6}$$

and thus the equality in displacement fields is observed between the two descriptions.

The two different descriptions (*i.e.* Lagrangian and Eulerian) have different strengths and weaknesses, and both are useful in different ways. Rather than selecting one over the other, the discussion now turns to highlighting several important differences between the two, beginning with a discussion on velocity.

Within a referential description, the position of each material point is furnished by Equation (3) and the velocity of a particular particle, originally at some point, $\mathbf{X}$, in the reference configuration, is expressed as:

$$\mathbf{v}(\mathbf{X},t) = \frac{\partial}{\partial t}\phi(\mathbf{X},t) \tag{7}$$

Similarly, the referential description yields an acceleration expression of the form:

$$\mathbf{a}(\mathbf{X},t) = \frac{\partial}{\partial t}\mathbf{v}(\mathbf{X},t) = \frac{\partial^2}{\partial t^2}\phi(\mathbf{X},t) \tag{8}$$

The foregoing are the first and second *partial time derivatives with material coordinate,* $\mathbf{X}$*, held constant*, respectively. If now we wish to consider the motion of particles passing through a specific location in space, then we adopt a spatial description and subsequently consider the *partial time derivative with spatial position held constant*. In this latter case we now have, for velocity:

$$\mathbf{v}(\mathbf{x},t) = \frac{\partial \mathbf{x}}{\partial t} \tag{9}$$

and for acceleration:

$$\mathbf{a}(\mathbf{x},t) = \frac{\partial}{\partial t}\mathbf{v}(\mathbf{x},t) = \frac{\partial^2 \mathbf{x}}{\partial t^2} \tag{10}$$

An important distinction to draw when considering Equations (9) and (10), as opposed to Equations (7) and (8), is that in the former case, the quantities are local with respect to the given particle located instantly at the point of interest, while the latter two are used to describe the motion of a specific particle at an arbitrary time. This difference may be highlighted by the consideration of a steady flow situation.

In a the case of *steady flow*, it is easy to imagine that the accelerations of the individual material points, as they proceed along their *stream lines* (a curve whose tangents are parallel with the particle velocity vector associated with particle instantaneously occupying the point of tangency) are non-zero. Whereas, the consideration of the time rate of change in velocity measured at a particular spatial point, anchored in space, will yield an acceleration of zero. The utility of Equation (10) becomes apparent, as it affords us a means for inferring the motion of a particular particle, just now being observed at a point within some control volume.

It is observed that the form of the derivatives appearing in Equations (7) and (8) are commonly referred to as *material time derivatives*; as it is that the material point is held constant as the derivative with respect to time is evaluated. Alternately, the form of the derivatives appearing in Equations (9) and (10) are commonly referred to as *spatial time derivative*; for analogous reasons.

If it were that only spatial data are available, the material time derivative could, nonetheless be evaluated as follows (using acceleration as an example):

$$\mathbf{v}\left(\mathbf{x},t\right)=\mathbf{v}\left(\phi\left(\mathbf{X},t\right),t\right)=\mathbf{v}\circ\phi \tag{11}$$

where the form of the velocity in the rightmost terms are given as a *composition* of functions; a notation that is common in the mathematical literature, and introduced here for completeness. Equation (11) may now be used to re-express the material time derivative using the *chain rule* as follows:

$$\frac{\partial\mathbf{v}\left(\mathbf{X},t\right)}{\partial t}=\frac{\partial\mathbf{v}\left(\mathbf{x},t\right)}{\partial t}+\frac{\partial\mathbf{v}\left(\mathbf{x},t\right)}{\partial\mathbf{x}}\frac{\partial\phi\left(\mathbf{X},t\right)}{\partial t} \tag{12}$$

it is noted that use has been made of Equation (3) in the last term on the right hand side of Equation (12). We may expand the result of Equation (12) as:

$$\mathbf{a}\left(\mathbf{X},t\right)=\mathbf{a}\left(\mathbf{x},t\right)+\mathbf{v}\left(\mathbf{X},t\right)\cdot\nabla\mathbf{v}\left(\mathbf{x},t\right) \tag{13}$$

It is pointed out that the velocity in the second term on the right hand side of Equation (13) may be changed to the spatial velocity, on account of the result from Equation (11); and thus:

$$\mathbf{a}\left(\mathbf{X},t\right)=\mathbf{a}\left(\mathbf{x},t\right)+\mathbf{v}\left(\mathbf{x},t\right)\cdot\nabla\mathbf{v}\left(\mathbf{x},t\right) \tag{14}$$

where the rightmost term on the right hand side of Equation (14) is frequently referred to as either the *transport* or *convective* term. It is pointed out that the

material velocity contained in the convective term in Equation (14) is known in terms of the spatial velocity (using Equation (11)), and thus the material time derivative is expressible entirely using spatial quantities.

The gradient operator appearing in Equation (14) is sometimes referred to as the *left gradient*, and defined as:

$$\nabla \mathbf{v} \equiv \begin{bmatrix} \frac{\partial v_x}{\partial x} & \frac{\partial v_y}{\partial x} & \frac{\partial v_z}{\partial x} \\ \frac{\partial v_x}{\partial y} & \frac{\partial v_y}{\partial y} & \frac{\partial v_z}{\partial y} \\ \frac{\partial v_x}{\partial z} & \frac{\partial v_y}{\partial z} & \frac{\partial v_z}{\partial z} \end{bmatrix} = \begin{bmatrix} v_{x,x} & v_{y,x} & v_{z,x} \\ v_{x,y} & v_{y,y} & v_{z,y} \\ v_{x,z} & v_{y,z} & v_{z,z} \end{bmatrix} \tag{15}$$

wherein the the indicial notation for partial differentiation has been introduced in Equation (15).

The specific result presented in Equation (12) may be generalized to any scalar field as:

$$\frac{Df}{Dt} = \frac{\partial f}{\partial t} + \mathbf{v} \cdot \nabla f \tag{16}$$

as well as any tensor field:

$$\frac{D\sigma}{Dt} = \frac{\partial \sigma}{\partial t} + \mathbf{v} \cdot \nabla \sigma \tag{17}$$

where the convention for referring to the material time derivative as $\frac{D}{Dt}$, is introduced. An additional convention, that represents spatial quantities without parenthetical arguments is adopted. Meaning that from this point forward, the following is implied (as an example): $\mathbf{v} = \mathbf{v}(\mathbf{x}, t)$; whereas the referential quantity (or material quantity) will always appear with an argument, as in $\mathbf{v}(\mathbf{X}, t)$.

1.1.1 Rate of deformation tensor

Consider two continuum particles located in a spatial reference frame. While it is that the original position of the points, in terms of material coordinates in a referential sense, is not known, the instantaneous spatial velocities are known. As a result, the velocity of one particle may be denoted as, $\mathbf{v}$, while the the velocity of the other particle, a distance $d\mathbf{x}$ away, is given by $\mathbf{v} + d\mathbf{v}$. The relative velocity of the first point, with respect to the second, is then:

$$d\mathbf{v} = \mathbf{L} \cdot d\mathbf{x}, \quad \mathbf{L} = (\nabla_{\mathbf{x}} \mathbf{v})^T \tag{18}$$

where $\nabla_{\mathbf{x}}$ denotes the spatial gradient, and thus $(\nabla_{\mathbf{x}} \mathbf{v})^T$ denotes the spatial gradient of velocity, now called $\mathbf{L}$.

The tensor, $\mathbf{L}$, may be written as the sum:

$$\mathbf{L} = \mathbf{D} + \mathbf{W} \tag{19}$$

where,

$$\mathbf{D} = \frac{1}{2}\left(\mathbf{L} + \mathbf{L}^T\right) \tag{20}$$

and,

$$\mathbf{W} = \frac{1}{2}\left(\mathbf{L} - \mathbf{L}^T\right) \tag{21}$$

D is called the *rate of deformation tensor* and **W** is called the *spin tensor* (the former being symmetric, and the latter being skew symmetric). Thus it is observed that the spatial velocity field can be expressed as:

$$d\mathbf{v} = \mathbf{D} \cdot d\mathbf{x} + \mathbf{W} \cdot d\mathbf{x} \tag{22}$$

If the rate of deformation tensor vanishes, then the motion in the spatial reference frame is a simple rigid body rotation. Conversely, if the spin tensor vanishes, then the motion is *irrotational*, and thus:

$$d\mathbf{v} = \mathbf{D} \cdot d\mathbf{x} \tag{23}$$

It is pointed out that there is no requirement of smallness on the part of the velocity and velocity gradients. The representation of motion in terms of the rate of deformation and spin may be finite in magnitude.

Properties of the rate of deformation tensor may be elucidated when considering a differential position vector, $d\mathbf{X}$, in the reference configuration. The instantaneous change in this vector length, in the spatial reference frame, is:

$$(d\mathbf{s})^2 = d\mathbf{x} \cdot d\mathbf{x} \tag{24}$$

the rate of deformation of this quantity is given using the chain rule:

$$\frac{d}{dt}(d\mathbf{s})^2 = 2d\mathbf{s}\frac{d}{dt}(d\mathbf{s}) \tag{25}$$

Using Equations (24) and (25):

$$\frac{d}{dt}(d\mathbf{s})^2 = 2d\mathbf{x} \cdot \frac{d}{dt}(d\mathbf{x}) \tag{26}$$

Using Equation (3), it is observed that:

$$\frac{d}{dt}(d\mathbf{x}) = \left[\frac{d}{dt}(\nabla\phi)^T\right] \cdot d\mathbf{X} + (\nabla\phi)^T \cdot \frac{d}{dt}d\mathbf{X} \tag{27}$$

the last term of which vanishes since the time rate of change of the material point in the reference configuration is zero, by definition. A change in differentiation order yields:

$$\frac{d}{dt}(d\mathbf{x}) = \frac{d}{dt}\left[\nabla\phi^T\right] \cdot d\mathbf{X} = \left(\nabla\mathbf{v}(\mathbf{X}, t)\right)^T \cdot d\mathbf{X} \tag{28}$$

It is observed that $(\nabla \mathbf{v}(\mathbf{X}, t))^T$ is the velocity gradient with respect to the material coordinates in a referential system; which is clearly different from $\mathbf{L}$, the spatial gradient of the velocity field. However, both of these can be made to yield the same quantity, as:

$$(\nabla \mathbf{v}(\mathbf{X}, t))^T \cdot d\mathbf{X} = d\mathbf{v} = \mathbf{L} \cdot d\mathbf{x} \tag{29}$$

and thus:

$$\frac{d}{dt}(d\mathbf{x}) = \mathbf{L} \cdot d\mathbf{x} \tag{30}$$

Using Equation (26), it is seen that:

$$\begin{aligned} \frac{d}{dt}\left[(d\mathbf{s})^2\right] &= 2d\mathbf{x} \cdot \mathbf{L} \cdot d\mathbf{x} \\ &= 2d\mathbf{x} \cdot \mathbf{D} \cdot d\mathbf{x} + 2d\mathbf{x} \cdot \mathbf{W} \cdot d\mathbf{x} \end{aligned} \tag{31}$$

Since the last term in Equation (31) vanishes due to the skew symmetry of $\mathbf{W}$, the following observation is made:

$$\frac{d}{dt}\left[(d\mathbf{s})^2\right] = 2d\mathbf{x} \cdot \mathbf{D} \cdot d\mathbf{x} \tag{32}$$

the rate of deformation of the squared length of the material occupying an instantaneous relative position $d\mathbf{x}$ at some location, is determined using the rate of deformation tensor, $\mathbf{D}$, at that same point. It is pointed out that the rate of deformation tensor is not the same thing as the time rate of change of strain. The former is obtained using the spatial gradient of the velocity field at a point, while the later is obtained using a material derivative of the displacement field.

1.1.2 Deformation gradient

Using the description of deformation furnished in Equation (3), as well as the *Jacobian matrix*, it is possible to characterize the deformation by defining an operator known as the *deformation gradient*:

$$\mathbf{F} = \frac{\partial \phi}{\partial \mathbf{X}} = (\nabla_0 \phi)^T \tag{33}$$

The effect of the deformation gradient is to map a linear differential in the referential coordinate system into its deformed counterpart in the spatial coordinate system. The following equation illustrates this idea through the contraction of the deformation gradient with an arbitrary linear differential selected from within the reference configuration:

$$d\mathbf{x} = \mathbf{F} \cdot d\mathbf{X}; \quad dx_i = F_{ij} dX_j \tag{34}$$

In the foregoing, subscript i refers to the motion, while subscript j refers to the partial derivative. Being more explicit, an example two dimensional case may

be considered, from with the following is obtained:

$$\mathbf{F} = (\nabla_0 \phi)^T = \begin{bmatrix} \frac{\partial \phi_1}{\partial \mathbf{X}_1} & \frac{\partial \phi_1}{\partial \mathbf{X}_2} \\ \frac{\partial \phi_2}{\partial \mathbf{X}_1} & \frac{\partial \phi_2}{\partial \mathbf{X}_2} \end{bmatrix} \tag{35}$$

The determinant of the deformation gradient also plays an important role in relating volume integrations performed in different reference frames as:

$$d\mathbf{V}_\Omega = \mid \mathbf{F} \mid d\mathbf{V}_{\Omega_0} \tag{36}$$

something that will be very useful for us to know, later in the course.

Commonly, certain restrictions on the motion of a body are assumed (or enforced) when considering a continuum within a finite element context:

- $\phi(\mathbf{X}, t)$ is continuously differentiable
- $\phi(\mathbf{X}, t)$ is one-to-one and onto (*bijection*)
- $\mid \mathbf{F} \mid > 0$

The first requirement is specified as a means to help ensure compatibility within the body, $\mathcal{B}$, as a result of any given deformation. It is pointed out that the requirement can be relaxed somewhat to permit discontinuities in ϕ, and its derivatives on sets of measure zero (*i.e.* at small cracks). The requirement regarding a one-to-one and onto mapping is a necessary and sufficient condition for the invertability of $\mathbf{F}$; something that is necessary for the existence of the reverse mapping from the spatial coordinates back to the referential coordinates. Additionally, the invertability requirement dictates that the determinant of the deformation be non-zero. However, our third requirement on motion of the body enforces the positivity of $\mid \mathbf{F} \mid$, as a means to ensure that mass is not destroyed, *etc.*

1.1.3 Rigid body rotation and coordinate transformation

A notional decomposition of the motion from the referential to the spatial coordinates may be presented as:

$$\phi(\mathbf{X}, t) = \mathbf{R}(t) \cdot \mathbf{X} + \mathbf{x}_T(t) \tag{37}$$

where $\mathbf{R}(t)$ is the *rotation tensor*, and $\mathbf{x}_T$ is the translation vector. The vanishing of the latter term leads to a motion that is a rigid body rotation; which preserves length:

$$d\mathbf{x} \cdot d\mathbf{x} = d\mathbf{X} \cdot \mathbf{R}^T \mathbf{R} \cdot d\mathbf{X} \tag{38}$$

as a result of the preservation of length, it is observed that the product $\mathbf{R}^T\mathbf{R}$ must be the identity tensor, $\mathbf{I}$, in order to guarantee that $d\mathbf{x} \cdot d\mathbf{x} = d\mathbf{X} \cdot d\mathbf{X}$. Based on the foregoing, it is observed that the rotation tensor, $\mathbf{R}$, is an *orthogonal tensor*, as it is that $\mathbf{R}^{-1} = \mathbf{R}^T$. As a result, any contraction of $\mathbf{R}$ with a

vector results in an orthogonal transformation (*e.g.* rigid body rotation).

As an initial step in the development of the rotation tensor, $\mathbf{R}$, consider the representation of a given vector quantity in terms of two separate orthogonal cartesian bases ($\mathbf{i}_i \cdot \mathbf{i}_j = \delta_{ij} = \hat{\mathbf{i}}_i \cdot \hat{\mathbf{i}}_j$):

$$\mathbf{r} = r_i \mathbf{i}_i = \hat{r}_i \hat{\mathbf{i}}_i \tag{39}$$

multiplying both sides of Equation (39) by the unit vector $\mathbf{i}_j$ yields:

$$r_i \mathbf{i}_i \cdot \mathbf{i}_j = \hat{r}_i \hat{\mathbf{i}}_i \cdot \mathbf{i}_j \rightarrow r_i \delta_{ij} = \hat{r}_i \hat{\mathbf{i}}_i \cdot \mathbf{i}_j \rightarrow r_j = R_{ji} \hat{r}_i \tag{40}$$

where $R_{ji} = \mathbf{i}_j \cdot \hat{\mathbf{i}}_i$. Thus, it is observed that:

$$\mathbf{r} = \mathbf{R} \cdot \hat{\mathbf{r}} \rightarrow r_i = R_{ij} \hat{r}_j \equiv R_{i\hat{j}} r_{\hat{j}} \tag{41}$$

Exploiting orthogonality of the rotation tensor, the inverse transformation appears as:

$$\hat{\mathbf{r}} = \mathbf{R}^T \cdot \mathbf{r} \rightarrow \hat{r}_j \equiv r_{\hat{j}} = R_{\hat{j}i} r_i \tag{42}$$

It is pointed out that in Equations (41) and (42), there is a single vector that is being referred to separate coordinates systems, that differ from one another by a rigid body rotation. As an example, the two dimensional specialization of the case represented by Equation (41) is given as:

$$\begin{aligned} \begin{bmatrix} r_x \\ r_y \end{bmatrix} &= \begin{bmatrix} R_{x\hat{x}} & R_{x\hat{y}} \\ R_{y\hat{x}} & R_{y\hat{y}} \end{bmatrix} \begin{bmatrix} \hat{r}_x \\ \hat{r}_y \end{bmatrix} \\ &= \begin{bmatrix} \mathbf{i}_x \cdot \hat{\mathbf{i}}_x & \mathbf{i}_x \cdot \hat{\mathbf{i}}_y \\ \mathbf{i}_y \cdot \hat{\mathbf{i}}_x & \mathbf{i}_y \cdot \hat{\mathbf{i}}_y \end{bmatrix} \begin{bmatrix} \hat{r}_x \\ \hat{r}_y \end{bmatrix} \\ &= \begin{bmatrix} cos\,(\theta) & -sin\,(\theta) \\ sin\,(\theta) & cos\,(\theta) \end{bmatrix} \begin{bmatrix} \hat{r}_x \\ \hat{r}_y \end{bmatrix} \end{aligned} \tag{43}$$

Suppose now that the desire is to rotate a given vector, $\mathbf{r}$, into another vector, $\mathbf{s}$, in a single coordinate system. It may be observed that the components of the rotated vector, $\mathbf{s}$, in the rotated coordinate (*i.e.* hatted) system, $\hat{s}_i$, are identical to the corresponding components of the vector, $\mathbf{r}$ in the unrotated coordinates, r_i:

$$\hat{s}_i = r_i \tag{44}$$

and so, applying Equation (42) to $\hat{s}_i$ yields:

$$\mathbf{r} = \mathbf{R}^T \cdot \mathbf{s} \Rightarrow \mathbf{s} = \mathbf{R} \cdot \mathbf{r} \tag{45}$$

Analogous expression for the rotational transformation of second order tensors appear as:

$$\mathbf{D} = \mathbf{R}\hat{\mathbf{D}}\mathbf{R}^T \Rightarrow \hat{\mathbf{D}} = \mathbf{R}^T\mathbf{D}\mathbf{R} \tag{46}$$

1.1.4 Finite strain

Considering, once again, the potential for *deformation*, alongside translation and rigid body rotations, the notion of a *deformation tensor* is motivated. Given some deformation, a positive definite quantification of this condition is furnished by the expression:

$$(ds)^2 = d\mathbf{X} \cdot \mathbf{C} \cdot d\mathbf{X} \tag{47}$$

while the inverse is given as:

$$(dS)^2 = d\mathbf{x} \cdot \mathbf{B}^{-1} \cdot d\mathbf{x} \tag{48}$$

If there is no deformation, the foregoing deformation tensors assume the form of identity tensors; a condition that is somewhat counterintuitive for a measure of deformation. As a consequence, it is common to introduce the notion of a *strain tensor* as the positive definite (when deformation is present) quantity in the referential description, known as the *Green-Lagrange strain*:

$$(ds)^2 - (dS)^2 = 2d\mathbf{X} \cdot \mathbf{E} \cdot d\mathbf{X} \tag{49}$$

quantifying spatial deformation in a referential description. Additionally, the *Eulerian strain* appears as:

$$(ds)^2 - (dS)^2 = 2d\mathbf{x} \cdot \mathbf{E}^* \cdot d\mathbf{x} \tag{50}$$

quantifying deformation in the spatial description.

Comparing Equations (47) and (49) in the Lagrangian description, it is observed that:

$$d\mathbf{X} \cdot \mathbf{C} \cdot d\mathbf{X} - d\mathbf{X} \cdot d\mathbf{X} = 2d\mathbf{X} \cdot \mathbf{E} \cdot d\mathbf{X} \tag{51}$$

which leads to:

$$2\mathbf{E} = \mathbf{C} - \mathbf{I} \tag{52}$$

An analogous approach applies to the Eulerian case:

$$2\mathbf{E}^* = \mathbf{I} - \mathbf{B}^{-1} \tag{53}$$

Use may be made of the deformation gradient in the formulation of deformation and strain tensors. In the referential description, it is observed that:

$$\begin{aligned}(ds)^2 = d\mathbf{x} \cdot d\mathbf{x} = \left(d\mathbf{X} \cdot \mathbf{F}^T\right) \cdot (\mathbf{F} \cdot d\mathbf{X}) = d\mathbf{X} \cdot \mathbf{C} \cdot d\mathbf{X} \\ \Rightarrow \mathbf{E} = \frac{1}{2}\left[\mathbf{F}^T\ \mathbf{F} - \mathbf{I}\right]\end{aligned} \tag{54}$$

A similar condition applies in the spatial description:

$$\begin{aligned}(dS)^2 = d\mathbf{X} \cdot d\mathbf{X} = \left[d\mathbf{x} \cdot \left(\mathbf{F}^{-1}\right)^T\right] \cdot \left[\left(\mathbf{F}^{-1}\right) \cdot d\mathbf{x}\right] = d\mathbf{x} \cdot \mathbf{B}^{-1} \cdot d\mathbf{x} \\ \Rightarrow \mathbf{E}^* = \frac{1}{2}\left[\mathbf{I} - \left(\mathbf{F}^{-1}\right)^T\ \mathbf{F}^{-1}\right]\end{aligned} \tag{55}$$

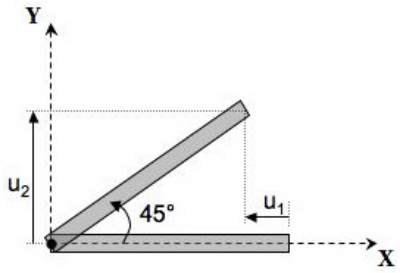

Figure 1: Large rotation of rigid rod

It is pointed out that all four of the foregoing deformation and strain tensors are symmetric.

Motivation for use of the of the *Green-Lagrange strain*, as compared with the usual linear *engineering strain*, in nonlinear finite element analysis, comes from its invariance under rigid body rotations; a critically important feature with respect to stability related finite element analyses that involve large displacements (rotations).

Consider a simple unit dimensional example problem depicted in Figure 1. This example will highlight two important ideas:

- the unsuitability of the *engineering strain* in cases of large rotation
- the invariance of the *Green-Lagrange strain* in such cases

Clearly, a strain measure that yields non-zero terms when a body merely rotates as a rigid body (*i.e.* no deformation) would prove pathological for applications involving geometric nonlinearity. Such a rigid body rotation condition is depicted in Figure 1, wherein a bar that is initially aligned with the *x-axis* of a two dimensional Cartesian reference frame, moves such that a rotation of $\frac{\pi}{4}$ radians occurs about its left end. The displacement of the free end may then be given as: $u_1 = -\left(L - \frac{\sqrt{2}}{2}L\right)$ and $u_2 = \frac{\sqrt{2}}{2}L$. Considering these displacements, the response of this structural element according to *enginering strain* may be examined:

$$\epsilon = \frac{du_1}{dx} = \frac{\frac{\sqrt{2}}{2}L - L}{L} = \frac{\sqrt{2}}{2} - 1 \neq 0 \tag{56}$$

Clearly the strains obtained from Equation (56), according to linear *engineering strain* theory, are fictitious, since there can be no deformation of the structural element under a pure rigid body rotation.

Considering now the Green-Lagrange strain measure applied to this same problem, the components of the tensor that characterize deformation along the

x-axis yields:

$$\begin{aligned} E_{11} &= \frac{1}{2}\left(\frac{\partial u_1}{\partial x_1} + \frac{\partial u_1}{\partial x_1} + \frac{\partial u_1}{\partial x_1}\frac{\partial u_1}{\partial x_1} + \frac{\partial u_2}{\partial x_1}\frac{\partial u_2}{\partial x_1}\right) \\ &= \frac{\partial u_1}{\partial x_1} + \frac{1}{2}\left(\frac{\partial u_1}{\partial x_1}\right)^2 + \frac{1}{2}\left(\frac{\partial u_2}{\partial x_1}\right)^2 \\ &= \left(\frac{\sqrt{2}}{2} - 1\right) + \frac{1}{2}\left(\frac{\sqrt{2}}{2} - 1\right)^2 + \frac{1}{2}\left(\frac{\sqrt{2}}{2}\right)^2 \\ &= \left(\frac{\sqrt{2}}{2} - 1\right) + \frac{1}{2}\left(\frac{1}{2} - \sqrt{2} + 1\right) + \frac{1}{4} = 0 \end{aligned} \tag{57}$$

It is thus seen that the *Green-Lagrange strain* remains invariant (*i.e.* null) during the rigid body rotation depicted in Figure 1.

Consideration may now be given to relating the Green-Lagrange strain to the rate of deformation tensor of Equation (19). Starting with the the use of the Chain Rule on the spatial gradient of the velocity of field, it is observed that:

$$\mathbf{L} = \frac{\partial \mathbf{v}}{\partial \mathbf{x}} = \frac{\partial \mathbf{v}}{\partial \mathbf{X}}\frac{\partial \mathbf{X}}{\partial \mathbf{x}} = \frac{\partial}{\partial t}\left(\frac{\partial \phi\left(\mathbf{X}, t\right)}{\partial \mathbf{X}}\right)\left(\frac{\partial \mathbf{x}}{\partial \mathbf{X}}\right)^{-1} = \dot{\mathbf{F}}\ \mathbf{F}^{-1} \tag{58}$$

Returning now to Equation (20), it is observed that:

$$\mathbf{D} = \frac{1}{2}\left(\mathbf{L} + \mathbf{L}^T\right) = \frac{1}{2}\left(\dot{\mathbf{F}}\ \mathbf{F}^{-1} + \mathbf{F}^{-T}\ \dot{\mathbf{F}}^T\right) \tag{59}$$

Taking now the time derivative of the Green-Langrange strain from Equation (54):

$$\dot{\mathbf{E}} = \frac{1}{2}\frac{D}{Dt}\left(\mathbf{F}^T\ \mathbf{F} - \mathbf{I}\right) = \frac{1}{2}\left(\mathbf{F}^T\ \dot{\mathbf{F}} + \dot{\mathbf{F}}^T\ \mathbf{F}\right) \tag{60}$$

Pre-multiplying Equation (59) by $\mathbf{F}^T$ and post-multiplying by $\mathbf{F}$ yields:

$$\begin{aligned} \mathbf{F}^T\ \mathbf{D}\ \mathbf{F} &= \frac{1}{2}\mathbf{F}^T\ \left(\dot{\mathbf{F}}\ \mathbf{F}^{-1} + \mathbf{F}^{-T}\ \dot{\mathbf{F}}^T\right)\ \mathbf{F} \\ &= \frac{1}{2}\left(\mathbf{F}^T\ \dot{\mathbf{F}}\ \mathbf{F}^{-1} + \mathbf{F}^T\ \mathbf{F}^{-T}\ \dot{\mathbf{F}}^T\right)\ \mathbf{F} \\ &= \frac{1}{2}\left(\mathbf{F}^T\ \dot{\mathbf{F}}\ \mathbf{F}^{-1}\ \mathbf{F} + \mathbf{I}\ \dot{\mathbf{F}}^T\ \mathbf{F}\right) \\ &= \frac{1}{2}\left(\mathbf{F}^T\ \dot{\mathbf{F}}\ \mathbf{I} + \mathbf{I}\ \dot{\mathbf{F}}^T\ \mathbf{F}\right) = \frac{1}{2}\left(\mathbf{F}^T\ \dot{\mathbf{F}} + \dot{\mathbf{F}}^T\ \mathbf{F}\right) \end{aligned} \tag{61}$$

The relationship between the time rate of change of Green-Lagrange strain, and the deformation rate is then given as:

$$\begin{aligned} \dot{\mathbf{E}} &= \mathbf{F}^T \cdot \mathbf{D} \cdot \mathbf{F} \\ \mathbf{D} &= \mathbf{F}^{-T} \cdot \dot{\mathbf{E}} \cdot \mathbf{F}^{-1} \end{aligned} \tag{62}$$

1.1.5 Stress

In the limit, as a traction acting at a surface of a continuous body (either an actual boundary of the problem domain, or equivalently, a notional, internal domain: as in a free body of a portion of the domain) is made to affect a smaller and smaller area, the *point-wise* quantity *stress* is uncovered. The continuum point at which the stress is acting may be conceived of (quite naturally in a Cartesian three-space) as a differential material element having three edges corresponding with hypothetical coordinate axes. Additionally, all edges in this element are vanishingly small; and hence the modifier *differential*. Within this context, it is then quite natural to conceive of stress as a *tensor* quantity. It is convenient, to now review a few key points regarding tensors, and their components and invariants.

It is instructive to think of the stress tensor as a linear operator whose components, in the given cartesian coordinate system, produce a traction vector corresponding to three stress components on the face of the differential material element that is orthogonal to a unit vector argument:

$$\mathbf{T}_{face} = \mathbf{n} \cdot \mathbf{T} \tag{63}$$

where $\mathbf{n}$ is a unit vector that serves to define the face of interest (*i.e.* the vector, $\mathbf{n}$, is taken as the normal to the face). This is more clearly illustrated with a hypothetical normal vector oriented along the *x-direction*:

$$\begin{bmatrix} T_{11} & T_{12} & T_{13} \end{bmatrix} = \begin{bmatrix} 1 & 0 & 0 \end{bmatrix} \begin{bmatrix} T_{11} & T_{12} & T_{13} \\ T_{21} & T_{22} & T_{23} \\ T_{31} & T_{23} & T_{33} \end{bmatrix} \tag{64}$$

Just as vectors are invariant quantities that can be described using suitable components within a given coordinate system associated with a specific ortho-normal basis (*i.e.* Equation (43)), so too can tensors (such as stress and strain) be expressed in terms of suitable components in any given set of coordinate axes. While it was that vector quantities could be described in terms of a linear combination of scalar magnitudes multiplying appropriate basis vectors, tensors employ linear combinations of scalar magnitudes acting on *dyads*. A dyad is an *open product* of two vectors defined as:

$$\hat{\mathbf{i}}_i \hat{\mathbf{i}}_j = \hat{\mathbf{i}}_i \otimes \hat{\mathbf{i}}_j = \begin{bmatrix} 1 \\ 0 \\ 0 \end{bmatrix} \begin{bmatrix} 0 & 1 & 0 \end{bmatrix} = \begin{bmatrix} 0 & 1 & 0 \\ 0 & 0 & 0 \\ 0 & 0 & 0 \end{bmatrix} \tag{65}$$

with the latter two, right-hand expression being a simple example using the first two ortho-normal basis vectors for Cartesian three-space. While it seems clear that a general second order tensor, such as stress, cannot in general be represented as a single dyad, such tensors can be expressed in terms of *dyadics*: linear combinations of dyads, amplified by suitable magnitudes (acting as coefficients for the component dyads).

A general stress tensor, $\mathbf{T}$, may be expressed as:

$$\begin{aligned}\mathbf{T} = T_{ij}\hat{\mathbf{i}}_i \otimes \hat{\mathbf{i}}_j = T_{11}\hat{\mathbf{i}}_1 \otimes \hat{\mathbf{i}}_1 + T_{12}\hat{\mathbf{i}}_1 \otimes \hat{\mathbf{i}}_2 + T_{13}\hat{\mathbf{i}}_1 \otimes \hat{\mathbf{i}}_3 \\ + T_{21}\hat{\mathbf{i}}_2 \otimes \hat{\mathbf{i}}_1 + T_{22}\hat{\mathbf{i}}_2 \otimes \hat{\mathbf{i}}_2 + T_{23}\hat{\mathbf{i}}_2 \otimes \hat{\mathbf{i}}_3 \\ + T_{31}\hat{\mathbf{i}}_3 \otimes \hat{\mathbf{i}}_1 + T_{32}\hat{\mathbf{i}}_3 \otimes \hat{\mathbf{i}}_2 + T_{33}\hat{\mathbf{i}}_3 \otimes \hat{\mathbf{i}}_3\end{aligned} \tag{66}$$

or, even more explicitly:

$$\begin{aligned}\mathbf{T} = T_{11}\begin{bmatrix}1&0&0\\0&0&0\\0&0&0\end{bmatrix} + T_{12}\begin{bmatrix}0&1&0\\0&0&0\\0&0&0\end{bmatrix} \\ + T_{13}\begin{bmatrix}0&0&1\\0&0&0\\0&0&0\end{bmatrix} + T_{21}\begin{bmatrix}0&0&0\\1&0&0\\0&0&0\end{bmatrix} \\ + T_{22}\begin{bmatrix}0&0&0\\0&1&0\\0&0&0\end{bmatrix} + T_{23}\begin{bmatrix}0&0&0\\0&0&1\\0&0&0\end{bmatrix} \\ + T_{31}\begin{bmatrix}0&0&0\\0&0&0\\1&0&0\end{bmatrix} + T_{32}\begin{bmatrix}0&0&0\\0&0&0\\0&1&0\end{bmatrix} \\ + T_{33}\begin{bmatrix}0&0&0\\0&0&0\\0&0&1\end{bmatrix}\end{aligned} \tag{67}$$

As in the case of elementary solid mechanics, it is possible to identify the specific orientation of the differential material element such that the resulting stress components posses strictly normal components to the faces of the material element (*i.e.* there are no shearing components present)

The state of stress wherein shears vanish is referred to as being *principal*. Such a state of stress would be characterized as one wherein the operation furnished in Equation (63) results in a traction vector that is merely some scalar multiple of the normal vector to the face of the differential material element in question:

$$\mathbf{n} \cdot \mathbf{T} = \lambda \mathbf{n} \tag{68}$$

or, in indicial notation:

$$(T_{ij} - \lambda \delta_{ij})\, n_i = 0 \tag{69}$$

In order that Equation (69) have a solution, other than the trivial case of $\mathbf{n} = \mathbf{0}$, the determinant of the parenthetical term must vanish:

$$\begin{vmatrix} T_{11} - \lambda & T_{12} & T_{13} \\ T_{21} & T_{22} - \lambda & T_{23} \\ T_{31} & T_{32} & T_{33} - \lambda \end{vmatrix} = 0 \tag{70}$$

As a result of the stress tensor being symmetric and composed of real numbers, the eigenvalues obtained from the solution of the cubic characteristic equation, emanating from Equation (70), are real. These three eigenvalues are known as the *principal stresses*. Additionally, if these principal stresses are *distinct* (*i.e.* not repeated) then the eigenvectors associated with these eigenvalues are mutually orthogonal. As it is that the only eigenvectors directions are defined (and not the magnitudes and positive sense), a positive sense leading to a *right-handed* coordinate system is usually adopted.

The expansion of the determinant described in Equation (70) can be be made in terms of scalar *invariants* of the stress tensor. These three quantities are invariant with respect to rotations of the cartesian reference frame at the continuum point where the state of stress is observed. Specifically, the characteristic equation from Equation (70) may be states as:

$$\lambda^3 - I_T\lambda^2 - II_T\lambda - III_T = 0 \tag{71}$$

where the quantities I_T, II_T, and III_T (subscript denotes stress) are scalar invariant quantities defined as:

$$\begin{aligned} I_T &= T_{ii} = tr\mathbf{T} \\ II_T &= \frac{1}{2}\left(T_{ij}T_{ij} - T_{ii}T_{jj}\right) = \frac{1}{2}T_{ij}T_{ij} - \frac{1}{2}I_T^2 = \frac{1}{2}\left(\mathbf{T}:\mathbf{T} - I_T^2\right) \\ III_T &= \frac{1}{6}e_{ijk}e_{pqr}T_{ip}T_{jq}T_{kr} = det\mathbf{T} \end{aligned} \tag{72}$$

The hydrostatic state of stress (*i.e.* the stress state tending to cause volumetric changes, only, in a homogeneous, isotropic medium) can be given in terms of the first invariant as:

$$\sigma\mathbf{I} = \frac{1}{3}T_{ii}\mathbf{I} = \frac{1}{3}I_T\mathbf{I} \tag{73}$$

It is mentioned that Equation (73) is also frequently referred to as the *spherical stress tensor*. A related quantity is the *stress deviator*; the quantity that measures the difference from the purely hydrostatic stress state. This latter quantity is given by the *deviatoric stress tensor*:

$$\mathbf{T} - \sigma\mathbf{I} \tag{74}$$

The deviatoric stress tensor gets its name from the fact that it represents the residual stress, after the stress causing volumetric change is subtracted off. The implication is that in a homogeneous, isotropic material, once the spherical stress tensor is removed from the total stress tensor, the portion that remains must be associated with a change (or *deviation*) in shape.

It is possible to, once again, define a set of scalar invariants; this time for the deviatoric stress tensor. These expressions are analogous to those of Equation

(72), but the resulting characteristic equation is simpler than that of Equation (71); as the trace of the deviatoric stress tensor is null:

$$\lambda^3 - J_2\lambda - J_3 = 0 \tag{75}$$

Here the J_2 and J_3 terms represent second and third deviatoric stress invariants, respectively.

While the stress tensor provided by Equation (73) is termed *hydrostatic*, it is only analogous to the notion of *true pressure* in a fluid when the deformation of the body is constantly updated (recall that *engineering* stress is related to the original geometry of the body; *i.e.* $\sigma = P \div A_o$ in the case of uniaxial tension in a bar). In such a circumstance, the stress at a point is referred to as the *Cauchy Stress Tensor*, and given as:

$$\mathbf{n} \cdot \sigma = \mathbf{t} \tag{76}$$

where the vector, $\mathbf{t}$, is the traction acting on an arbitrary surface in the *current configuration*. This leads to the consideration of a differential force resultant acting on a differential area element, normal to the unit vector, $\mathbf{n}$:

$$\mathbf{n} \cdot \sigma \; d\Gamma = \mathbf{t} \; d\Gamma = d\mathbf{f} \tag{77}$$

The foregoing is in contrast to the *first Piola-Kirchhoff stress tensor* (*PK1* tensor), yielding the differential force:

$$\mathbf{n}_o \cdot \mathbf{P} \; d\Gamma_o = \mathbf{t}_o \; d\Gamma_o = d\mathbf{f} \tag{78}$$

Another useful stress tensor, for use with referential descriptions, is the *Second Piola-Kirchhoff Stress* (also called the *PK2* stress); yielding yet another differential force:

$$\mathbf{n}_o \cdot \mathbf{S} \; d\Gamma_o = \mathbf{F}^{-1} \cdot \mathbf{t}_o \; d\Gamma_o = \mathbf{F}^{-1} \cdot d\mathbf{f} \tag{79}$$

It is noted that the PK1 stress tensor is non-symmetrical. In contrast, the PK2 tensor is symmetrical. Additionally, the PK2 stress tensor plays a prominent role in nonlinear analysis involving large deformations, as it is *energy conjugate* to the Green-Lagrange strain tensor (in the sense of producing a valid expression for work).

As the preceding stress equations involve the consideration of differential areas, $d\mathbf{\Gamma}$, in different reference frames, it is useful to review the development of *Nanson's formula* for differential area transformation. The review begins with the postulated existence of two differential areas: one in the referential description, $d\mathbf{\Gamma}_o$; and this same differential area, deformed and in the current configuration, $d\mathbf{\Gamma}$. These two quantities may be conveniently expressed in terms of cross products involving two adjacent and non-parallel edges of the of the differential areas:

$$\mathbf{n}_o \; d\Gamma_o = d\mathbf{X} \times \delta\mathbf{X} \rightarrow \mathbf{n} \; d\Gamma = d\mathbf{x} \times \delta\mathbf{x} \tag{80}$$

or in Cartesian components:

$$(n_o)_i \; d\Gamma_o = e_{ijk} dX_j \delta X_k \rightarrow n_q \; d\Gamma = e_{qrs} dx_r \delta x_s \tag{81}$$

To better explain these relationships, previous developments related to the deformation tensor of Equation (47), as well as the strain invariants described in Equation (72), are now considered.

When considering the *stretching* of a linear differential element, defined as $\frac{ds}{dS}$; the ratio of the element lengths in the current and referential configurations, respectively, are considered. It is common for the stretch in the material element originally oriented with $\mathbf{n}_o$, in the reference configuration, to be labeled as $\mathbf{\Lambda}$; whereas the stretch of an element oriented along $\mathbf{n}$, in the current configuration, is denoted by λ. If now Equations (47) and (48) are divided by $(dS)^2$ and $(ds)^2$, respectively, the following is obtained:

$$\begin{aligned} \Lambda^2 &= \frac{d\mathbf{X}}{dS} \cdot \mathbf{C} \cdot \frac{d\mathbf{X}}{dS} = \mathbf{n}_o \cdot \mathbf{C} \cdot \mathbf{n}_o \\ \frac{1}{\lambda^2} &= \frac{d\mathbf{x}}{ds} \cdot \mathbf{B}^{-1} \cdot \frac{d\mathbf{x}}{ds} = \mathbf{n} \cdot \mathbf{B}^{-1} \cdot \mathbf{n} \end{aligned} \tag{82}$$

As a concrete example, the case of the unit extension of a differential material element whose side is initially parallel with the X_1-axis is considered as $\frac{ds-dS}{dS} = \frac{ds}{dS} - 1$; thus yielding:

$$E_{(1)} = \Lambda_{(1)} - 1 = \sqrt{C_{11}} - 1 = \sqrt{1 + 2E_{11}} - 1 \tag{83}$$

In Equation (83), $E_{(1)}$ is the unit elongation, and use has been made of Equation (47), in going from the second to third equality.

Extending the ideas from Equation (83) to the case of a differential volume element having sides that are parallel with the principal directions of $\mathbf{C}$ and $\mathbf{E}$ within the referential coordinate axes, then the following extension becomes natural:

$$\begin{aligned} \frac{dV}{dV_o} = \Lambda_{(1)}\Lambda_{(2)}\Lambda_{(3)} &= \sqrt{(1 + 2E_1)\,(1 + 2E_2)\,(1 + 2E_3)} \\ &= \sqrt{C_1 C_2 C_3} = \sqrt{III_C} \end{aligned} \tag{84}$$

where III_C is the third invariant of the Green Deformation Tensor, $\mathbf{C}$. Likewise, an analogous expression for the case in which the differential element ends up with its sides aligned with the principal spatial coordinate axes may be expressed as:

$$\frac{dV}{dV_o} = \lambda_{(1)}\lambda_{(2)}\lambda_{(3)} = \frac{1}{\sqrt{B_1^{-1} B_2^{-1} B_3^{-1}}} = \frac{1}{\sqrt{III_{B^{-1}}}} \tag{85}$$

These foregoing results may be related to a previously developed notion (*i.e.* Equation (36)).

Recall the use of the deformation gradient determinant, $\mid F \mid$, in volume integration:

$$\int f(\mathbf{x})\, dx_1 dx_2 dx_3 = \int f \circ \phi(\mathbf{X}) \mid \mathbf{F} \mid dX_1 dX_2 dX_3 \tag{86}$$

It is noted that as long as the deformation is continuous, the determinant of the deformation gradient is always positive. It is now possible elucidate the implication of Equation (36):

$$\mid \mathbf{F} \mid = \frac{dV}{dV_o} = \frac{\rho_o}{\rho} \tag{87}$$

The inverse relationship also holds:

$$\mid \mathbf{F} \mid^{-1} = \frac{dV_o}{dV} = \frac{\rho}{\rho_o} \tag{88}$$

The foregoing results from Equations (87) and (88) may be used in conjunction with the results from Equations (84) and (85) to yield the results that:

$$III_C = \mid \mathbf{F} \mid^2 \tag{89}$$

and,

$$III_{B^{-1}} = \mid \mathbf{F} \mid^{-2} \tag{90}$$

Recalling, now, that determinant of an arbitrary 3-by-3 matrix (m-rows by n-columns) may be given as a permutation:

$$\mid a_n^m \mid = e_{ijk} a_1^i a_2^j a_3^k \tag{91}$$

A similar result may be obtained with arbitrary column numbers for a (*i.e.* not 1, 2, and 3):

$$e_{pqr} \mid a_n^m \mid = e_{ijk} a_p^i a_q^j a_r^k \tag{92}$$

This result may be used to further develop Equations (87) and (88):

$$e_{ijk} \frac{\rho_o}{\rho} = e_{ijk} \mid \mathbf{F} \mid = e_{rst} \frac{\partial x_r}{\partial X_i} \frac{\partial x_s}{\partial X_j} \frac{\partial x_t}{\partial X_k} \tag{93}$$

as well as:

$$e_{rst} \frac{\rho}{\rho_o} = e_{rst} \mid \mathbf{F} \mid^{-1} = e_{ijk} \frac{\partial X_i}{\partial x_r} \frac{\partial X_j}{\partial x_s} \frac{\partial X_k}{\partial x_t} \tag{94}$$

Re-expressing Equation (81) as:

$$(n_o)_i \, d\Gamma_o = e_{ijk} \frac{\partial X_j}{\partial x_s} \frac{\partial X_k}{\partial x_t} dx_s \delta x_t \tag{95}$$

Multiplying both sides of Equation (95) by $\frac{\partial X_i}{\partial x_r}$, and using Equations (94) and (81), yields:

$$n_r \, d\Gamma = \frac{\rho_o}{\rho} \frac{\partial X_i}{\partial x_r} (n_o)_i \, d\Gamma_o \tag{96}$$

or, in tensor form:

$$\mathbf{n}\, d\Gamma = \mid \mathbf{F} \mid \mathbf{n}_o \cdot \mathbf{F}^{-1} d\Gamma_o \tag{97}$$

Oftentimes, Equation (97) appears in terms of *vector areas*:

$$d\mathbf{A} = \frac{\rho_o}{\rho} d\mathbf{A}_o \cdot \mathbf{F}^{-1} = \mid \mathbf{F} \mid d\mathbf{A}_o \cdot \mathbf{F}^{-1} \tag{98}$$

The foregoing expression for *Nanson's Formula* are useful in discussions pertaining to transforming between the various measures of stress introduced earlier (*i.e.* Cauchy, PK1, and PK2).

Using the notion of force per unit undeformed area, the Piola-Kirchhoff stresses arise naturally. The PK1 stress tensor, $\mathbf{P}$ furnishes the actual force $d\mathbf{f}$ acting on the deformed area element, $d\Gamma$, but measured per unit undeformed area $d\Gamma_o$; thus yielding:

$$\mathbf{n}_o \cdot \mathbf{P}\, d\Gamma_o = d\mathbf{f} = \mathbf{n} \cdot \sigma\, d\Gamma \tag{99}$$

Equation (99) is then seen to yield the actual differential force acting on the deformed area in the current configuration, but it does so using information regarding the body in question in a previously deformed state (*i.e.* in terms of a referential description). In contrast, the PK2 stress tensor, $\mathbf{S}$, furnishes a differential force, $d\tilde{\mathbf{f}}$, that is related to the current differential force vector, $d\mathbf{f}$, through the application of the inverse deformation gradient:

$$d\tilde{\mathbf{f}} = \mathbf{F}^{-1} \cdot d\mathbf{f} \tag{100}$$

The foregoing may be used to arrive at the useful additional expressions:

$$\mathbf{n}_o \cdot \mathbf{S}\, d\Gamma_o = d\tilde{\mathbf{f}} = \mathbf{F}^{-1} \cdot d\mathbf{f} = \mathbf{F}^{-1} \cdot \mathbf{n} \cdot \sigma\, d\Gamma = \mathbf{n} \cdot \sigma \left(\mathbf{F}^{-1}\right)^T d\Gamma \tag{101}$$

The expressions in Equations (77), (78), and (79) are now seen more clearly, thus permitting additional insights that enable mapping from one stress tensor to another.

By using Nanson's Formula, it is possible to consider how it is that the Cauchy stress tensor is related to the Piola-Kirchhoff stress tensors; beginning with the PK1 stress:

$$\begin{aligned}
\mathbf{n}_o \cdot \mathbf{P}\, d\Gamma_o &= \mathbf{n} \cdot \sigma\, d\Gamma \qquad (102)\\
\mathbf{n}_o \cdot \mathbf{P}\, d\Gamma_o &= \frac{\rho_o}{\rho} \mathbf{n}_o \cdot \mathbf{F}^{-1}\, \sigma\, d\Gamma_o \\
0 &= \mathbf{n}_o \cdot \mathbf{P}\, d\Gamma_o - \frac{\rho_o}{\rho} \mathbf{n}_o \cdot \mathbf{F}^{-1}\, \sigma\, d\Gamma_o \\
0 &= \mathbf{n}_o d\Gamma_o \cdot \left(\mathbf{P} - \frac{\rho_o}{\rho} \mathbf{F}^{-1}\, \sigma \right)
\end{aligned}$$

Equations (102) lead to the tensor transformation between the Cauchy and PK1 stress tensors:

$$\mathbf{P} = \frac{\rho_o}{\rho}\mathbf{F}^{-1}\ \sigma \tag{103}$$

and, inversely:

$$\sigma = \frac{\rho}{\rho_o}\mathbf{F}\ \mathbf{P} \tag{104}$$

In the case of the PK2 stress the following relations hold:

$$\begin{aligned}\mathbf{n}_o \cdot \mathbf{S}\ d\Gamma_o &= \mathbf{F}^{-1} \cdot \left(\frac{\rho_o}{\rho}\mathbf{n}_o\ d\Gamma_o \cdot \mathbf{F}^{-1}\ \sigma\right) \\ &= \left(\frac{\rho_o}{\rho}\mathbf{n}_o\ d\Gamma_o \cdot \mathbf{F}^{-1}\ \sigma\right) \cdot \left(\mathbf{F}^{-1}\right)^T\end{aligned} \tag{105}$$

thus, leading to the tensor transformation from the Cauchy and PK1 stress tensors into the PK2 stress tensor:

$$\mathbf{S} = \frac{\rho_o}{\rho}\mathbf{F}^{-1}\ \sigma\ \left(\mathbf{F}^{-1}\right)^T = \mathbf{P}\left(\mathbf{F}^{-1}\right)^T \tag{106}$$

and, inversely for the PK2 into the PK1 stress:

$$\mathbf{P} = \mathbf{S}\ \mathbf{F}^T \tag{107}$$

and similarly, the inversion from PK2 to Cauchy stress:

$$\sigma = \frac{\rho}{\rho_o}\mathbf{F}\ \mathbf{S}\ \mathbf{F}^T \tag{108}$$

1.1.6 General principles

The general principles underpinning continuum mechanics require mathematical descriptions of physical phenomena to enable the statement of *balance laws*. An illustration of such a physical phenomenon comes in the form of the vitally important example of *flux across a surface*. If a differential portion the boundary of a body, $\mathcal{B}$, is denoted as $d\Gamma$ (possessing a normal vector to its surface, denoted by $\mathbf{n}$), then any physical quantity moving through $d\Gamma$ may be described using the notion of *flux*. Considering that the velocity of the quantity in question may be denoted by a vector, $\mathbf{v}$, then the *flux of volume* appears as:

$$\mathbf{v} \cdot \mathbf{n} d\Gamma \tag{109}$$

The physical interpretation of Equation (109) is quite simply: the volume of material flowing through the differential boundary element, $d\Gamma$, *per unit time*. If the differential time interval, dt, were added, as a multiple, to Equation (109), then the volume of material passing through the boundary, $d\Gamma$ would be the result.

Considering the complete boundary, Γ, of the body $\mathcal{B}$, then the so-called *volume flux* appears as:

$$Volume\ Flux = \int_{\Gamma} \mathbf{v} \cdot \mathbf{n} d\Gamma \tag{110}$$

The utility of Equation (110) in expressing quantities useful in conservation laws, is perhaps obvious, but it is nonetheless instructive to point out a few useful examples in this regard:

$$Mass\ Flux = \int_{\Gamma} \rho \mathbf{v} \cdot \mathbf{n} d\Gamma \tag{111}$$

$$Momentum\ Flux = \int_{\Gamma} \rho \mathbf{v} \left(\mathbf{v} \cdot \mathbf{n} \right) d\Gamma \tag{112}$$

$$Kinetic\ Energy\ Flux = \int_{\Gamma} \frac{1}{2} \rho v^2 \left(\mathbf{v} \cdot \mathbf{n} \right) d\Gamma \tag{113}$$

The foregoing equations of flux may be generalized as:

$$Material\ Property\ Flux = \int_{\Gamma} \rho \not{A} \mathbf{v} \cdot \mathbf{n} d\Gamma = \int_{\Gamma} \rho \not{A} \mathbf{v} d\mathbf{A} \tag{114}$$

where the quantity, $d\mathbf{A}$, is taken to mean *vector differential element of area*.

Of course, the implication in the previously defined flux equations was the motion of mass through the differential boundary, $d\Gamma$, associated with the body of interest. Such *mechanical fluxes*, as they are usually known, do not in anyway imply that physical quantities that best occur in a vacuum (*i.e.* without mass transport) are somehow excluded from consideration within the scope of the previously defined notions. Indeed non-mechanical fluxes (*e.g.* current flow, heat flow, *etc.*) can be similarly described. Considering the case of heat flux:

$$Heat\ flux\ through\ a\ boundary = \int_{\Gamma} \mathbf{q} \cdot \mathbf{n} d\Gamma \tag{115}$$

where $\mathbf{q}$ is the *heat flux vector*; given in units of power per unit area.

An important point of departure for any discussion of the general principles (or *conservation laws*) in continuum mechanics is a discussion of the *Divergence Theorem* of Gauss. In words, this theorem generally states that the outer normal component of a vector field, taken over a closed surface, is equal to the divergence of the same vector field over the volume bounded by the closed surface. Mathematically, the Divergence Theorem appears in vector form as:

$$\int_{\Gamma} \mathbf{v} \cdot \mathbf{n} d\Gamma = \int_{\Omega} \nabla \cdot \mathbf{v} d\Omega \tag{116}$$

In Cartesian form, the Divergence Theorem takes the form:

$$\int_{\Gamma} v_i n_i d\Gamma = \int_{V} \frac{\partial v_i}{\partial x_i} d\Omega \tag{117}$$

Other special cases for the Cartesian representation of the Divergence Theorem include the case of a scalar field:

$$\int_{\Gamma} f n_i d\Gamma = \int_{V} \frac{\partial f}{\partial x_i} d\Omega \tag{118}$$

as well as the case of a second order tensor:

$$\int_{\Gamma} T_{ij} n_i d\Gamma = \int_{V} \frac{\partial T_{ij}}{\partial x_i} d\Omega \tag{119}$$

A generalization of Gauss's divergence Theorem sometimes appears using the so-called *star product*. The star product can be used to denote dot and cross products, as well as diads, *etc.* The generalized Divergence Theorem is frequently stated as:

$$\int_{\Gamma} \mathbf{n} \star \mathscr{A} d\Gamma = \int_{\Omega} \nabla \star \mathscr{A} d\Omega \tag{120}$$

While it is clear that the Divergence Theorem requires differentiability on the part of the quantities appearing within the volume integrations, discontinuities may, nonetheless, be treated using *jump conditions*. In such a case, the problem domain is discretized into sub-domains that are suitablely differentiable for application of the Divergence Theorem. The set of all interfaces joining such domains is denoted as Γ_{int}. Using this approach a piecewise application of the Divergence Theorem is possible; as now illustrated for the case of the Cartesian components of a discontinuous scalar field:

$$\int_{\Omega} \frac{\partial f}{\partial x_i} d\Omega = \int_{\Gamma} f n_i d\Gamma + \int_{\Gamma_{int}} [\![f n_i]\!] d\Gamma \tag{121}$$

and the Cartesian components of a discontinuous vector field:

$$\int_{\Omega} \frac{\partial v_i}{\partial x_i} d\Omega = \int_{\Gamma} n_i v_i d\Gamma + \int_{\Gamma_{int}} [\![n_i v_i]\!] d\Gamma \tag{122}$$

where $[\![f\mathbf{n}]\!]$ and $[\![\mathbf{n} \cdot \mathbf{v}]\!]$ are the jumps defined as:

$$[\![f\mathbf{n}]\!] = f^A \mathbf{n}^A + f^B \mathbf{n}^B \tag{123}$$

$$[\![\mathbf{n} \cdot \mathbf{v}]\!] = v_i^A n_i^A + v_i^B n_i^B = \left(v_i^A - v_i^B \right) n_i^A = \left(v_i^B - v_i^A \right) n_i^B \tag{124}$$

and in addition:

$$[\![f\mathbf{n}]\!] \cdot \mathbf{n}^A = f^A - f^B \tag{125}$$

The Divergence Theorem is extremely important, not only for its role creating useful forms for the balance laws of continuum mechanics, but also for its general utility in arriving at the fundamental formulations in computational mechanics. However, it initial use within the current discussion concerns the former case, and thus a consideration of the *conservation of mass* and *continuity equation* follows.

Consider a body, $\mathcal{B}$, having mass, M, and enclosed by a boundary, Γ. The distribution of mass within $\mathcal{B}$ varies in both space and time:

$$\rho\left(\mathbf{x},t\right) \quad \forall \mathbf{x} \in \Omega \subset \mathbb{R}^3, t \in [0,\infty) \tag{126}$$

and thus, at a given instant of time, the mass of body, $\mathcal{B}$ is:

$$M = \int_\Omega \rho \, d\Omega \tag{127}$$

thus leading directly to the following statement concerning the rate of change in the total mass of $\mathcal{B}$:

$$\frac{\partial M}{\partial t} = \int_\Omega \frac{\partial \rho}{\partial t} d\Omega \tag{128}$$

If mass is neither created, nor destroyed within the body, then the change in mass per unit time must occur as a result of a mass flux across some, or all of boundary, Γ. Assuming that the mass is increasing (*i.e.* here is a net *inflow* of mass to body $\mathcal{B}$), Equation (111) may be employed as follows:

$$\frac{\partial M}{\partial t} = -\int_\Gamma \rho \mathbf{v} \cdot \mathbf{n} d\Gamma \tag{129}$$

It is pointed out that the negative sign on the right hand side of Equation (129) is included to denote *inflow*, as the positive normal, $\mathbf{n}$, was taken as positive when pointing out from the enclosed volume, Ω.

Gauss' Divergence Theorem may now be applied to Equation (129); resulting in:

$$\frac{\partial M}{\partial t} = -\int_\Omega \nabla \cdot \left(\rho \mathbf{v}\right) d\Omega \tag{130}$$

Equations (128) and (130) maybe combined:

$$\int_\Omega \left[\frac{\partial \rho}{\partial t} + \nabla \cdot \left(\rho \mathbf{v}\right)\right] d\Omega = 0 \tag{131}$$

It is clear that irrespective of the choice for Ω, the integral of Equation (131) must vanish. This result leads to a statement of the *continuity equation* of continuum mechanics:

$$\frac{\partial \rho}{\partial t} + \nabla \cdot \left(\rho \mathbf{v}\right) = 0 \tag{132}$$

Equation (132) may be re-cast in terms of the material time derivative as:

$$\frac{D\rho}{Dt} + \rho \nabla \cdot \mathbf{v} = 0 \tag{133}$$

Since, in the case of Equation (133) the focus is on a material body (*i.e.* there is no mass flux across the material boundary), the material density is taken as constant, and thus brought out from the divergence term. The form of the

continuity equation furnished in Equation (132) is sometimes referred to as the *conservative form*. Some useful observations may now be made concerning the implications of Equation (132).

Considering a simple re-arrangement of the continuity equation leads to:

$$\nabla \cdot \mathbf{v} = -\frac{1}{\rho}\frac{D\rho}{Dt} \tag{134}$$

Simply stated, Equation (134) requires that the divergence in the velocity field measures the rate of flow of material at a particle in the body, $\mathcal{B}$. This effect manifests in units of rate of density change in the neighborhood of the particle. Thus, in the case of incompressibility, $\nabla \cdot \mathbf{v} = 0$.

Considering, now, the case of material coordinates (the previous development implied a spatial description), the conservation of mass yields:

$$\int_{\Omega_o} \rho\left(\mathbf{X}, t_o\right) d\Omega_o = \int_{\Omega} \rho\left(\mathbf{x}, t\right) d\Omega \tag{135}$$

In words, Equation (135) states that the mass of a body occupying a volume Ω_o at time t_o is identical to the mass at some future time, t; when the body occupies the volume Ω. Using the result of Equation (87), the foregoing may be restated as:

$$\int_{\Omega} \rho\left(\mathbf{x}, t\right) d\Omega = \int_{\Omega_o} \rho\left(\mathbf{x}, t\right) \mid \mathbf{F} \mid d\Omega_o \tag{136}$$

where $\mid \mathbf{F} \mid$ is the determinant of the deformation gradient (positivity is implied). Other authors may denote this same quantity as $\mid \mathbf{J} \mid$: the absolute value of the *Jacobian determinant*. The latter term is a more general mathematical term, while the former case possesses suggestive geometric implications that are germane to the present discussion. This leads to the statement:

$$\int_{\Omega_o} \left[\rho\left(\mathbf{X}\right) - \rho\left(\mathbf{x}\right) \mid \mathbf{F} \mid\right] d\Omega_o = 0 \tag{137}$$

thus leading too:

$$\rho\left(\mathbf{x}\right) \mid \mathbf{F} \mid = \rho\left(\mathbf{X}\right) \tag{138}$$

Equation (138) may be differentiated with respect to time to arrive at the form of the continuity equation that is applicable in the material reference frame:

$$\frac{d}{dt}\left(\rho\left(\mathbf{x}\right) \mid \mathbf{F} \mid\right) = 0 \tag{139}$$

It is pointed out that the spatial and material descriptions of the continuity equations appear quite different, but their equivalence can be seen in the proofs contained in most elementary texts on continuum mechanics.

In considering the balance laws of continuum mechanics, it is oftentimes helpful to be able to take material time derivatives of integrals for scalar fields taken over a fixed material domains, in order to describe physical quantities such as internal energy, heat, *etc.*, and denoted by $\mathscr{A}$. In general, domains of constant material may have boundaries that deform in order to continually enclose the particles of interest during the motion of the body (*i.e.* the integral quantities of Equations (110) and (111) vanish for the material domain); thus leading to an integral of the form:

$$I(t) = \int_{\Omega} \mathscr{A}(\mathbf{x}, t)\, d\Omega \tag{140}$$

The dependence of the volume, Ω, on time complicates the form of the material time derivative of Equation (140); preventing the commuting of the time derivative to the interior of the integral. Indeed, as a first step towards taking the material time derivative of Equation (140), the integral is transformed in order that it may be taken over a fixed volume in the referential configuration. By using the relations $\mathbf{x} = \phi(\mathbf{X}, t)$, and $d\Omega = \mid \mathbf{F}(\mathbf{X}, t) \mid d\Omega_o$, the time rate of change in $I(t)$ becomes:

$$\dot{I} = \frac{D}{Dt} \int_{\Omega} \mathscr{A}(\mathbf{x}, t)\, d\Omega = \frac{\partial}{\partial t} \int_{\Omega_o} \mathscr{A}(\phi(\mathbf{X}, t), t) \mid \mathbf{F}(\mathbf{X}, t) \mid d\Omega_o \tag{141}$$

Since the volume of integration within Equation (141) is now constant in time, the time derivative commutes, and a subsequent application of the product rule yields:

$$\frac{D}{Dt} \int_{\Omega} \mathscr{A}(\mathbf{x}, t)\, d\Omega = \int_{\Omega_o} \left[\dot{\mathscr{A}}(\phi(\mathbf{X}, t), t) \mid \mathbf{F}(\mathbf{X}, t) \mid + \mathscr{A}(\phi(\mathbf{X}, t), t) \mid \dot{\mathbf{F}}(\mathbf{X}, t) \mid \right] d\Omega_o \tag{142}$$

where $\dot{\mathscr{A}}$ signifies the material time derivative of the scalar field $\mathscr{A}$. Equation (142) may now be converted back to the spatial reference frame; once again using $\mathbf{x} = \phi(\mathbf{X}, t)$, and $d\Omega = \mid \mathbf{F}(\mathbf{X}, t) \mid d\Omega_o$:

$$\begin{aligned} \frac{D}{Dt} \int_{\Omega} \mathscr{A}(\mathbf{x}, t)\, d\Omega &= \int_{\Omega_o} \left[\dot{\mathscr{A}}(\phi(\mathbf{X}, t), t) + \mathscr{A}(\phi(\mathbf{X}, t), t) \frac{\mid \dot{\mathbf{F}}(\mathbf{X}, t) \mid}{\mid \mathbf{F}(\mathbf{X}, t) \mid} \right] \mid \mathbf{F}(\mathbf{X}, t) \mid d\Omega_o \\ &= \int_{\Omega} \left[\dot{\mathscr{A}}(\mathbf{x}, t) + \mathscr{A}(\mathbf{x}, t) \frac{\mid \dot{\mathbf{F}}(\mathbf{X}, t) \mid}{\mid \mathbf{F}(\mathbf{X}, t) \mid} \right] d\Omega \\ &= \int_{\Omega} \left[\dot{\mathscr{A}}(\mathbf{x}, t) + \mathscr{A}(\mathbf{x}, t)\, \nabla \cdot \mathbf{v}(\mathbf{x}, t) \right] d\Omega \end{aligned} \tag{143}$$

where smoothness in the spatial velocity field, $\mathbf{v}$, has been assumed.

Omitting the arguments to the tensor quantities, and subsequently applying the the Divergence Theorem of Gauss (Equation (116)) to the last term in Equation (143), furnishes the more common form of *Reynolds Transport Theorem*:

$$\frac{D}{Dt} \int_{\Omega} \mathscr{A}\, d\Omega = \int_{\Omega} \dot{\mathscr{A}}\, d\Omega + \int_{\Gamma} \mathscr{A} \mathbf{v} \cdot \mathbf{n}\, d\Gamma \tag{144}$$

Equation (144) describes the time rate of change of an integral taken over a material volume by setting up a mathematical description of the body within the spatial reference frame. The volume of the body, considered in the spatial frame, is simply the instantaneous volume that the body assumes at the time instant, t. As a result of the fact that the actual material body possesses a bounding surface that is deforming in space and time, non-vanishing flux terms reemerge in this spatial representation. With all of this in mind, the meaning of Equation (144) may be given in words as: the rate of increase in the amount of $\mathscr{A}$, possessed by the material body that is instantaneously within the spatial volume Ω is equal to the rate of increase in the total amount of $\mathscr{A}$ inside of the control surface Γ minus the net rate of outward flux of $\mathscr{A}$ carried by mass transport through the Γ. An analogous expression for the material time derivative of a line integral $\int_c f(\mathbf{x})\, d\mathbf{x}$ may be obtained using Equations (28) and (29):

$$\frac{D}{Dt}\int_c f(\mathbf{x})\, d\mathbf{x} = \int_c \left[\frac{df}{dt} d\mathbf{x} + f(\mathbf{x})\, \mathbf{L}\cdot d\mathbf{x}\right] \tag{145}$$

The foregoing treatment of balance laws is helpful to keep in mind as discussion now shifts to balance laws that are directly at the heart of finite element formulations. The *conservation of linear momentum* is equivalent to Newton's Second Law of Motion; but rather than being posed as a differential equation, as in the latter case, the conservation form is furnished via integration.

External agencies may impose actions on a given body, $\mathcal{B}$, whose material points occupy a domain Ω that is bounded by Γ. These actions are usually described in terms of *tractions* (mechanical effects imposed along a boundary), and *body forces* (effects acting on all particles within the domain; as so-called *actions-at-a-distance*, *e.g.* gravitational attraction, inertial forces, magnetic attraction, *etc.*) Thus, the *total force* is given as:

$$\mathbf{f}(t) = \int_\Omega \rho\mathbf{b}(\mathbf{x},t)\, d\Omega + \int_\Gamma \mathbf{t}(\mathbf{x},t)\, d\Gamma \tag{146}$$

Additionally, as *linear momentum per unit volume* appears as $\rho\mathbf{v}(\mathbf{x},t)$, the linear momentum of the entire body, $\mathcal{B}$, is:

$$\mathbf{p}(t) = \int_\Omega \rho\mathbf{v}(\mathbf{x},t)\, d\Omega \tag{147}$$

The *conservation of linear momentum* requires that the time rate of change of linear momentum balances the applied total force:

$$\frac{D\mathbf{p}}{Dt} = \mathbf{f} \Rightarrow \frac{D}{Dt}\int_\Omega \rho\mathbf{v} d\Omega = \int_\Omega \rho\mathbf{b}(\mathbf{x},t)\, d\Omega + \int_\Gamma \mathbf{t}(\mathbf{x},t)\, d\Gamma \tag{148}$$

Dropping the tensor arguments and applying Reynolds Transport Theorem, along with Gauss' Divergence Theorem, to the left hand side of Equation (148) results in:

$$\frac{D}{Dt}\int_\Omega \rho\mathbf{v} d\Omega = \int_\Omega \left[\frac{D}{Dt}(\rho\mathbf{v}) + (\rho\mathbf{v})\,\nabla\cdot\mathbf{v}\right] d\Omega \tag{149}$$

Using the *product rule of differentiation* on the first term in the right hand side of Equation (149) result in:

$$\frac{D}{Dt}\int_{\Omega}\rho\mathbf{v}d\Omega=\int_{\Omega}\left[\rho\frac{D\mathbf{v}}{Dt}+\mathbf{v}\left(\frac{D\rho}{Dt}+\rho\nabla\cdot\mathbf{v}\right)\right]d\Omega \tag{150}$$

It is noticed that the parenthetical term on the right hand side of Equation (150) is identical with Equation (133), the *continuity equation*, and thus vanishes; leaving:

$$\frac{D}{Dt}\int_{\Omega}\rho\mathbf{v}d\Omega=\int_{\Omega}\rho\frac{D\mathbf{v}}{Dt}d\Omega \tag{151}$$

Continuing in our development of Equation (148), the Divergence Theorem may be applied to the traction term on the right hand side; as modified using *Cauchy's Law* (Equation (76)):

$$\int_{\Gamma}\mathbf{t}d\Gamma=\int_{\Gamma}\mathbf{n}\cdot\sigma d\Gamma=\int_{\Omega}\nabla\cdot\sigma d\Omega \tag{152}$$

It is pointed out that within the notes, thus far, the convention of adopting the *left gradient operator* has somewhat informally been followed. From this point forward, it will be formally followed, unless otherwise noted. In the case of Equation (152), this convention mandates that, since the normal, $\mathbf{n}$, is to the left, the divergence is to the left. When the divergence is to the left, the implication is that the contraction occurs on the first index; the converse is also true. Since the Cauchy stress tensor is symmetrical, this distinction is somewhat academic. However, when an asymmetrical stress tensor, or a non-Cartesian reference frame is considered, this distinction become vital. To emphasize the meaning of the foregoing, the Cartesian component form of Equation (152) is now given:

$$\int_{\Gamma}t_j d\Gamma=\int_{\Gamma}n_i\sigma_{ij}d\Gamma=\int_{\Omega}\frac{\partial\sigma_{ij}}{\partial x_i}d\Omega \tag{153}$$

Substituting Equations (152) and (151) into Equation (148) yields:

$$\int_{\Omega}\left(\rho\frac{D\mathbf{v}}{Dt}-\rho\mathbf{b}-\nabla\cdot\sigma\right)d\Omega=0 \tag{154}$$

Assuming that the integrand of Equation (154) is C^1, and recognizing that the integration is valid over any arbitrary domain, the following partial differential equation is obtained:

$$\rho\frac{D\mathbf{v}}{Dt}=\nabla\cdot\sigma+\rho\mathbf{b} \tag{155}$$

Equation (155) is frequently referred to as the *momentum equation*. As a result of the product of density and velocity change, the momentum change term on the left hand side is oftentimes called the *inertial term*. The divergence of the stress field leads to a statement on the *internal forces* within the body.

Energy conservation is yet another of the important balance laws of continuum mechanics. The present discussion considers only the context of thermomechanical systems (*i.e.* those systems where energy change is induced by mechanical work or heat). This conservation law requires that the time rate of change in total energy be equal to the rate of mechanical work done on a body (by surface tractions and body forces); as well as through the introduction of heat energy (by heat flux through the surface and by heat generation within the body, *e.g.* through an exothermic chemical reaction). The total energy of a body comprises contributions from both stored internal energy, as well as kinetic energy, and thus the time rate of change of the energy is given in terms of power, $\mathscr{P}$:

$$\mathscr{P}^{total} = \mathscr{P}^{stored} + \mathscr{P}^{kinetic} \tag{156}$$

where,

$$\mathscr{P}^{stored} = \frac{D}{Dt}\int_{\Omega} \rho w^{stored} d\Omega \tag{157}$$

and,

$$\mathscr{P}^{kinetic} = \frac{D}{Dt}\int_{\Omega} \frac{1}{2}\rho \mathbf{v}\cdot\mathbf{v} d\Omega \tag{158}$$

In the Equation (157), the quantity w^{stored} is the stored energy per unit mass (*i.e.* potential energy).

Consideration of the external actions leads to important expressions involving, first, mechanical actions (due to body forces and tractions, respectively):

$$\mathscr{P}^{mechanical} = \int_{\Omega} \mathbf{v}\cdot\rho\mathbf{b} d\Omega + \int_{\Gamma} \mathbf{v}\cdot\mathbf{t} d\Gamma \tag{159}$$

and subsequently the contributions from thermal effects (due to heat generation and heat flux, respectively):

$$\mathscr{P}^{thermal} = \int_{\Omega} \rho I d\Omega - \int_{\Gamma} \mathbf{n}\cdot\mathbf{q} d\Gamma \tag{160}$$

where the negative on the heat flux power term is due to the fact that the heat flow in the direction of the outward normal is considered positive with respect to the commonly held sign convention. In the foregoing, the term, I, denotes heat generation, per unit time, per unit volume; while the term, $\mathbf{q}$, denotes the heat flux (possessing units of power per unit area).

In concise notation, the principle of energy conservation may be stated as:

$$\mathscr{P}^{total} = \mathscr{P}^{mechanical} + \mathscr{P}^{thermal} \tag{161}$$

Equation (161) is frequently referred to in the literature as the *First Law of Thermodynamics*.

Applying Reynold's Transport Theorem and Equation (151) to the left hand side of Equation (161) results in:

$$\begin{aligned}\frac{D}{Dt}\int_\Omega \left[\rho w^{stored} + \frac{1}{2}\rho \mathbf{v}\cdot\mathbf{v}\right] d\Omega &= \int_\Omega \left[\rho \frac{Dw^{stored}}{Dt} + \frac{1}{2}\rho \frac{D\left(\mathbf{v}\cdot\mathbf{v}\right)}{Dt}\right] d\Omega \\ &= \int_\Omega \left[\rho \frac{Dw^{stored}}{Dt} + \rho \mathbf{v}\cdot\frac{D\mathbf{v}}{Dt}\right] d\Omega \end{aligned} \tag{162}$$

Considering, now, the traction term within Equation (159), Cauchy's Law and the Divergence Theorem may be applied as follows:

$$\begin{aligned}\int_\Gamma \mathbf{v}\cdot\mathbf{t} d\Gamma &= \int_\Gamma \mathbf{n}\cdot\sigma\cdot\mathbf{v} d\Gamma \\ &= \int_\Omega \nabla\cdot\left(\sigma\cdot\mathbf{v}\right) d\Omega \\ &= \int_\Omega \left(\sigma_{ij}v_j\right)_{,i} d\Omega = \int_\Omega \left(v_{j,i}\sigma_{ij} + v_j\sigma_{ij,i}\right) d\Omega \\ &= \int_\Omega \left(D_{ji}\sigma_{ij} + W_{ji}\sigma_{ij} + v_j\sigma_{ij,i}\right) d\Omega \end{aligned} \tag{163}$$

In Equation (163), use has been made of Equation (22); where D and W are the rate of deformation and spin tensors, respectively. Since the Cauchy stress tensor is symmetrical, and the spin tensor is skew symmetrical, Equation (163) simplifies, to be:

$$\begin{aligned}\int_\Gamma \mathbf{v}\cdot\mathbf{t} d\Gamma &= \int_\Omega \left(D_{ji}\sigma_{ij} + v_j\sigma_{ij,i}\right) d\Omega \\ &= \int_\Omega \left(\mathbf{D}\colon\sigma + \left(\nabla\cdot\sigma\right)\cdot\mathbf{v}\right) d\Omega \end{aligned} \tag{164}$$

Substitution of all of the foregoing into Equation (162) (with an application of the Divergence Theorem to the heat flux term) yields:

$$\int_\Omega \left(\rho\frac{Dw^{stored}}{Dt} - \mathbf{D}\colon\sigma + \nabla\cdot\mathbf{q} - \rho I + \mathbf{v}\cdot\left(\rho\frac{D\mathbf{v}}{Dt} - \nabla\cdot\sigma - \rho\mathbf{b}\right)\right) d\Omega = 0 \tag{165}$$

It is pointed out the last parenthetical term within the integrand of Equation (165) vanishes due to the conservation of linear momentum (*i.e.* Equation (155)). In light of this fact, as well as the fact that the integrand from Equation (165) holds for any arbitrary boundary, the following PDE for energy conservation is obtained:

$$\rho\frac{Dw^{stored}}{Dt} = \mathbf{D}\colon\sigma - \nabla\cdot\mathbf{q} + \rho I \tag{166}$$

If heat flux, $\mathbf{q}$, and heat generation, I, are neglected, the conservation of energy no longer appears as a PDE:

$$\rho\frac{Dw^{stored}}{Dt} = \mathbf{D}\colon\sigma \tag{167}$$

the scalar product of the Cauchy stress and the rate of deformation. Thus the change in internal power, per unit volume, due to stress and strain are described by the *power conjugate* quantities of Cauchy stress and the rate of deformation. The rate of change in the total stored energy within a body is obtained by integration over the domain:

$$\frac{DW^{int}}{Dt} = \int_{\Omega} \rho \frac{Dw^{stored}}{Dt} d\Omega = \int_{\Omega} \mathbf{D} \colon \sigma d\Omega = \int_{\Omega} D_{ij}\sigma_{ij} d\Omega = \int_{\Omega} \frac{\partial v_i}{\partial x_j}\sigma_{ij} d\Omega \tag{168}$$

The foregoing treatment of conservation laws within continuum mechanics can be brought closer to the nonlinear finite element context by beginning to introduce terminology that is more consistent with the finite element literature, and adopting mechanical response measures that are more suitable for for use in finite element formulations.

In the finite element literature, the name *Total Lagrangian* is usually assigned to referential context that is referred to as being, simply, *Langrangian* in the context of continuum mechanics. Thus, in a Total Lagrangian (TL) context, the independent variables in time and space are t and $\mathbf{X}$. Additionally, several important dependent quantities are the initial density, $\rho_o(\mathbf{X}, t)$, the displacement field, $\mathbf{u}(\mathbf{X}, t)$. Examples of other dependent quantities include the power conjugate pair PK1 stress $\mathbf{P}$ and the time rate of change in the deformation gradient $\dot{\mathbf{F}}$. It is pointed out that some authors (including Belytschko, Liu, and Moran) refer to the tensor $\mathbf{P}$ as the *nominal stress*, and subsequently refer to the PK1 stress as $\mathbf{P}^T$. This difference is largely academic, and thus the current treatment will persist in referring to $\mathbf{P}$ as the PK1 stress tensor.

With regard to external actions, the current treatment will denote tractions, that are measured within a Total Lagrangian (TL) reference frame, as $\mathbf{t}_o$. Similarly, for body forces the result $\rho_o\mathbf{b}$ furnishes the body force per unity initial volume of the body. Of course, the conservation of mass ensures that $\rho_o\mathbf{b} = \rho\mathbf{b}$ as demonstrated by the following:

$$d\mathbf{f} = \rho\mathbf{b}d\Omega = \rho\mathbf{b} \mid \mathbf{F} \mid d\Omega_o = \rho_o\mathbf{b}d\Omega_o \tag{169}$$

where $d\mathbf{f}$ is the resultant body force measured with respect to the reference configuration.

The linear momentum in the TL reference frame is thus able to be written as:

$$\mathbf{p}(t) = \int_{\Omega_o} \rho_o \mathbf{v}(\mathbf{X}, t)\, d\Omega_o \tag{170}$$

Consideration of the external actions within the TL leads to:

$$\mathbf{f}(t) = \int_{\Omega_o} \rho_o \mathbf{b}(\mathbf{X}, t)\, d\Omega_o + \int_{\Gamma_o} \mathbf{t}_o(\mathbf{X}, t)\, d\Gamma_o \tag{171}$$

Subsequent application of Newton's second law, $\frac{d\mathbf{p}}{dt} = \mathbf{f}$, leads to:

$$\frac{d}{dt}\int_{\Omega_o} \rho_o \mathbf{v} d\Omega_o = \int_{\Omega_o} \rho_o \mathbf{b} d\Omega_o + \int_{\Gamma_o} \mathbf{t}_o d\Gamma_o \tag{172}$$

Since the material domain in the TL formulation is static in time, Reynold's Transport Theorem is not needed, and thus the time derivative may be taken inside the integral in Equation (172), yielding:

$$\int_{\Omega_o} \rho_o \frac{\partial \mathbf{v}\left(\mathbf{X}, \mathbf{t}\right)}{\partial t} d\Omega_o = \int_{\Omega_o} \rho_o \mathbf{b} d\Omega_o + \int_{\Gamma_o} \mathbf{t}_o d\Gamma_o \tag{173}$$

The last term in Equation (173) may be transformed using Cauchy's Law and the Divergence Theorem:

$$\int_{\Gamma_o} \mathbf{t}_o d\Gamma_o = \int_{\Gamma_o} \mathbf{n}_o \cdot \mathbf{P} d\Gamma_o = \int_{\Omega_o} \nabla_o \cdot \mathbf{P} d\Omega_o \tag{174}$$

where ∇_o represents the gradient taken with respect to the TL reference frame. Substitution of Equation (174) into Equation (173) leads to:

$$\int_{\Omega_o} \left(\rho_o \frac{\partial \mathbf{v}\left(\mathbf{X}, t\right)}{\partial t} - \rho_o \mathbf{b} - \nabla_o \cdot \mathbf{P} \right) d\Omega_o = 0 \tag{175}$$

Exploiting the arbitrariness of the domain of integration leads to the PDE describing conservation of linear momentum in the TL reference frame:

$$\rho_o \frac{\partial \mathbf{v}\left(\mathbf{X}, t\right)}{\partial t} = \rho_o \mathbf{b} + \nabla_o \cdot \mathbf{P} \tag{176}$$

The conservation of energy follows in a similar manner.

Consider first a statement concerning the conservation of thermo-mechanical power in an arbitrary body, reckoned with respect to the initial configuration (*i.e.* adopting a TL reference frame):

$$\begin{aligned} \frac{d}{dt}\int_{\Omega_o} \left(\rho_o w^{stored} + \frac{1}{2}\rho_o \mathbf{v}\cdot\mathbf{v} \right) d\Omega_o = \int_{\Omega_o} \mathbf{v}\cdot\rho_o \mathbf{b} d\Omega_o + \int_{\Gamma_o} \mathbf{v}\cdot\mathbf{t}_o d\Gamma_o \\ + \int_{\Omega_o} \rho_o I d\Omega_o - \int_{\Gamma_o} \mathbf{n}_o \cdot \tilde{\mathbf{q}} d\Gamma_o \end{aligned} \tag{177}$$

The last term in Equation (177) represents the heat flux currently occurring into the body, but measured per unit area of the body in its initial state. The tilde is used to distinguish this heat flux from the earlier one, $\mathbf{q}$, taken with respect to the current configuration. A simple transformation is available for readily going between the two. This transformation takes as its point of departure the equivalence between the heat flux in the body at time t, as measured with respect

to the current domain boundary, Γ, and the same heat transfer, measured with respect to the surface of the body in its initial state:

$$\int_{\Gamma} \mathbf{n} \cdot \mathbf{q} d\Gamma = \int_{\Gamma_o} \mathbf{n}_o \cdot \tilde{\mathbf{q}} d\Gamma_o \tag{178}$$

By applying Equation (97) to Equation (178) the desired transformation is obtained:

$$\tilde{\mathbf{q}} = \mid \mathbf{F} \mid^{-1} \mathbf{F}^T \cdot \mathbf{q} \tag{179}$$

Returning to the consideration of Equation (177) leads to the recognition that since the domain of the integrand is fixed in time, the use of Reynold's Transport Theorem is not required, and thus the time derivative may be brought into the integrand:

$$\begin{aligned} &\frac{d}{dt} \int_{\Omega_o} \left(\rho_o w^{stored} + \frac{1}{2} \rho_o \mathbf{v} \cdot \mathbf{v} \right) d\Omega_o \\ &= \int_{\Omega_o} \left(\rho_o \frac{\partial w^{stored} \left(\mathbf{X}, t \right)}{\partial t} + \rho_o \mathbf{v} \cdot \frac{\partial \mathbf{v} \left(\mathbf{X}, t \right)}{\partial t} \right) d\Omega_o \end{aligned} \tag{180}$$

whereas the traction power term on the right hand side of Equation (177) can be modified using the definition of the PK1 stress, as well as the Divergence Theorem:

$$\begin{aligned} \int_{\Gamma_o} \mathbf{v} \cdot \mathbf{t}_o d\Gamma_o &= \int_{\Gamma_o} \mathbf{v} \cdot \left(\mathbf{n}_o \cdot \mathbf{P} \right) d\Gamma_o \\ &= \int_{\Omega_o} \nabla_o \cdot \left(\mathbf{v} \cdot \mathbf{P} \right) d\Omega_o \\ &= \int_{\Omega_o} \left(\frac{\partial v_j}{\partial X_i} P_{ij} + v_j \frac{\partial P_{ij}}{\partial X_i} \right) d\Omega_o \\ &= \int_{\Omega_o} \left(\frac{\partial F_{ji}}{\partial t} P_{ij} + \frac{\partial P_{ij}}{\partial X_i} v_j \right) d\Omega_o \\ &= \int_{\Omega_o} \left(\frac{\partial \mathbf{F}^T}{\partial t} : \mathbf{P} + \left(\nabla_o \cdot \mathbf{P} \right) \cdot \mathbf{v} \right) d\Omega_o \end{aligned} \tag{181}$$

Employing Equations (180) and (181) within Equation (177) results in (with an additional application of the Divergence Theorem):

$$\begin{aligned} &\int_{\Omega_o} \rho \frac{\partial w^{stored}}{\partial t} - \frac{\partial \mathbf{F}^T}{\partial t} : \mathbf{P} + \nabla_o \cdot \tilde{\mathbf{q}} - \rho_o I \\ &+ \left(\rho_o \frac{\partial \mathbf{v} \left(\mathbf{X}, t \right)}{\partial t} - \nabla_o \cdot \mathbf{P} - \rho_o \mathbf{b} \right) \cdot \mathbf{v} d\Omega_o = 0 \end{aligned} \tag{182}$$

where the term inside the parentheses is the Lagrangian form of the momentum equation (and thus it vanishes); leaving:

$$\int_{\Omega_o} \rho \frac{\partial w^{stored}}{\partial t} - \frac{\partial \mathbf{F}^T}{\partial t} : \mathbf{P} + \nabla_o \cdot \tilde{\mathbf{q}} - \rho_o I d\Omega_o = 0 \tag{183}$$

Furthermore, the recognition of the arbitrary nature involved in the specification of the domain of integration leads directly to the strong form statement of the energy conservation in a TL reference frame:

$$\rho_o \frac{\partial w^{int}(\mathbf{X}, t)}{\partial t} = \frac{\partial \mathbf{F}^T}{\partial t} : \mathbf{P} - \nabla_o \cdot \tilde{\mathbf{q}} + \rho_o I \tag{184}$$

or, in a slightly different notational presentation:

$$\rho_o \dot{w}^{int} = \dot{\mathbf{F}}^T : \mathbf{P} - \nabla_o \cdot \tilde{\mathbf{q}} + \rho_o I \tag{185}$$

It is observed from Equations (184) and (185) that the PK1 stress and the material time derivative of the deformation gradient are power conjugate to one another. It is further noted that:

$$\mathbf{D} : \sigma \mid \mathbf{F} \mid = \dot{\mathbf{F}}^T : \mathbf{P} \tag{186}$$

Discussion now shifts to the consideration of frame invariance, and its importance within the proper framing of constitutive theories.

1.1.7 Polar decomposition and frame invariance

A useful point of departure regarding any discussion on frame invariance involves the consideration of the *polar decomposition theorem*. This discussion complements the earlier treatment regarding rigid body rotations; wherein the rotation tensor, $\mathbf{R}$, was seen to be *orthogonal* (*i.e.* $\mathbf{R}^{-1} = \mathbf{R}^T$).

The statement of the polar decomposition theorem is straightforwardly posed as:

$$\mathbf{F} = \mathbf{R}\,\mathbf{U} \tag{187}$$

where is the tensor, $\mathbf{F}$, is the deformation gradient mapping a differential line segment in the reference configuration, $d\mathbf{X}$ into the equivalent differential line segment within current configuration, $d\mathbf{x}$. The tensor $\mathbf{U}$ is a symmetrical map that is alternately referred to as the *right stretch tensor*, or *stretch tensor*, for reasons that will become clear in the the sequel. However, a consideration of orthogonality and symmetry leads to the following observation:

$$\mathbf{F}^T\,\mathbf{F} = (\mathbf{R}\,\mathbf{U})^T\ (\mathbf{R}\,\mathbf{U}) = \mathbf{U}^T\,\mathbf{R}^T\,\mathbf{R}\,\mathbf{U} = \mathbf{U}\mathbf{U} \tag{188}$$

which enables the writing the down of $\mathbf{U}$ as:

$$\mathbf{U} = \left(\mathbf{F}^T\,\mathbf{F}\right)^{\frac{1}{2}} \tag{189}$$

It is pointed out that the stretch tensor, $\mathbf{U}$, is the symmetric map taking a the set of all vectors at a point into new vectors: with changed length, and also a rotation (except for the case of the subset of vectors coinciding with the principal directions of $\mathbf{U}$ - these experience stretching only). It is noticed that the operation of raising the tensor product $\left(\mathbf{F}^T\,\mathbf{F}\right)$ to the one half power involves

the transformation of the tensor product using its eigenvectors to arrive at the diagnolized form:

$$\mathbf{\Phi}^T \left(\mathbf{F}^T \mathbf{F}\right) \mathbf{\Phi} = \lambda_{ii}\mathbf{I} \tag{190}$$

The diagonal terms of the tensor resulting from the transformation described in Equation (190) are then raised to the one half power, and the resulting matrix subjected to the inverse transformation to yield the results described by Equation (189). The inverse transformation is always available, as the the symmetric tensor $\mathbf{U}$ is positive definite. It is noted that the quantity $\mathbf{U} - \mathbf{I}$ is sometimes called the *Biot strain tensor*.

Discussion now shifts to the topic of frame invariance; a point which can be motivated through the consideration of the linear hypoelastic material response:

$$\frac{D\sigma}{Dt} = \mathbf{C}^{\sigma D} : \mathbf{D} \tag{191}$$

The inappropriateness of this material law for use in the cases of large rotations is easily observed through a thought experiment. Consider a 2D truss element that is prestressed while it is aligned with one axis of a Cartesian reference frame. If the truss is rotated as a *rigid body*, in order that its alignment now coincides with the orthogonal axis, then it is expected that the rate of deformation, $\mathbf{D}$, must vanish but the components of the Cauchy stress tensor must be different in order to express the fact that the locked in prestress is now pointing in a direction that is orthogonal to its initial position. Thus we can observe that the hypoelastic material law will not serve as a suitable constitutive relation for use with large rotations. The present discussion now shifts to the development of suitable rates for the foregoing, and other more general, scenarios.

Consider the case of the *Jaumann rate*. The Jaumann rate of the Cauchy stress leads to an objective constitutive relation that accounts for issues like the one mentioned in the previous paragraph. The form of the Jaumann rate takes the form:

$$\sigma^{\nabla J} = \frac{D\sigma}{Dt} - \mathbf{W}\,\sigma - \sigma\,\mathbf{W}^T \tag{192}$$

where Equation (192) makes use of the material time derivative of the Cauchy stress tensor, in addition to the spin tensor $\mathbf{W}$ from Equation (21). Also in Equation (192), the superscript, ∇, denotes an objective rate, while the superscript, J, describes it as the Jaumann rate. A simple rearranging of terms leads to an objective description of the constitutive relation sought by Equation (191):

$$\frac{D\sigma}{Dt} = \sigma^{\nabla J} + \mathbf{W}\,\sigma + \sigma\,\mathbf{W}^T \tag{193}$$

which can be re-expressed as the sum of a *material term* and a *rotational term* as:

$$\frac{D\sigma}{Dt} = \mathbf{C}^{\sigma J} : \mathbf{D} + \mathbf{W}\,\sigma + \sigma\,\mathbf{W}^T \tag{194}$$

wherein $\mathbf{C}^{\sigma J}$: $\mathbf{D}$ is the Jaumannian form of the objective hypoelastic constitutive relation, and $\mathbf{W}\ \sigma + \sigma\ \mathbf{W}^T$ accounts for the influence of rotation. Other objective rates are also available: the *Truesdell rate* and the *Green-Nagdi rate*.

1.2 Review of strong forms, weak forms, and topics from mathematics

It is very useful to review fundamental mathematical terminology and notions as the present treatment begins shifting to the development of the governing nonlinear finite element equations. Discussions commences with useful definitions from *set theory*.

1.2.1 Concepts from set theory

A *set* is any well defined collection of objects. These individual objects, within the set, are called *elements*. Consider an element, a, from within a set A:

$$a \in A \tag{195}$$

As an example of the notion of a set, consider the set of all positive integers that are smaller than 100:

$$Z = \{x\colon x \in \mathbb{Z}, 0 < x < 100\} \tag{196}$$

Additionally, the set of all positive integers that is smaller than 50, and larger than 1 is:

$$W = \{y\colon y \in \mathbb{Z}, 1 < y < 50\} \tag{197}$$

Furthermore, W is observed to be contained within Z; and thus W is termed a *subset* of Z:

$$W \subset Z \tag{198}$$

It is pointed out that any set is a subset of itself; while a proper subset is a subset that contains fewer elements than the set to which it is a subset.

The *union* of two sets is written as $A \cup B$, and defined as:

$$A \cup B = \{x\colon x \in A \text{ or } x \in B\} \tag{199}$$

whereas the intersection of two sets is written as $A \cap B$, and defined as:

$$A \cap B = \{x\colon x \in A \text{ and } x \in B\} \tag{200}$$

The concepts of *open* and *closed sets* is likewise important; and subsequently treated.

An example of a neighborhood is given in the consideration of any point k on the real line, $\mathbb{R}$, wherein a positive constant, ϵ, is defined. The neighborhood of c is defined as an open interval:

$$(c-\epsilon, c+\epsilon) = \{k\colon c-\epsilon < k < c+\epsilon\} \tag{201}$$

where the points, k, are referred to as *interior points*. The *closure* of the *open interval* that defines the neighborhood in Equation (201) is the union of the interior points and the points on the boundary of the interval:

$$[c-\epsilon, c+\epsilon] = \{k\colon c-\epsilon \leq k \leq c+\epsilon\} \tag{202}$$

1.2.2 Concepts from functional analysis

Consider a set of functions that are well defined. This set is referred to as a *function space*. An element of this function space is said to be *integrable* on some *measurable set*, Ω, *iff*:

$$\int_{\Omega} |f| d\Omega < \infty, \quad \forall f \in F \tag{203}$$

where F is the function space in question. The space of *square integrable* functions is defined as:

$$L^2(\Omega) = \{u\colon \int_{\Omega} |u|^2 d\Omega < \infty\} \tag{204}$$

It is interesting to observe that:

$$L^{\infty}(\Omega) \subset \cdots \subset L^p(\Omega) \subset \cdots \subset L^1(\Omega) \tag{205}$$

Furthermore, it is noticed that the space of continuous functions, $C(\Omega)$, is not a subspace of any L^p; as the following illustration points out.

Consider a function $u(x) = \frac{1}{x}$; a member of $C(\Omega)$ in the *open interval* $(0,1)$. It is clear that while $u(x) \in C(0,1)$, $u(x) \notin L^{\infty}(0,1)$ (which, in itself, is a subspace of all $L^p(0,1)$). However, if instead of focusing on the unbounded case of $u(x) = \frac{1}{x}$, the general case of *bounded* continuous functions is considered (denoted as $C(\bar{\Omega})$) then $C(\bar{\Omega}) \subset L^{\infty}(\Omega)$. In summary, it is pointed out that function spaces are simply sets of functions that behave in a precisely defined manner.

It turns out that the suggestive language of geometry (as related to the elementary school notion of a vector as a directed line segment) is useful and important in considering the properties of abstract function spaces. Indeed, any abstract function space may be considered as a vector space if it satisfies the following six axioms:

1. $\forall u, v \in X$ and $\alpha, \beta \in \mathbb{R}$ yields $\alpha u + \beta v \in X$
2. $u + v = v + u$ and $u + (v + w) = (u + v) + w \quad \forall u, v, w \in X$

3. $\exists\, 0 \in X \ni u + 0 = u \quad \forall u \in X$ (termed the *zero element*)
4. $\forall u \in X \;\exists\; -u \in X \ni u + (-u) = 0$; thus defining *vector differencing* as $u + (-v)$
5. $(\alpha\beta)\, u = \alpha\,(\beta u)\;\; \forall \alpha, \beta \in \mathbb{R}$ and $\forall u \in X$
6. $(\alpha + \beta)\, u = \alpha u + \beta u$ and $\alpha\,(u + v) = \alpha u + \alpha v,\;\; \forall \alpha, \beta \in \mathbb{R}$ and $\forall u, v \in X$

Examples of function spaces satisfying properties 1-6 include $C^m\,(\Omega)$, $L^P\,(\Omega)$, and $L^\infty\,(\Omega)$.

Recalling, once again, elementary mathematics, the *scalar product*, or *dot product* or *inner product*, was denote as $\mathbf{u}\cdot\mathbf{v}$; yielding a scalar quantity $|u||v|cos\,(\theta)$ (θ being the included angle between the intersecting directed line segments $\mathbf{u}$ and $\mathbf{v}$). More formally, and on a real vector space, X, the properties of an inner product are abstracted in the following four axioms: $\forall\, u, v, w \in X$ and $\alpha, \beta \in \mathbb{R}$ where $(\cdot, \cdot)$ denotes *inner product*

1. $(u, v) \in \mathbb{R}$ (*i.e.* it is a *scalar product*)
2. $(u, v) = (v, u)$; symmetry property
3. $(\alpha u + \beta v, w) = \alpha\,(u, w) + \beta\,(v, w)$; linearity property
4. $(u, u) \geq 0$ and $(u, u) = 0 \iff u = 0$; positive definiteness

The inner product applied to the usual Euclidean space, $\mathbb{R}^3$, and defined as $(\mathbf{x}, \mathbf{y}) = \mathbf{x}\cdot\mathbf{y} = x_1y_1 + x_2y_2 + x_3y_3$ satisfies the four previously specified properties of an inner product. Consider, now, the abstract function space $L^2\,(\Omega)$ on the open interval (a, b) (denoted as $L^2\,(a, b)$) which may be endowed with an inner product of the form:

$$(u, v) \equiv \int_a^b u\,(x)\, v\,(x)\, dx \quad \forall u, v \in L^2\,(a, b) \tag{206}$$

The notion of *orthogonality* in Euclidean space (where vectors are said to be orthogonal, or perpendicular, when $\mathbf{u} \cdot \mathbf{v} = 0$) may be abstracted, to any space endowed with an inner product, to mean that elements within the space are orthogonal when $(u, v) = 0$.

Continuing on with allusions to notions from elementary mathematics, consideration of the length of a directed line segment yields an analog for abstract vector spaces: the *norm*. An operation known as a norm, and denoted as $\|\cdot\|$ is defined on an abstract vector space, X, if the following four axioms are satisfied: $\forall u, v \in X$ and $\alpha \in \mathbb{R}$

1. $\|u\| \in \mathbb{R}$ (the norm is a scalar)
2. $\|u\| \geq 0$ and $\|u\| = 0 \iff u = 0$; positive definiteness

3. $\|\alpha u\| = |\alpha| \|u\|$; positive homogeneity
4. $\|u + v\| \leq \|u\| + \|v\|$; triangle inequality

An example of a discrete norm defined on $\mathbb{R}^n$ is:

$$\|x\|_{\ell^p} = \left(|x_1|^p + |x_2|^p + \cdots + |x_n|^p\right)^{\frac{1}{p}} \quad \forall x \in \mathbb{R}^n \tag{207}$$

while a continuous norm, defined on $L^P(\Omega)$ is:

$$\|u\|_{L^p} = \left[\int_\Omega \mid u \mid^p d\Omega\right]^{\frac{1}{p}} \quad \forall u \in L^p(\Omega) \tag{208}$$

Additionally, a so-called *sup-norm* may be defined on the space of bounded continuous functions (as a subspace of $L^\infty(\Omega)$):

$$\|u\|_{L^\infty} = \max_{x \in \bar{\Omega}} \mid u \mid \quad \forall u \in C\left(\bar{\Omega}\right) \tag{209}$$

In light of the foregoing, the notion of a *normed space* may be introduced as the vector space and the norm to be applied therein; denoted as $(X, \|\cdot\|)$, for example.

While the notion of a normed space is more general than that of an inner product space, all inner product spaces are normed spaces because the inner product may be used to define an operation that satisfies the four requirements of a norm. As an example, consider $\mathbf{u} \in \mathbb{R}^3$, wherein $\|\mathbf{u}\| = (\mathbf{u} \cdot \mathbf{u})^{\frac{1}{2}}$, or more generally, consider an arbitrary function belonging to an inner product space, then a norm may defined for this space as: $\|u\| = (u, u)^{\frac{1}{2}}$.

Interestingly, when abstracting the elementary notion of length assigned to a directed line segment, and having the form $d(x, y) = \sqrt{(x_1 - y_1)^2 + (x_2 - y_2)^2 + (x_3 - y_3)^2}$, to abstract function spaces, there becomes no need to have these be vector spaces (as was required in the case of normed and inner product spaces). All that is required of the *metric space* is that it admit an operation having the properties that: $\forall u, v, w \in X$ (where X is a metric space)

1. $d(u, v) \geq 0$ and $d(u, v) = 0 \iff u = v$
2. $d(u, v) = d(v, u)$ (the operation is symmetric)
3. $d(u, w) \leq d(u, v) + d(v, w)$ (triangle inequality)

Since in nonlinear finite element analysis inner product spaces are normally considered, it is convenient to generate metrics using norms; as in:

$$d(u, v) = \|u - v\| \tag{210}$$

These concepts are behind what motivates the integral equations that are at the heart of the nonlinear finite element method.

Consider some arbitrary partial differential equation (PDE), represented as $\mathcal{L}(u(\mathbf{x})) = 0$, $\forall \mathbf{x} \in \Omega$, and where $\mathcal{L}(\cdot)$ is some differential operator defined on some inner product space Ω. If instead of the solution $u(\mathbf{x})$ (that satisfies the PDE exactly), an approximate solution, $\hat{u}(\mathbf{x})$ is considered, then there will be some error in the solution; in that the right hand side of the PDE will not be strictly zero. This error is termed the *residual*, and thus defined as $\mathcal{R} = \mathcal{L}(\hat{u}(\mathbf{x}))$.

In the nonlinear finite element method, the approximate solution is frequently a lower dimensional representation of the actual solution, that lives in some inner product space. A cartoon of this relationship may be given in terms of $\mathbb{R}^3$; where $\mathbb{R}^3$ represents the inner product space where the exact solution appears as a point. The subspace where a specific class of lower order approximate solutions live may be conceived of as a plane within $\mathbb{R}^3$.

Each of the individual approximate solutions within the given sub-space possesses an accompanying residual (in comparison with the exact solution $u(\mathbf{x})$). Since the exact solution space is an inner product space (and thus, also, a vector space) then the residual appears as a directed line segment connecting the point of a given approximate solution (lying on the plane) with the exact solution (appearing as a point within $\mathbb{R}^3$). In the case of the smallest residual (*i.e.* best approximation), this vector should be smaller than any other associated vectors from within the given class of approximate solutions. One way of thinking about this is that the smallest residual vector would be the one that is normal to the subspace of the approximate solutions (*i.e.* the perpendicular distance is the closest that any arbitrary point in $\mathbb{R}^3$ can be to a flat plane within the same space).

More formally, the foregoing notions regarding the best approximate solution may be treated through the consideration of a space, $\mathcal{V}$, where the exact solution $u(\mathbf{x})$ lives. Denoting the subspace where the approximate solutions, $\hat{u}(\mathbf{x})$, lives, as $\mathcal{V}_h$, the objective in the nonlinear finite element method is to find:

$$\hat{u}(\mathbf{x}) \in \mathcal{V}_h \ni \int_\Omega v\left(\mathcal{L}\left(\hat{u}(\mathbf{x})\right)\right) d\Omega = 0 \quad \forall v \in \mathcal{V}_h,\ \forall \mathbf{x} \in \Omega \tag{211}$$

where the integral in Equation (211) is an inner product; thus leading to the orthogonality condition described in the foregoing. Indeed, Equation (211) is the prototypical form of the *weighted residual* statement of the problem with the governing PDE $\mathcal{L}(u(\mathbf{x})) = 0$; although the subspace $\mathcal{V}_h$ must be much more carefully defined.

In keeping with a numerical implementation, the discrete form of the approximate solution:

$$\hat{u}(\mathbf{x}) = u_i N_i(\mathbf{x}) \tag{212}$$

is considered in the sequel. Specifically, the $N_i(\mathbf{x})$ are the so-called finite element *basis functions*, and the u_i are the primary unknowns pursued in the finite

element solution. The finite element method uses the prototypical weighted residual formulation presented in Equation (211) to pursue an approximate solution to some governing PDE. Indeed, the finite element solution finds the best approximation to the actual solution, from within a given subspace. In the case of the approximate solution described by Equation (212), $i = 1, 2, \ldots dim\left(\mathcal{V}_h\right)$, and $\mathcal{V}_h = span\left(N_i\right)$. It is further pointed out that the approximate solution of Equation (212) must satisfy the homogeneous *essential* (or *Dirichlet*) boundary conditions associated with the boundary value problem in question; the *natural* (or *Neumann*) boundary conditions will be seen to be implied in the integral statement itself. Other than essential homogeneous boundary conditions will be treated later in this section.

While the generic form of Equation (211) is consistent with the so-called *weighted residual* form of the problem at hand, the specific case described by Equation (211) is known more precisely as a *Galerkin projection*. This is the case since the function v (known as the *test function*) and the function $\hat{u}$ (known as the *trial function*) live in the same space, $\mathcal{V}_h$.

It is instructive to apply the foregoing to a simple one dimensional example boundary value problem:

$$\begin{aligned} u''\left(\mathbf{x}\right) + f\left(\mathbf{x}\right) &= 0, \quad \forall x \in \Omega = \mathbb{R}\left(0,1\right) \\ u\left(0\right) &= 0 \\ u'\left(1\right) &= \beta \end{aligned} \tag{213}$$

Employing a trial solution of the form provided in Equation (212) results in a residual appearing as:

$$\mathcal{R}\left(\mathbf{x}\right) = f\left(\mathbf{x}\right) + N_i''\left(\mathbf{x}\right) u_i \tag{214}$$

since:

$$\begin{aligned} \hat{u}\left(\mathbf{x}\right) &= N_i\left(\mathbf{x}\right) u_i \\ \hat{u}'\left(\mathbf{x}\right) &= \frac{dN_i\left(\mathbf{x}\right)}{d\mathbf{x}} u_i + \frac{du_i}{d\mathbf{x}} N_i\left(\mathbf{x}\right) = N_i'\left(\mathbf{x}\right) u_i \\ \hat{u}''\left(\mathbf{x}\right) &= \frac{dN_i'\left(\mathbf{x}\right)}{d\mathbf{x}} u_i + \frac{du_i}{d\mathbf{x}} N_i'\left(\mathbf{x}\right) = N_i''\left(\mathbf{x}\right) u_i \end{aligned} \tag{215}$$

The Galerkin form of the weighted residual statement for the problem in Equation (213) then becomes:

$$\begin{aligned} \int_0^1 N_j\left(\mathbf{x}\right)\left(N_i''\left(\mathbf{x}\right) u_i + f\left(\mathbf{x}\right)\right) dx = 0 \quad i,j = 1 \ldots M \\ -\int_0^1 N_j\left(\mathbf{x}\right) N_i''\left(\mathbf{x}\right) u_i \, dx = \int_0^1 N_j\left(\mathbf{x}\right) f\left(\mathbf{x}\right) dx \end{aligned} \tag{216}$$

As it is that the *integration by parts* formula will be useful in the foregoing, it

is briefly re-derived from the *product rule* of elementary calculus:

$$\frac{d\left(uv\right)}{dx} = \frac{du}{dx}v + \frac{dv}{dx}u$$
$$\int_a^b \frac{d\left(uv\right)}{dx}dx = \int_a^b \frac{du}{dx}vdx + \int_a^b \frac{dv}{dx}udx$$
$$\int_a^b u\frac{dv}{dx}dx = uv\mid_a^b - \int_a^b v\frac{du}{dx}dx \tag{217}$$

Applying the familiar form in the final line of Equation (217) to the left hand side of Equation (216) yields:

$$u \equiv N_j\left(\mathbf{x}\right) \quad dv \equiv N_i''\left(\mathbf{x}\right)$$
$$du \equiv N_j'\left(\mathbf{x}\right) \quad v \equiv N_i'\left(\mathbf{x}\right)$$
$$\int_0^1 N_j\left(\mathbf{x}\right)\left(N_i''\left(\mathbf{x}\right)\right)u_i\,dx = N_j\left(\mathbf{x}\right)N_i'\left(\mathbf{x}\right)u_i\mid_0^1 - \int_0^1 N_j'\left(\mathbf{x}\right)N_i'\left(\mathbf{x}\right)u_i\,dx \tag{218}$$

Subsequently substituting the foregoing into Equation (216) yields:

$$\int_0^1 N_j'\left(\mathbf{x}\right)N_i'\left(\mathbf{x}\right)u_i\,dx = N_j\left(1\right)\hat{u}'\left(1\right) - N_j\left(0\right)\hat{u}'\left(0\right) + \int_0^1 N_j\left(\mathbf{x}\right)f\left(\mathbf{x}\right)dx \tag{219}$$

which is subsequently recognized as being:

$$\int_0^1 N_j'\left(\mathbf{x}\right)N_i'\left(\mathbf{x}\right)u_i\,dx = N_j\left(1\right)\beta + \int_0^1 N_j\left(\mathbf{x}\right)f\left(\mathbf{x}\right)dx \tag{220}$$

It is pointed out that the terms $N\left(0\right)$ vanishes on account of our selection of shape functions that satisfy the problem's Dirichlet boundary conditions. Interestingly, the Neumann conditions arose as a natural consequence of the application of integration by parts formula. Thus it can be said that the Neumann conditions are implied in the integral statement of the problem.

When considering other than homogeneous Dirichlet boundary conditions, it is convenient to stipulate a slight difference between the space of trial and test functions. At this point, too, it is useful to add some additional precision to the definition of these spaces.

It continues to be true that the test functions might only satisfy the homogeneous case of the Dirichlet boundary condition (it turns out that this will lead to more convenient mathematical forms, after the integration by parts), but in the case of the trial functions, the exact Dirichlet conditions of the problem (homogeneous or not) must be strictly satisfied; as is easily done by a superposition with a suitable function that assumes the correct values at the desired boundary locations:

$$\hat{u}\left(\mathbf{x}\right) = \psi\left(\mathbf{x}\right) + N_i\left(\mathbf{x}\right)u_i \tag{221}$$

Additionally, based on the integral form of Equation (220), that results from application of the integration by parts formula, it is noticed that the square of the first derivative of the shape function $N(\mathbf{x})$ is required to be integrated; along with the shape function by itself. This fact, coupled with the desire for the vanishing of the test functions on the problem boundary where Dirichlet conditions are imposed (for convenience), results in the need for two separate spaces. One for the trial functions:

$$\hat{u} \in H_{\psi}^{m}(\Omega) = \{u \colon D^{\alpha} u \in L^{2}(\Omega) \, \forall \alpha \ni |\alpha| < m \text{ and } u = \psi \text{ on } \partial\Omega\} \tag{222}$$

and one for the test functions:

$$v \in H_{o}^{m}(\Omega) = \{v \colon D^{\alpha} v \in L^{2}(\Omega) \, \forall \alpha \ni |\alpha| < m \text{ and } v = 0 \text{ on } \partial\Omega\} \tag{223}$$

where $2m$ is the highest derivative occurring within the governing PDE for the problem under investigation, D^{α} is the *weak partial derivative* of order α and below. However, as a practical matter, the superposition furnished in Equation (221) permits the test functions and finite element shape functions to be from the same space (Equation (223)); with ψ being used to then satisfy the required Dirichlet conditions as a result of the superposition. As a result, the application of the Galerkin method, within the nonlinear finite element context, draws its finite element shape functions (for use as test functions, and for the interior portion of the trial functions) from the space of functions H_{o}^{m}.

The foregoing general notions may be applied, as an illustration, to an n-dimensional diffusion problem; given as:

$$\begin{aligned} -\nabla \cdot (k(\mathbf{x}) \nabla u(\mathbf{x})) &= f(\mathbf{x}), \quad \forall \mathbf{x} \in \Omega \subset \mathbb{R}^{n} \\ -k(\mathbf{x}) \nabla u(\mathbf{x}) \cdot \mathbf{n} &= g(\mathbf{x}), \quad \forall \mathbf{x} \in \partial\Omega_{N} \\ u(\mathbf{x}) &= \psi(\mathbf{x}), \quad \forall \mathbf{x} \in \partial\Omega_{E} \end{aligned} \tag{224}$$

where $u(\mathbf{x})$ is being sought over a domain, Ω, with a boundary $\partial\Omega = \partial\Omega_{N} \cup \partial\Omega_{E}$; where $\partial\Omega_{N}$ and $\partial\Omega_{E}$ are non-overlapping (*i.e.* $\partial\Omega_{N} \cap \partial\Omega_{E} = \emptyset$). $g(\mathbf{x})$, $f(\mathbf{x})$, and $\psi(\mathbf{x})$ are known functions. In applying an approximate solution of the form $\hat{u}(\mathbf{x}) = \psi(\mathbf{x}) + N_{i}(\mathbf{x}) u_{i}$, the Galerkin weak form of the problem may be pursued.

Commencing with the construction of a weighted residual statement, it follows that:

$$\int_{\Omega} W_{i}(\mathbf{x}) \left(-\nabla \cdot (k(\mathbf{x}) \nabla \hat{u}(\mathbf{x})) - f(\mathbf{x})\right) d\Omega = 0 \tag{225}$$

At this point, it is now useful to introduce the n-dimensional form of the integration by parts formula, known as *Green's Lemma*:

$$-\int_{\Omega} \nabla \cdot (\nabla u) \, v_{i} \, d\Omega = \int_{\Omega} \nabla u \cdot \nabla v_{i} \, d\Omega - \int_{\partial\Omega} v_{i} \nabla u \cdot \mathbf{n} \, d(\partial\Omega) \tag{226}$$

Green's Lemma may be applied to the first term within the parentheses of the integrand given in Equation (225):

$$-\int_{\Omega}\left(\nabla\cdot\left(k\left(\mathbf{x}\right)\nabla\hat{u}\left(\mathbf{x}\right)\right)\right)W_i\left(\mathbf{x}\right)d\Omega=\int_{\Omega}k\left(\mathbf{x}\right)\nabla\hat{u}\left(\mathbf{x}\right)\cdot\nabla W_i\left(\mathbf{x}\right)d\Omega - \int_{\partial\Omega}W_i\left(\mathbf{x}\right)k\left(\mathbf{x}\right)\nabla\hat{u}\left(\mathbf{x}\right)\cdot\mathbf{n}\,d\left(\partial\Omega\right) \quad (227)$$

thus leading to an expanded weak form:

$$\int_{\Omega}k\left(\mathbf{x}\right)\nabla\hat{u}\left(\mathbf{x}\right)\cdot\nabla W_i\left(\mathbf{x}\right)d\Omega=\int_{\Omega}W_i\left(\mathbf{x}\right)f\left(\mathbf{x}\right)d\Omega + \int_{\partial\Omega}W_i\left(\mathbf{x}\right)k\left(\mathbf{x}\right)\nabla\hat{u}\left(\mathbf{x}\right)\cdot\mathbf{n}\,d\left(\partial\Omega\right) \quad (228)$$

Substituting the expanded approximate solution, $\hat{u}\left(\mathbf{x}\right)$, into the foregoing, and employing Galerkin's method (*i.e.* $W_i\left(\mathbf{x}\right)=N_i\left(\mathbf{x}\right)$), yields:

$$\int_{\Omega}k\left(\mathbf{x}\right)\nabla N_i\left(\mathbf{x}\right)\cdot\nabla N_j\left(\mathbf{x}\right)u_j\,d\Omega=\int_{\Omega}f\left(\mathbf{x}\right)N_i\left(\mathbf{x}\right)d\Omega + \int_{\partial\Omega}N_i\left(\mathbf{x}\right)k\left(\mathbf{x}\right)\nabla\hat{u}\left(\mathbf{x}\right)\cdot\mathbf{n}\,d\left(\partial\Omega\right) - \int_{\Omega}k\left(\mathbf{x}\right)\nabla N_i\left(\mathbf{x}\right)\cdot\nabla\psi\left(\mathbf{x}\right)d\Omega \quad (229)$$

where use has been made of the essential boundary condition in the last integral. Similarly, the Neumann condition may be applied to the second to last integral; resulting in:

$$\int_{\Omega}k\left(\mathbf{x}\right)\nabla N_i\left(\mathbf{x}\right)\cdot\nabla N_j\left(\mathbf{x}\right)u_j\,d\Omega=\int_{\Omega}f\left(\mathbf{x}\right)N_i\left(\mathbf{x}\right)d\Omega - \int_{\partial\Omega_N}g\left(\mathbf{x}\right)N_i\left(\mathbf{x}\right)d\left(\partial\Omega\right) - \int_{\Omega}k\left(\mathbf{x}\right)\nabla N_i\left(\mathbf{x}\right)\cdot\nabla\psi\left(\mathbf{x}\right)d\Omega \quad (230)$$

1.3 Review of isoparametric finite element formulations

In many practical applications of the finite element method it is a non-trivial matter to arrive at the form of the set of finite element basis functions, N_i, that are spatially, globally defined within a given problem domain, Ω, and that span the solution space of interest. Further complicating the matter is that these basis functions must vanish at the locations where Dirichlet conditions are to be imposed; while at the same time being nearly orthogonal to one another (to avoid ill-conditioning during computational implementation). As a result, it is natural to consider a given problem domain, Ω, as comprising pairwise disjoint subsets, A_i (*i.e.* $A_i\cap A_j=\emptyset\quad\forall i,j=1,2,\ldots\ni j\neq i$), known as a

partition of Ω. Assuming that $\Omega \subseteq \bigcup_i A_i$, then the partition also is a *cover* of Ω. The partition associated with such a cover is what is meant when referring to the *mesh* defined on a given problem domain. The mesh provides a convenient framework within which a computationally expedient approach to the finite element method may be conceived. It is pointed out that the requirement of disjointedness only holds for the classical *h-method*; overlapping covers are admissible within the more general finite element approaches such as: *GFEM, Xfem, PU-FEM, hp clouds, etc.* For now, the discussion will be restricted to the classical h-method.

Given a mesh, comprised of what are referred to as *elements*, the goal becomes one of finding simple polynomial shape functions, h_i (defined over individual elements), such that they may be used to form global finite element basis functions, N_i, that vanish over most elements, except for a local patch that shares a specific node. In this way, the enforcing of Dirichlet conditions is simplified, and *bandedness* of the system matrix is enhanced (more will be said about this later).

In pursuit of such an approach, a *partition of unity* is typically adopted as the paradigm governing the selection of the finite element shape functions, h_i. For convenience and computational expediency, these functions are typically polynomials. Additionally, in keeping with the requirement that the global finite element basis functions be non-zero over only small patches of elements within the mesh, the notion of a partition of unity is adopted; where the support for the partition is restricted to the set of elements sharing a given node. This means that the local finite element shape functions must behave as a Kronecker delta when constituting a local approximation, $\hat{u}$, to a solution, u:

$$\hat{u}_i = h_j\left(x_i\right) u_j = \delta_{ij} u_j \approx u_i \tag{231}$$

As will be seen later, this results in the unknown coefficients of the finite element shape functions being the actual field values of the unknown function being sought through the finite element method. Additionally, in the case of an *isoparametric* finite element formulation, the local finite element shape functions, h_i, are also used to interpolate the element geometric coordinates; as well as the field variables.

Within the isoparametric approach, it is frequently convenient to conceive of a *parent element*, of simple and regular geometry, that may serve as an archetype for all finite elements of such type, that occur within a given mesh. In this way, shape functions, and the inverse and determinant of a *Jacobian* involving the same, are employed to map the parent element into an actual finite element within a mesh that covers the problem domain of interest. A very simple example of this concept occurs in the consideration of a 2-D linear truss finite element (depicted in Figure 2).

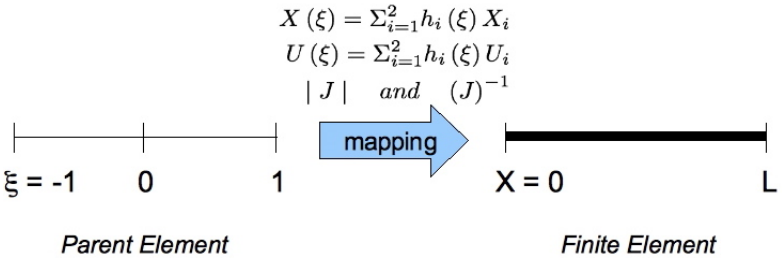

Figure 2: Isoparametric truss

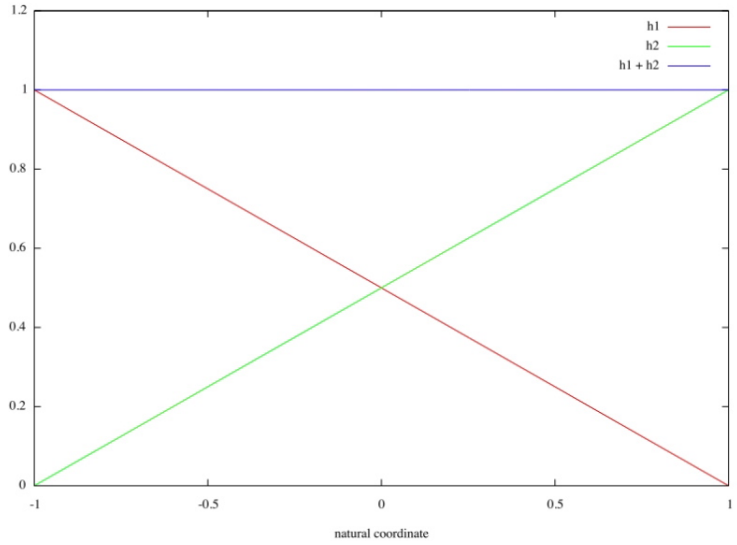

Figure 3: Isoparametric truss finite element linear shape functions

The parent element for the current 2-D linear truss element appears on the left side of Figure 2. The following discussion will serve as an example regarding the mapping of the parent element onto the actual problem domain (appearing on the right side of Figure 2). The local, or *natural*, coordinates are denoted by ξ, and so the following finite element shape functions are used in the current formulation (as a result of their obvious satisfaction of the partition of unity requirement: see Figure 3.)

$$h_1(\xi) = \frac{1}{2}(1-\xi) \tag{232}$$

$$h_2(\xi) = \frac{1}{2}(1+\xi) \tag{233}$$

Using these finite element shape functions, it is possible, within the isoparametric element approach, to interpolate both the physical problem coordinates,

X, and field variables, **U** (in the case of a 2D truss element, these are simply the member end displacements). In the case of each component of the interpolated physical coordinates, the following relation holds for an individual element:

$$X(\xi) = \Sigma_{i=1}^{2} h_i(\xi) X_i \tag{234}$$

where X_i are the *nodal coordinates* (measured with respect to the coordinates employed within the physical problem domain) associated with each of the individual member ends; and

$$U(\xi) = \Sigma_{i=1}^{2} h_i(\xi) U_i \tag{235}$$

where U_i are the *nodal displacements* (with respect to the coordinate of the physical system) associated with the member ends. As Equations (234) and (235) show, it is only the finite element shape function that has a spatial dependence (the nodal values of the coordinates and displacement components are constants). Thus, when considering a treatment of strains, within the isoparametric finite element formulation, the following approach is adopted.

Consider an application of the chain rule to the case of uniaxial strain; as it applies to the case depicted in Figure (2):

$$\epsilon = \frac{dU}{d\xi}\frac{d\xi}{dX} \tag{236}$$

A focus on a uniaxial state of stress permits the consideration of a scalar displacement field, in terms of the two individual members ends, denoted as U_i where i ranges from one to two (in the case of Figure (2)):

$$\frac{dU}{d\xi} = \frac{U_2 - U_1}{2} \tag{237}$$

As similar consideration of the displacements leads to:

$$\frac{dX}{d\xi} = \frac{X_2 - X_1}{2} = \frac{L}{2} \tag{238}$$

A substitution of Equations (238) and (237) into Equation (236) leads to the intuitive result that:

$$\epsilon = \frac{U_2 - U_1}{L} \tag{239}$$

It is common practice, within applications of the finite element method to solids and structures, to define a *strain-displacement matrix*; given as:

$$\epsilon = \mathbf{B}\mathbf{U} \tag{240}$$

In terms of the example truss problem, considered in Figure (2), the strain-displacement matrix takes the form (in light of Equation (239)):

$$\mathbf{B} = \frac{1}{L}\begin{bmatrix} -1 & 1 \end{bmatrix} \tag{241}$$

Consistent with the weak form of the governing equations obtained for the 1-D system associated with Equation (220), the so-called *stiffness matrix* may be formed by a consideration of the right hand side of Equation (220), and the subsequent application of Equation (241):

$$\begin{aligned}\mathbf{K} &= \int_{\Omega_\xi} J^{-1}\frac{dh(\xi)}{d\xi}\,\mathbf{C}\,J^{-1}\frac{dh(\xi)}{d\xi}\mid J\mid d\Omega_\xi \\ &= \int_{\Omega_\xi}\mathbf{B}^T\mathbf{C}\mathbf{B}\mid J\mid d\Omega_\xi \\ &= \frac{AE}{L^2}\int_{-1}^{1}\left[\begin{array}{c}-1\\1\end{array}\right]\left[\begin{array}{cc}-1 & 1\end{array}\right]\mid J\mid d\xi\end{aligned} \tag{242}$$

The use of the determinant of the Jacobian, $\mid J \mid$, is motivated by a consideration of Equation (36); wherein the isoparametric mapping described in Figure (2) serves as an equivalent "deformation." In the case of the 1-D isoparametric truss element formulation, the jacobian determinant volume map takes the form:

$$A\,dX = \mid J \mid A\,d\xi \tag{243}$$

whereupon Equation (238) may be applied to yield:

$$\mid J \mid = \frac{L}{2} \tag{244}$$

An application of Equation (244) to Equation (242) allows for the statement of the explicit form of the isoparametric truss stiffness matrix (given in global, problem coordinates):

$$\mathbf{K} = \frac{AE}{L}\left[\begin{array}{cc}1 & -1\\-1 & 1\end{array}\right] \tag{245}$$

where A is the truss cross-sectional area and E is the modulus of elasticity (as a specialization of the more general constitutive tensor $\mathbf{C}$).

A variation on the example problem from Equation (213) will now be used to demonstrate a useful means for treating the presence of Dirichlet conditions in the finite element system:

$$\begin{aligned}u''(\mathbf{x}) + f(\mathbf{x}) = 0, \quad \forall x \in \Omega = \mathbb{R}(0,L)\\ u(0) = u_L\\ u(L) = u_R\end{aligned} \tag{246}$$

The corresponding weak form that is integrated over the parent element and mapped onto the finite element in the physical problem space is:

$$\int_{-1}^{1} J^{-1}\nabla h_i(\xi)\cdot J^{-1}\nabla h_j(\xi)\mid J\mid d\xi = \int_{-1}^{1}\tilde{f}(\xi)\,h_i(\xi)\mid J\mid d\xi \tag{247}$$

where $\tilde{f}(\xi)$ is the simultaneous mapping of $f(x)$ into the local coordinates, and its subsequent restriction to a particular parent element domain. It is observed that the left hand side of Equation (246) is identical to the stiffness matrix, $\mathbf{K}$, from Equation (242). It is noted that in the general finite element literature (*i.e.* not restricted to solids and structures), it not uncommon to have the term denoted as A, and thus:

$$A_{ij}(\xi) = \int_{-1}^{1} J^{-1}\nabla h_i(\xi) \cdot J^{-1}\nabla h_j(\xi) \mid J \mid d\xi \tag{248}$$

Additionally, the forcing term from the right hand side of Equation (246) is similarly denoted by b:

$$b_i(\xi) = \int_{-1}^{1} \tilde{f}(\xi)\, h_i(\xi) \mid J \mid d\xi \tag{249}$$

Assuming the validity of the finite element shape functions given in Equations (232) and (233), integration of Equation (248) yields:

$$\mathbf{A} = \frac{1}{L}\begin{bmatrix} 1 & -1 \\ -1 & 1 \end{bmatrix} \tag{250}$$

Similarly, Equation (249) can be integrated to yield:

$$\mathbf{b} = \frac{L}{2}\begin{bmatrix} \tilde{f}_{(-1)} \\ \tilde{f}_{(1)} \end{bmatrix} \tag{251}$$

where $\tilde{f}_{(-1)}$ and $\tilde{f}_{(1)}$ are the values of $\tilde{f}(\xi)$; evaluated at the parent element ends.

The complete system associated with the components furnished in Equations (250) and (251) appears as:

$$\begin{bmatrix} \frac{1}{L} & -\frac{1}{L} \\ -\frac{1}{L} & \frac{1}{L} \end{bmatrix}\begin{bmatrix} u_{(-1)} \\ u_{(1)} \end{bmatrix} = \frac{L}{2}\begin{bmatrix} \tilde{f}_{(-1)} \\ \tilde{f}_{(1)} \end{bmatrix} \tag{252}$$

Incorporation of the first of the Dirichlet conditions from Equation (246) (for the purposes of illustration) can be handled straightforwardly as:

$$\begin{bmatrix} 1 & 0 \\ -\frac{1}{L} & \frac{1}{L} \end{bmatrix}\begin{bmatrix} u_{(-1)} \\ u_{(1)} \end{bmatrix} = \begin{bmatrix} u_L \\ \frac{L}{2}\tilde{f}_{(1)} \end{bmatrix} \tag{253}$$

However, it is noticed that the approach described in Equation (253) destroys the symmetry in the system; an important characteristic to preserve for efficiency when dealing with large systems of equations. A simple way to correct this problem rests in a simple algebraic trick: taking the product of the specified quantity multiplied by the column in the stiffness matrix where its influence is felt, during the matrix multiplication operation, and subsequently subtracting this column matrix from the right hand side of Equation (252) (*i.e.* the b term);

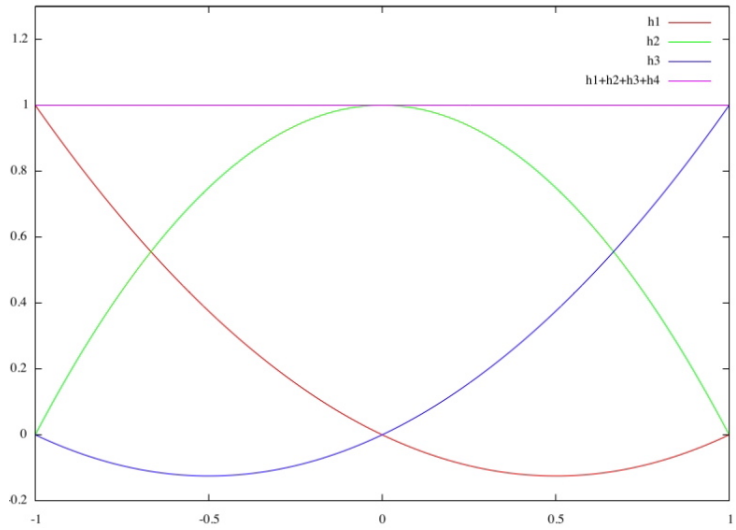

Figure 4: Isoparametric truss finite element quadratic shape functions

once again setting the required row entries to correspond with the prescribed values (as in Equation (253). This approach is applied to the example problem as:

$$\begin{bmatrix} 1 & 0 \\ 0 & \frac{1}{L} \end{bmatrix} \begin{bmatrix} u_{(-1)} \\ u_{(1)} \end{bmatrix} = \begin{bmatrix} u_L \\ \frac{L}{2}\tilde{f}_{(1)} + \frac{1}{L}u_L \end{bmatrix} \tag{254}$$

whereas the actual system (properly specialized for the complete set of Dirichlet conditions furnished in Equation (246) appears as:

$$\begin{bmatrix} 1 & 0 \\ 0 & 1 \end{bmatrix} \begin{bmatrix} u_{(-1)} \\ u_{(1)} \end{bmatrix} = \begin{bmatrix} u_L \\ u_R \end{bmatrix} \tag{255}$$

The foregoing example problem can be extended to consider the case of a three node parent element; in which case the finite element shape functions, h, would have the form:

$$h_1(\xi) = \frac{1}{2}\xi(\xi - 1) \tag{256}$$

$$h_2(\xi) = (1 + \xi)(1 - \xi) \tag{257}$$

$$h_3(\xi) = \frac{1}{2}\xi(1 + \xi) \tag{258}$$

which also satisfy the partition of unity requirement, as displayed in Figure (4).
The 1D finite element shape functions provided in Equations (232), (233) and (256) - (258) may be employed as building blocks for a general method of constructing higher dimensional finite element shape functions through the use of an analogy to the dyadic product introduced earlier in the notes as Equation (65).

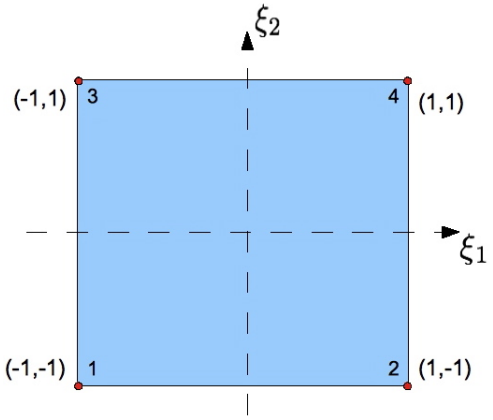

Figure 5: 2D parent element with four nodes

Consideration may now be given to the four node parent element provided in Figure (5). The required linear finite element shape functions for the formulation of such an element can be obtained using an approach modeled after the dyadic product. Consider a case where each of the four required finite element shape functions, $h_1(\xi_1,\xi_2), h_2(\xi_1,\xi_2), h_3(\xi_1,\xi_2)$, and $h_4(\xi_1,\xi_2)$, appear in a matrix form as:

$$\begin{bmatrix} h_1(\xi_1,\xi_2) & h_3(\xi_1,\xi_2) \\ h_2(\xi_1,\xi_2) & h_4(\xi_1,\xi_2) \end{bmatrix} \tag{259}$$

Such a case could have been arrived at using the open product (*i.e.* dyadic product) of two column matrices as:

$$\begin{bmatrix} h_1(\xi_1) \\ h_2(\xi_1) \end{bmatrix} \otimes \begin{bmatrix} h_1(\xi_2) \\ h_2(\xi_2) \end{bmatrix} = \begin{bmatrix} h_1(\xi_1)\,h_1(\xi_2) & h_1(\xi_1)\,h_2(\xi_2) \\ h_2(\xi_1)\,h_1(\xi_2) & h_2(\xi_1)\,h_2(\xi_2) \end{bmatrix} \tag{260}$$

whereupon, the required finite element shape functions for the element depicted in Figure (5) become:

$$\begin{aligned} h_1(\xi_1,\xi_2) &= \frac{1}{4}(1-\xi_1)(1-\xi_2) \\ h_2(\xi_1,\xi_2) &= \frac{1}{4}(1+\xi_1)(1-\xi_2) \\ h_3(\xi_1,\xi_2) &= \frac{1}{4}(1-\xi_1)(1+\xi_2) \\ h_4(\xi_1,\xi_2) &= \frac{1}{4}(1+\xi_1)(1+\xi_2) \end{aligned} \tag{261}$$

Obviously, this result can be generalized in a trivial way and extended to higher dimensional elements, and elements with more than two nodes in the parent elements whose finite element shape functions form the building blocks of the shape functions that are analogous to those depicted in Equation (259).

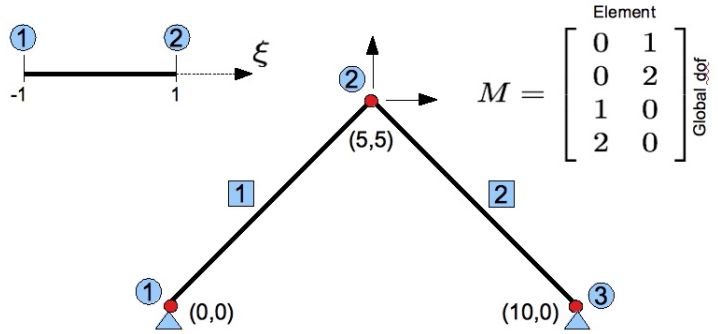

Figure 6: Example 2D truss problem

Assuming that numerical integration is employed in the evaluation of the types of integrals that appear in Equations (248) and (249), a general finite element algorithm, for use with iso-parametric parent elements that are mapped on finite elements comprising a mesh covering a problem domain, can be arrived at, or found in the literature. The application of numerical integration, and element assembly are important considerations; as are other effective means for treating essential boundary conditions. Later discussions in this work will begin by taking steps that specialize general finite element algorithms in order to be more efficient for applications involving structural elements; the ultimate focus of the present exposition.

As a foray into a consideration of structural elements, it is instructive to consider the process of *assembly* underpinning the so-called *direct stiffness method*, as it applies to a very simple 2-D truss problem. As it is that this particular example problem involves truss elements that can be oriented arbitrarily with respect to the global coordinate system (implied by the nodal coordinates associated with the truss arch structure depicted in Figure (6), a slight modification of the local element stiffness matrix, $\mathbf{K}^e$, associated with the parent element depicted in the same figure appears as:

$$\begin{aligned}\mathbf{K}^e &= \begin{bmatrix} c_1 & 0 \\ c_2 & 0 \\ 0 & c_1 \\ 0 & c_2 \end{bmatrix} \frac{AE}{L} \begin{bmatrix} 1 & -1 \\ -1 & 1 \end{bmatrix} \begin{bmatrix} c_1 & c_2 & 0 & 0 \\ 0 & 0 & c_1 & c_2 \end{bmatrix} \\ &= \frac{AE}{L} \begin{bmatrix} c_1^2 & c_1c_2 & -c_1^2 & -c_1c_2 \\ c_1c_2 & c_2^2 & -c_1c_2 & -c_2^2 \\ -c_1^2 & -c_1c_2 & c_1^2 & c_1c_2 \\ -c_1c_2 & -c_2^2 & c_1c_2 & c_2^2 \end{bmatrix} \end{aligned} \tag{262}$$

where the upper right superscript in the the designation $\mathbf{K}^e$ is meant to differentiate the local element stiffness matrix from the global system matrix to be designated as $\mathbf{K}$. It is pointed out that the quantities c_1 and c_2 represent

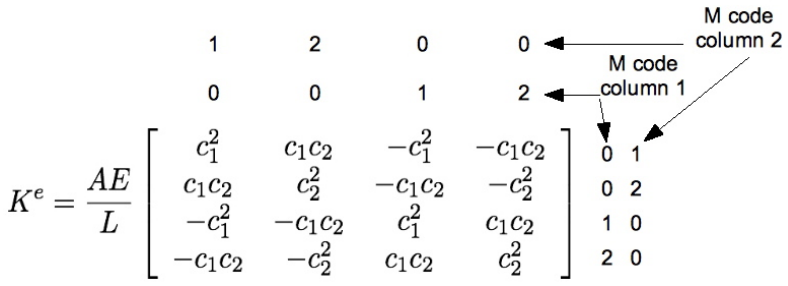

$$K^e = \frac{AE}{L}\begin{bmatrix} c_1^2 & c_1c_2 & -c_1^2 & -c_1c_2 \\ c_1c_2 & c_2^2 & -c_1c_2 & -c_2^2 \\ -c_1^2 & -c_1c_2 & c_1^2 & c_1c_2 \\ -c_1c_2 & -c_2^2 & c_1c_2 & c_2^2 \end{bmatrix}$$

Figure 7: System stiffness assembly for example 2D truss problem

the appropriate direction cosines effecting the coordinate rotations necessary to bring the local coordinate of the parent element into consonance with the appropriate finite element orientation within the global system frame of reference. The local 1-diection of the parent element originates at the end of the parent element corresponding to the smallest of the nodal numbers; extending through the higher numbered end node. The angles within the direction cosines are defined with this convention in mind.

Additionally, it is observed that the matrix depicted in the upper right of Figure (6) represents the element connectivity within the larger system. Specifically, the *M-code* matrix, M, lists zeros where homogeneous Dirichlet conditions are enforced, and integers elsewhere (corresponding to the global system degree of freedom numbering (usually optimized to minimize the bandwidth of the resulting system). The individual columns correspond with specific elements (*i.e.* column 1 pertains to element 1, *etc.*), and the rows correspond with what, if any, global degrees of freedom (dofs) correspond with the element ends. In this way, the individual element element stiffness matrices given in Equation (262) can be used to form the global stiffness matrix as depicted in Figure (7); yielding:

$$\mathbf{K} = \frac{AE}{L}\begin{bmatrix} c_1^2 & c_1c_2 \\ c_1c_2 & c_2^2 \end{bmatrix} + \frac{AE}{L}\begin{bmatrix} c_1^2 & c_1c_2 \\ c_1c_2 & c_2^2 \end{bmatrix} = \frac{2AE}{L}\begin{bmatrix} c_1^2 & c_1c_2 \\ c_1c_2 & c_2^2 \end{bmatrix} \quad (263)$$

The M-code can be similarly used to assemble a global force vector from the local force vectors considered on an individual, element-by-element basis.

2 Nonlinearity

Returning to a more general context (*i.e.* one that is not restricted to structural elements), a discussion of nonlinear partial differential equations (PDEs) is now undertaken.

2.1 Introduction to nonlinear PDEs and their solution

As a point of departure, consider the two nonlinear ODEs (defined on the interval $(0,1)$, and including Dirichlet conditions) as a basis for the subsequent discussion:

$$\begin{aligned} \frac{d^2u}{dx^2} + f(u) &= 0, & u(0) &= u_L, \quad u(1) = u_R \\ \frac{d}{dx}\left(\lambda(u)\frac{du}{dx}\right) &= 0, & u(0) &= u_L, \quad u(1) = u_R \end{aligned} \tag{264}$$

Assuming an approximate solution of the usual form,

$$u(\mathbf{x}) \approx \hat{u}(\mathbf{x}) = \sum_{j=1}^{n} u_j N_j(\mathbf{x}) \tag{265}$$

permits a consideration of the weak forms of the model problems. In a way that is analogous to problem treated in Equation (213) the Galerkin method may be applied to the model problems; resulting in:

$$\begin{aligned} \sum_{j=1}^{n}\left(\int_0^1 N_i'(\mathbf{x}) N_j'(\mathbf{x})\, dx\right) u_j &= \int_0^1 f\left(\sum_{s=1}^{n} u_s N_s(\mathbf{x})\right) N_i(\mathbf{x})\, dx, \quad i = 1,\ldots,n \\ \sum_{j=1}^{n}\left(\int_0^1 \lambda(\hat{u}(\mathbf{x})) N_i'(\mathbf{x}) N_j'(\mathbf{x})\, dx\right) u_j &= 0, \quad i = 1,\ldots,n \end{aligned} \tag{266}$$

These two weak forms may be expressed in a more compact notation as:

$$\begin{aligned} \mathbf{A}\mathbf{u} &= \mathbf{b}(\mathbf{u}) \\ \mathbf{A}(\mathbf{u})\,\mathbf{u} &= \mathbf{b} \end{aligned} \tag{267}$$

Or even more succinctly still, as:

$$\mathbf{F}(\mathbf{u}) = 0 \tag{268}$$

where $\mathbf{F}(\mathbf{u}) = \mathbf{A}\mathbf{u} - \mathbf{b}(\mathbf{u})$ in the case of the first model problem, and $\mathbf{F}(\mathbf{u}) = \mathbf{A}(\mathbf{u})\,\mathbf{u} - \mathbf{b}$, in the case of the second.

2.2 Picard iterations

Arguably, the simplest approach to the solution of nonlinear systems, such as those of Equation (267), would be to apply the iterative method attributed to Picard. Through subsequent applications of *Picard iteration*, the correct solution to each of the examples in Equation (267) is approached as:

$$\begin{aligned} \mathbf{A}\mathbf{u}^{k+1} &= \mathbf{b}\left(\mathbf{u}^k\right), & k &= 0,1,2,\ldots \\ \mathbf{A}\left(\mathbf{u}^k\right)\mathbf{u}^{k+1} &= \mathbf{b}, & k &= 0,1,2,\ldots \end{aligned} \tag{269}$$

where $\mathbf{u}^k$ is assumed to be available as an earlier solution within the iterative solution framework. Within such an iterative context, the question of *stopping criteria* immediately becomes relevant; additionally, starting conditions are at issue as well.

It is not uncommon to initiate Picard iteration with the zero vector (*i.e.* $\mathbf{u}^0 = \mathbf{0}$). As for a stopping criterion, essentially any discrete norm might be used to measure convergence in subsequent iterations, as $\|\mathbf{u}^{k+1} - \mathbf{u}^k\|$. Of course, the selection of a tolerance for the norm, signaling sufficient solution accuracy, is up to the analyst to select.

While it can sometimes be that Picard iteration may experience convergence problems when applied broadly to different classes of PDEs, some improvements can be achieved through the use of a technique known as *over-relaxation*. This approach involves the identification of an initial next step in the solution process, $\mathbf{u}^*$, using the approaches given in Equation (269):

$$\begin{aligned} \mathbf{A}\mathbf{u}^* &= \mathbf{b}\left(\mathbf{u}^k\right), & k &= 0, 1, 2, \ldots \\ \mathbf{A}\left(\mathbf{u}^k\right)\mathbf{u}^* &= \mathbf{b}, & k &= 0, 1, 2, \ldots \end{aligned} \tag{270}$$

whereupon, an over-relaxation parameter, ω, is introduced by fiat; subsequently leading to an identification of the next solution point:

$$\mathbf{u}^{k+1} = \omega \mathbf{u}^* + (1 - \omega)\,\mathbf{u}^k \tag{271}$$

where the prescribed over-relaxation parameter ranges as: $\omega \in (0, 1]$.

2.3 Newton-Raphson method

It is instructive to introduce the fundamental concepts associated with the *Newton-Raphson Method* through the consideration of a scalar form of the equations appearing as Equation (267); expressed more compactly as $F(u) = 0$. As it is that the Newton-Raphson Method is iterative, it is assumed that earlier approximations to the desired solution are available; being denoted as u^k. This earlier approximation to the problem solution does not satistfy the requirement wherein $F(u) = 0$, and thus an improvement is sought through the solution of an easier, surrogate problem for the more complex nonlinear problem at hand. The surrogate problem is expressed using a new function that is parameterized using the previously obtained solution, u^k; appearing as:

$$F(u) \approx M\left(u; u^k\right) \tag{272}$$

The vanishing of Equation (272) is subsequently used to furnish an improved approximation to the solution of the more complex original problem $F(u) = 0$. A useful approach to adopt is one where $M\left(u; u^k\right)$ is the linear portion of a

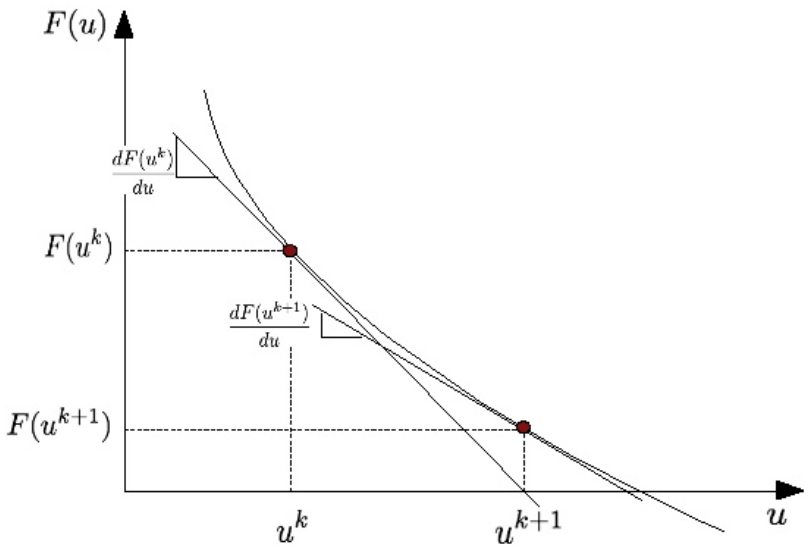

Figure 8: Schematic depiction of Newton-Raphson method applied to a scalar problem

Taylor series expansion of $F(u)$ about the point $u = u^k$ (with simplification):

$$\begin{aligned} M\left(u;u^k\right) &= F\left(u^k\right) + \frac{dF\left(u^k\right)}{du}\left(u-u^k\right) \\ F\left(u^k\right) &= -\frac{dF\left(u^k\right)}{du}\left(u-u^k\right) \\ -\frac{F\left(u^k\right)}{\frac{dF(u^k)}{du}} &= u-u^k \end{aligned} \tag{273}$$

The final line of the foregoing equation may be recast, in a form conducive to isolating the updated approximate solution to the original nonlinear problem, as:

$$u^{k+1} = u^k - \frac{F\left(u^k\right)}{\frac{dF(u^k)}{du}} \tag{274}$$

A graphical depiction of the foregoing nonlinear scalar problem is displayed schematically in Figure (8). Of course, all of the foregoing may be easily generalized to the multidimensional case.

In the multidimensional case, the more easily solved surrogate problem appears as $\mathbf{M}\left(\mathbf{u};\mathbf{u}^k\right)$; a linearization of the solution about the previously solved state being a commonly adopted approach:

$$\mathbf{M}\left(\mathbf{u};\mathbf{u}^k\right) = \mathbf{F}\left(\mathbf{u}^k\right) + \mathbf{J}\left(\mathbf{u}^k\right)\cdot\left(\mathbf{u}-\mathbf{u}^k\right) \tag{275}$$

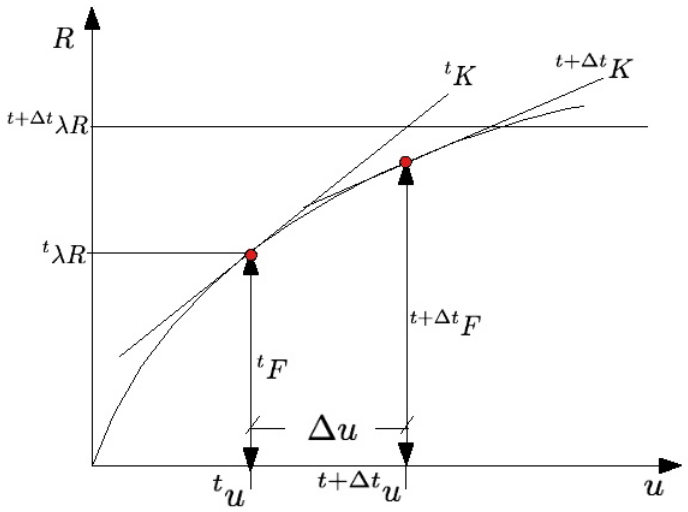

Figure 9: Schematic depiction of Newton-Raphson method applied to a single degree of freedom structure

where $\mathbf{J}\left(\mathbf{u}^k\right) \equiv \left(\nabla \mathbf{F}\left(\mathbf{u}^k\right)\right)^T$ is the *Jacobian* of $\mathbf{F}\left(\mathbf{u}^k\right)$, whose entry (i,j) is given as $\frac{\partial F_i}{\partial u_j}$. It is efficient to recast the solution approach furnished in Equation (274), in order that the increment in the nonlinear solution is solved for within each iteration as:

$$\mathbf{J}\left(\mathbf{u}^k\right)\Delta\mathbf{u}^{k+1} = F\left(\mathbf{u}\right) \tag{276}$$

where $\Delta\mathbf{u}^{k+1} = \mathbf{u}^{k+1} - \mathbf{u}^k$. Over-relaxation (sometimes also called *line searches*) can be applied to the Newton-Raphson method as well; resulting in an updated solution of the form:

$$\mathbf{u}^{k+1} = \mathbf{u}^k + \omega\Delta\mathbf{u}^{k+1} \tag{277}$$

While Picard iteration may have issues with convergence, the Newton Raphson method enjoys a quadratic convergence rate (*i.e.* $\mid \mathbf{u} - \mathbf{u}^{k+1} \mid \leq C \mid \mathbf{u} - \mathbf{u}^k \mid^2$, for a constant C).

The form of the Newton-Raphson method presented in Equation (276) is particularly useful in nonlinear structural mechanics where the $\mathbf{J}\left(\mathbf{u}^k\right)$ can be thought of as a *tangent stiffness matrix*, $\mathbf{K}_T$ (the linear portion of a Taylor series expansion carried out about the previous solution point within the method), and the right hand side of Equation (276) can be viewed as an out-of-balance force (sometimes called a *Residual*).

The Newton-Raphson method can be applied to a hypothetical single degree of freedom structural problem as a means for introducing notation and conventions that will prove useful in discussions centering on the *modified spherical arc length method*, to be introduced in the sequel. In the meantime a consideration

of Figure (9) may proceed.

The structure under consideration in Figure 9 is initially subject to some baseline loading, R. Subsequent load levels are achieved through the specification of a *Load Proportionality Factor* (LPF), λ. The solution increments (previously denoted by k) are denoted with a left super-script; where the variable name t is now adopted to facilitate later consideration of time, in transient dynamic contexts. Beginning with a consideration of the previously converged solution, where the structure assumed the configuration that is consistent with ${}^{t}u$ (under the external action of ${}^{t}\lambda R$), the Jacobian is formulated as the tangent stiffness ${}^{t}K$. The imbalance between the previously converged response (quantified by the *internal force vector* ${}^{t}F$) and the new desired load intensity, ${}^{t+\Delta t}\lambda R$, are treated iteratively during the increment that is solving for the configuration at $t+\Delta t$. In such a framework, the new configuration of the structure, denoted as ${}^{t+\Delta t}u$, results in an internal action for the structure of ${}^{t+\Delta t}F$; which does not balance the applied action ${}^{t+\Delta t}\lambda R$; thus additional iterations are required within the increment $t+\Delta t$. Thus, the subsequent structural configurations, at each iteration within the load increment for $t+\Delta t$, may be given generally as ${}^{t+\Delta t}u^{(i)}$; where the variable i denotes the particular iteration of interest. With this in mind, the case depicted in Figure (9), could have presented the current (within the current iteration for the given increment) solution configuration as ${}^{t+\Delta t}u^{(1)}$. It is then possible to summarize the Newton-Raphson approach to the solution of a particular iteration, within a given increment, as:

$$\begin{aligned} {}^{t+\Delta t}K^{(i-1)}\Delta u^{(i)} &= {}^{t+\Delta t}\lambda R - {}^{t+\Delta t}F^{(i-1)} \\ {}^{t+\Delta t}u^{(i)} &= \Delta u^{(i)} + {}^{t+\Delta t}u^{(i-1)} \end{aligned} \tag{278}$$

As an example, the starting iteration for increment $t+\Delta t$ in Figure (9) would appear as:

$$\begin{aligned} {}^{t}K\Delta u^{(1)} &= {}^{t+\Delta t}\lambda R - {}^{t}F \\ {}^{t+\Delta t}u^{(1)} &= \Delta u^{(1)} + {}^{t}u \end{aligned} \tag{279}$$

while the second iteration would then appear as:

$$\begin{aligned} {}^{t+\Delta t}K^{(1)}\Delta u^{(2)} &= {}^{t+\Delta t}\lambda R - {}^{t+\Delta t}F^{(1)} \\ {}^{t+\Delta t}u^{(2)} &= \Delta u^{(2)} + {}^{t+\Delta t}u^{(1)} \end{aligned} \tag{280}$$

One important drawback to the Newton - Raphson method rests in its inability to traverse limit points in the equilibrium path. At such locations, in configuration space, the tangent stiffness matrix becomes singular, and thus the usual approach to factorizing the matrix, and subsequently solving for displacement increments, will not be possible. In such cases an *arc length method* may be employed.

2.4 Modified spherical arc length method

There are many different arc length methods to choose from, but the underlying structure is the same: the incremental equilibrium equation is augmented with an additional constraint equation that dictates a parametric relationship between the displacement and load increments within a given iteration. In general, if the problem at hand has n degrees of freedom, then the $n+1$ dimensional problem being solved in the arc length method becomes:

$$\begin{aligned} {}^{\tau}\mathbf{K}\Delta\mathbf{U}^{(i)} &= \left({}^{t+\Delta t}\lambda^{(i-1)} + \Delta\lambda^{(i)}\right)\mathbf{R} - {}^{t+\Delta t}\mathbf{F}^{(i-1)} \\ 0 &= f\left(\Delta\lambda^{(i)}, \Delta\mathbf{U}^{i}\right) \end{aligned} \tag{281}$$

In Equation (281) the τ appears on the stiffness term, ${}^{\tau}\mathbf{K}$, since it may be that the stiffness is not being updated at every iteration (referred to as a *modified Newton - Raphson method*). Additionally, the quantity $\Delta\lambda^{(i)}$ refers to the increment in the load proportionality that takes ${}^{t+\Delta t}\lambda^{(i-1)}$ into ${}^{t+\Delta t}\lambda^{(i)}$. In the current discussion, the parametric equation, relating displacement and load increments, is furnished as:

$$\begin{aligned} \Delta l^2 &= \left[\left({}^{t+\Delta t}\lambda^{(i-1)} - {}^{t}\lambda\right) + \Delta\lambda^{(i)}\right]^2 + \mathbf{U}^{(i)T}\mathbf{U}^{(i)} \\ \mathbf{U}^{(i)} &= {}^{t+\Delta t}\mathbf{U}^{(i)} - {}^{t}\mathbf{U} \end{aligned} \tag{282}$$

Besides facilitating the traversing of limit points, the approach espoused in Equation (281) is useful when adaptivity in the solution is desirable. For example, during the evolution of the incremental solution, it may that regions of greater nonlinearity are encountered; thus it would desirable to be able to reduce the arc length in regions where the solution is particularly difficult to track (as well as increase it in regions where solution nonlinearity is more mild). The arc length method permits this. As previously noted, there are many different implementation strategies for the arc length method. The version presented is a hybrid of several dominant techniques that appears to perform efficiently and robustly. The discussion of the present *modified spherical arc length method* will commence with a consideration of required starting protocols. It will be seen that the parameters employed during the initial iteration will impact the remainder of the incrementally evolving solution.

Prior to the start of the first increment, the analyst must specify three solution parameters:

1. The reference load vector, $\mathbf{R}$, (to be scaled by the load proportionality factor (LPF), λ, during the course of the solution evolution);

2. An initial displacement, ${}^{\Delta t}\mathbf{U}_k^*$, to initiate the model response in the desired sense (*i.e.* in a manner that is consistent with subsequent loading within the problem);

3. A scalar constant, α, used to limit the size of any subsequent displacement increments as:

$$\|\mathbf{U}\| \leq \alpha \|^{\Delta t}\mathbf{U}\| \tag{283}$$

where $\|\cdot\|$ denotes the Euclidean norm.

To begin the solution, the solution time, Δt, is considered. The initial incremental equilibrium equation can be expressed as:

$${}^{0}\mathbf{K}\Delta\mathbf{U}^{(i)} = \left({}^{\Delta t}\lambda^{(i-1)} + \Delta\lambda^{(i)}\right)\mathbf{R} - {}^{\Delta t}\mathbf{F}^{(i-1)} \tag{284}$$

However, within the first iteration, the solution time appears as $\Delta t^{(1)}$, and thus the incremental equilibrium equations appear as:

$${}^{0}\mathbf{K}\Delta\mathbf{U}^{(1)} = \Delta\lambda^{(1)}\mathbf{R} \tag{285}$$

However, since we do not yet know $\Delta\lambda^{(1)}$ we instead solve the following variant; where the entire reference load vector, $\mathbf{R}$, used (the resulting over-estimated displacement is subsequently corrected):

$${}^{0}\mathbf{K}\Delta\mathbf{U}^{(1)} = \mathbf{R} \tag{286}$$

The use of Equation (286) implies that $\Delta\mathbf{U}^{(1)}$ is $\frac{1}{\Delta\lambda^{(1)}}$ too large; and thus must be reduced by the amount:

$${}^{\Delta t}\lambda_k^{(1)} \equiv \frac{{}^{\Delta t}U_k^*}{\Delta U_k^{(1)}} \tag{287}$$

where the subscript, k, refers to a specific degree of freedom within the displacement vector $\mathbf{U}$. We now have our first load proportionality factor. Additionally, through the use of Equation (287) we see that the updated displacement increment is presented as:

$${}^{\Delta t}\mathbf{U}^{(1)} = {}^{\Delta t}\lambda^{(1)}\Delta\mathbf{U}^{(1)} = {}^{\Delta t}\mathbf{U}^* \tag{288}$$

The foregoing is depicted, in a schematic sense for one degree of freedom, in Figure (10), so as to summarize the steps leading to ${}^{\Delta t}\mathbf{U}^{(1)}$ and ${}^{\Delta t}\lambda^{(1)}$ in the first iteration within the Δt increment. Subsequent iterations within the Δt increment proceed as follows.

Instead of using Equation (284) directly, a modification is employed:

$${}^{0}\mathbf{K}\Delta\bar{\mathbf{U}}^{(i)} = {}^{\Delta t}\lambda^{(i-1)}\mathbf{R} - {}^{\Delta t}\mathbf{F}^{(i-1)} \tag{289}$$

In the case of solution time $\Delta t^{(2)}$, the displacement increment, $\bar{\mathbf{U}}^{(2)}$, is obtained from the foregoing; whereupon the increment in LPF, $\Delta\lambda^{(2)}$, is arrived at from:

$$\Delta\lambda_k^{(2)} = -\frac{\bar{U}_k^{(2)}}{\Delta U_k^{(1)}} \tag{290}$$

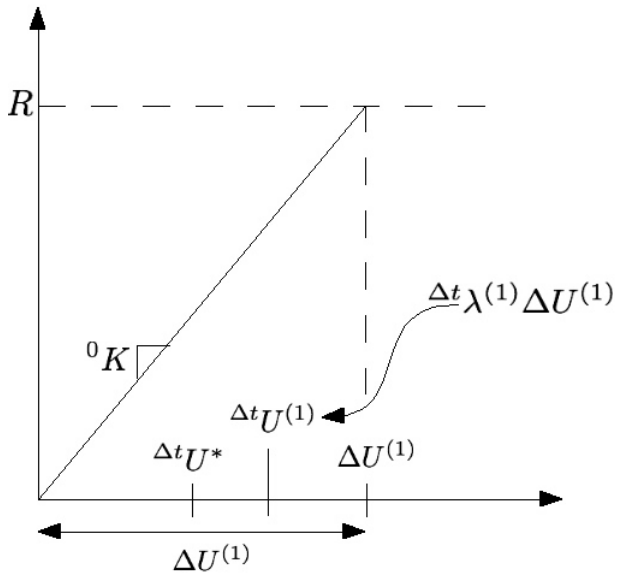

Figure 10: Schematic depiction of the first iteration, within the first increment, using the modified spherical arc length method

where the denominator term on the right hand side is the over-estimated displacement increment obtained using Equation (286). The incremental LPF from Equation (290) is subsequently used to compute a negative displacement; bringing the structure "backwards", in configuration space (with respect to the direction of loading) as:

$$\Delta \mathbf{U}^{(2)} = \Delta \bar{\mathbf{U}}^{(2)} + \Delta\lambda^{(2)} \Delta \mathbf{U}^{(1)} \tag{291}$$

whereupon the new configuration, for the increment at time $\Delta t^{(2)}$ is:

$$^{\Delta t}\mathbf{U}^{(2)} = ^{\Delta t}\mathbf{U}^{(1)} + \Delta \mathbf{U}^{(2)} \tag{292}$$

The accompanying new LPF is also reduced, taking the form:

$$^{\Delta t}\lambda^{(2)} = ^{\Delta t}\lambda^{(1)} + \Delta\lambda^{(2)} \tag{293}$$

The iterating within the time increment Δt continues until convergence in energy is achieved:

$$\frac{\Delta \mathbf{U}^{(i)} \cdot \left(^{\Delta t}\lambda^{(i-1)}\mathbf{R} - ^{\Delta t}\mathbf{F}^{(i-1)} \right)}{\Delta \mathbf{U}^{(1)} \cdot \left(^{\Delta t}\lambda^{(1)}\mathbf{R} \right)} \leq ETOL \tag{294}$$

where $ETOL$ is a suitably chosen energy tolerance. Figure (11) displays the approach, schematically, for the single degree of freedom case. For subsequent increments within the evolving nonlinear solution, the arc length used in each

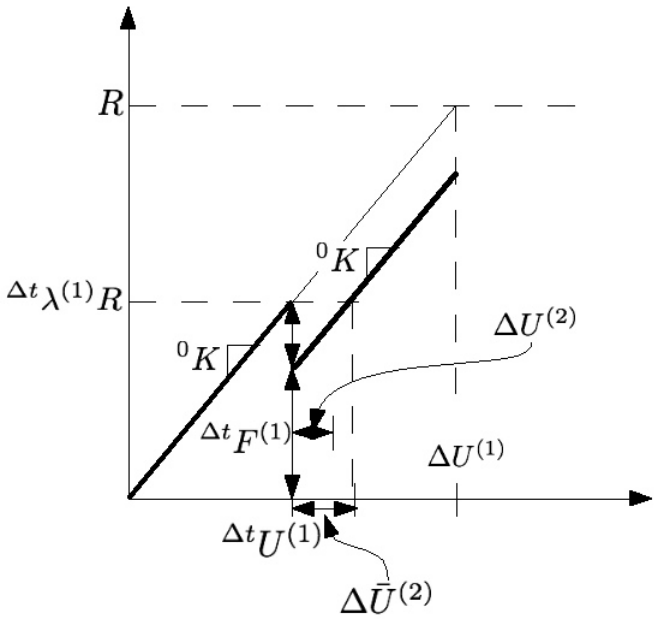

Figure 11: Schematic depiction of the subsequent iterations, within the first increment, using the modified spherical arc length method

iteration is computed based based on the results obtained within the previous increments as:

$$\Delta l = \beta\sqrt{\mathbf{U}\cdot\mathbf{U}+\lambda^2} \tag{295}$$

where β is a scaling parameter to be defined later (see Equations (311) and (312)), and the displacement and load increments used in Equation (295) are computed as:

$$\begin{aligned}\mathbf{U} &= {}^t\,\mathbf{U} - {}^{t-\Delta t}\,\mathbf{U}\\ \lambda &= {}^t\,\lambda - {}^{t-\Delta t}\,\lambda\end{aligned} \tag{296}$$

This process can be illustrated through the consideration of the equations that accompany iteration $i = 1$ within the solution increment for time $t + \Delta t$. Employing the tangent stiffness of the structure from some arbitrary time, τ, (*i.e.* employing the modified Newton - Raphson method), the error from the previous time increment can be solved for (in order that we do not inadvertently accumulate error between increments) as:

$${}^\tau\mathbf{K}\Delta\bar{\mathbf{U}}^{(1)} = {}^t\,\lambda\mathbf{R} - {}^t\,\mathbf{F} \tag{297}$$

whereupon a reference displacement increment can be computed for the current time increment as:

$${}^\tau\mathbf{K}\Delta\bar{\bar{\mathbf{U}}}^{(1)} = \mathbf{R} \tag{298}$$

It is now possible to compute the updated LPF, $\Delta\lambda^{(1)}$, using the previously computed arc length, Δl:

$$\left({}^{t+\Delta t}\lambda^{(1-1)} - {}^{t}\lambda + \Delta\lambda^{(1)}\right)^2 + \Delta\mathbf{U}^{(1)} \cdot \Delta\mathbf{U}^{(1)} = \Delta l^2$$
$$\left(\Delta\lambda^{(1)}\right)^2 + \Delta\mathbf{U}^{(1)} \cdot \Delta\mathbf{U}^{(1)} = \Delta l^2 \tag{299}$$

It is pointed out that Equation (299) has been specialized to account for the conditions accompanying the initial iteration within an increment wherein $\Delta\mathbf{U}$ is used (in lieu of $\mathbf{U}$) since the displacement increment between iteration is the same as that occurring between the increment. Additionally, the term ${}^{t+\Delta t}\lambda^{(1-1)} - {}^{t}\lambda$ vanishes; as it is that within the first iteration ${}^{t+\Delta t}\lambda^{(1-1)} - {}^{t}\lambda = {}^{t+\Delta t}\lambda^{(0)} - {}^{t}\lambda = 0$. The net result of the foregoing is that $\Delta\mathbf{U}^{(1)}$ depends on $\Delta\lambda^{(1)}$. The displacement increment for the initial iteration is then given as:

$$\Delta\mathbf{U}^{(1)} = \Delta\bar{\mathbf{U}}^{(1)} + \Delta\lambda^{(1)}\Delta\bar{\bar{\mathbf{U}}}^{(1)} \tag{300}$$

thus leading to the following quadratic equation:

$$\left(\Delta\lambda^{(1)}\right)^2 + \left(\Delta\bar{\mathbf{U}}^{(1)} + \Delta\lambda^{(1)}\Delta\bar{\bar{\mathbf{U}}}^{(1)}\right) \cdot \left(\Delta\bar{\mathbf{U}}^{(1)} + \Delta\lambda^{(1)}\Delta\bar{\bar{\mathbf{U}}}^{(1)}\right) = \Delta l^2 \tag{301}$$

Since $\Delta\lambda^{(1)}$ is now known, the entire updated iterative solution, within the current increment, may be summarized as:

$${}^{t+\Delta t}\mathbf{U}^{(1)} = {}^{t}\mathbf{U} + \Delta\mathbf{U}^{(1)}$$
$${}^{t+\Delta t}\lambda^{(1)} = {}^{t}\lambda + \Delta\lambda^{(1)} \tag{302}$$

This can be generalized to subsequent iterations (*i.e.* $i = 2, 3, \ldots$) within the increment for $t + \Delta t$ by proceeding with the solution of:

$${}^{\tau}\mathbf{K}\Delta\bar{\bar{\mathbf{U}}}^{(1)} = \mathbf{R} \tag{303}$$

for $\Delta\bar{\bar{\mathbf{U}}}^{(1)}$ (to be re-used in subsequent iterations within the increment), and then subsequently solving:

$${}^{\tau}\mathbf{K}\Delta\bar{\mathbf{U}}^{(i)} = {}^{t+\Delta t}\lambda^{(i-1)}\mathbf{R} - {}^{t+\Delta t}\mathbf{F}^{(i-1)} \tag{304}$$

(so as to not accumulate error in the solution from iteration to iteration). The foregoing may then be used to solve for the updated displacement, ${}^{t+\Delta t}\mathbf{U}^{(i)}$, as:

$${}^{t+\Delta t}\mathbf{U}^{(i)} = {}^{t+\Delta t}\mathbf{U}^{(i-1)} + \Delta\bar{\mathbf{U}}^{(i)} + \Delta\lambda^{(i)}\Delta\bar{\bar{\mathbf{U}}}^{(1)} \tag{305}$$

where $\Delta\lambda^{(i)}$ comes from the solution of the following quadratic equation:

$$\left(\left({}^{t+\Delta t}\lambda^{(i-1)} - {}^{t}\lambda\right) + \Delta\lambda^{(i)}\right)^2 + \mathbf{U}^{(i)} \cdot \mathbf{U}^{(i)} = \Delta l^2 \tag{306}$$

whose displacement increment terms, $\mathbf{U}^{(i)}$, are given by:

$$\mathbf{U}^{(i)} = {}^{t+\Delta t}\mathbf{U}^{(i)} - {}^{t}\mathbf{U} \tag{307}$$

Thus, the expanded form of the quadratic yielding the desired increment in the LPF becomes:

$$\left(\left({}^{t+\Delta t}\lambda^{(i-1)} - {}^{t}\lambda\right) + \Delta\lambda^{(i)}\right)^2 + \left[\left({}^{t+\Delta t}\mathbf{U}^{(i-1)} + \Delta\bar{\mathbf{U}}^{(i)} + \Delta\lambda^{(i)}\Delta\bar{\bar{\mathbf{U}}}^{(1)}\right) - {}^{t}\mathbf{U}\right] \cdot \left[\left({}^{t+\Delta t}\mathbf{U}^{(i-1)} + \Delta\bar{\mathbf{U}}^{(i)} + \Delta\lambda^{(i)}\Delta\bar{\bar{\mathbf{U}}}^{(1)}\right) - {}^{t}\mathbf{U}\right] = \Delta l^2 \tag{308}$$

Once the LPF increment has been solved for using Equation (308), then the updated LPF for the iteration may be stated as:

$${}^{t+\Delta t}\lambda^{(i)} = {}^{t+\Delta t}\lambda^{(i-1)} + \Delta\lambda^{(i)} \tag{309}$$

Once again, iterations continue until the energy tolerance, given in Equation (294), is satisfied.

Some important observations concerning the solution of the required quadratic equations are furnished as:

1. if no real roots are obtained, then abort the increment and subsequently restart with a smaller arc length; such as $\Delta l^{new} = \frac{\Delta l^{old}}{2}$
2. if two real roots are obtained, then the selected root becomes the one for which γ is largest; where $\gamma = \mathbf{U}^{(i-1)} \cdot \mathbf{U}^{(i)}$

Additionally, upon convergence to a displacement within an increment, the following check is performed:

$$\|{}^{t+\Delta t}\mathbf{U} - {}^{t}\mathbf{U}\|_{\ell^2} \leq \alpha \|{}^{\Delta t}\mathbf{U}\|_{\ell^2} \tag{310}$$

whereupon, if the check of Equation (310) fails, then the increment is abandoned and then restarted with:

$$\Delta l^{new} = \Delta l^{old} \frac{\alpha \|{}^{t+\Delta t}\mathbf{U}\|_{\ell^2}}{\|{}^{t+\Delta t}\mathbf{U} - {}^{t}\mathbf{U}\|_{\ell^2}} \tag{311}$$

However, if the test of Equation (310) is passed, then the solution is permitted to advance to the next increment; applying the updated arc length:

$$\Delta l^{new} = \Delta l^{old} \sqrt{\frac{N_1}{N_2}} \frac{\alpha \|{}^{t+\Delta t}\mathbf{U}\|_{\ell^2}}{\|{}^{t+\Delta t}\mathbf{U} - {}^{t}\mathbf{U}\|_{\ell^2}} \tag{312}$$

where $N_1 \equiv$ optimum number of iterations, and $N_2 \equiv$ number of iterations used in the previous increment. This last step enhances solution efficiency by adapting to the degree of local nonlinearity that the problem is exhibiting, as the solution is evolving.

2.5 Nonlinear continua

In formulating a tractable approach to the solution of nonlinear finite element idealizations of solids and structures, it is important to apply what we have reviewed in the preceding treatment, as practical means for solving problems. Specifically, the principal of conservation of linear momentum will be subsequently applied using the work conjugate material time derivative of the deformation gradient, $\dot{\mathbf{F}}$, and PK1 stress, $\mathbf{P}$; as a result of their simplicity when formulating important finite element expressions. However, as a result of the lack of symmetry in $\dot{\mathbf{F}}$ and $\mathbf{P}$, the Green-Lagrange (G-L) strain and PK2 stress will be adopted later in these notes; as implementation within the Total Lagrangian (T. L.) formulation progresses. Similarly, the power conjugate rate of deformation tensor and Cauchy stress rate are used within Updated Lagrangian (U. L.) formulations, while implementation will involve G-L strain and PK2 stress. It is pointed out that some authors in the literature apply the true strain and Cauchy stress in a work conjugate pairing for the U. L. formulation as well. The two approaches for the U. L. formulation are identical, and only differ as a matter of taste. We will adopt the power formulation so as to illustrate the usage of some of the quantities that we have previously reviewed in these notes. It is further noted that the T. L. and U. L. formulations yield identical results when implemented within a finite element framework. The choice of one formulation over the other, usually rests in the expediency of one formulation over the other as a result of peculiarities within a given problem.

2.6 Lagrangian Reference frames

Lagrangian reference frames are referential in nature: measuring the various mechanical response measures in terms of the initial, unstressed state in the case of the T. L., or with respect to the previously converged equilibrium configuration in the U. L. case. In either case, the referential description is required since the alternative would involve measuring the needed mechanical properties in the current configuration with respect to an unknown deformation state; which is actually the primary unknown sought during the usual nonlinear finite element solution.

2.6.1 Total Lagrangian (T. L.)

We may state the appropriate strong form of the conservation in linear momentum for the T. L. reference frame, in component form, as:

$$\frac{\partial P_{ji}}{\partial X_j} + \rho_o b_i = \rho_o \ddot{u}_i \tag{313}$$

We may subsequently consider a set of test and trial functions as:

$$\delta\mathbf{u}\left(\mathbf{X}\right) \in \mathcal{U}_0, \quad \mathbf{u}\left(\mathbf{X}, t\right) \in \mathcal{U} \tag{314}$$

where $\mathcal{U}$ is the space of displacement functions that satisfies the actual Dirichlet condition of the problem (*i.e* a space of *kinematically admissible* functions);

while $\mathcal{U}_0$ is a similar space, except that the functions must satisfy the homogeneous Dirichlet condition. It is pointed out that a suggestive notation is adopted for the test functions: including a δ symbol. This is done in order to obviate the parallels between the weak formulation and the *principle of virtual work* that is applied later in the course. A weak form may be subsequently obtained using the foregoing notation:

$$\int_{\Omega_o} \delta u_i \left(\frac{\partial P_{ji}}{\partial X_j} + \rho_o b_i - \rho_o \ddot{u}_i \right) d\Omega_o = 0 \tag{315}$$

The foregoing is not as helpful as it could be, since there is a requirement of C^1 continuity implied in Equation (315) as part of the derivative on the PK1 stress. Fortunately, integration by parts may be applied to this term as follows:

$$\int_{\Omega_o} \delta u_i \frac{\partial P_{ji}}{\partial X_j} d\Omega_o = \int_{\Omega_o} \frac{\partial}{\partial X_j} \left(\delta u_i P_{ji} \right) d\Omega_o - \int_{\Omega_o} \frac{\partial \left(\delta u_i \right)}{\partial X_j} P_{ji} d\Omega_o \tag{316}$$

Gauss' Divergence Theorem may be subsequently applied to the first term on the right side of the equal sign above, to yield:

$$\int_{\Omega_o} \frac{\partial}{\partial X_j} \left(\delta u_i P_{ji} \right) d\Omega_o = \int_{\Gamma_o} \delta u_i \left(n_o \right)_j P_{ji} d\Gamma_o \tag{317}$$

The integrand on the right hand side of Equation (317) is simply the Neumann condition on the boundary tractions which can be stated as:

$$\left(n_o \right)_j P_{ji} = \left(t_o \right)_i \tag{318}$$

where t_o is the traction vector on the boundary. Equation (317) may then be re-stated as:

$$\int_{\Omega_o} \frac{\partial}{\partial X_j} \left(\delta u_i P_{ji} \right) d\Omega_o^t = \int_{\Gamma_o^t} \delta u_i \left(t_o \right)_i d\Gamma_o^t \tag{319}$$

where Γ_o^t is the portion of the domain boundary where Dirichlet conditions are not specified, and the following conditions apply: $\Gamma = \Gamma^t \cup \Gamma^u$ and $\Gamma^t \cap \Gamma^u = \emptyset$ (where Γ^u is the portion of the boundary where the essential boundary conditions are specified). It is also noted that the first term within the left hand side of the integrand in Equation (319) may be modified, so as to be put in terms of the deformation gradient, as follows:

$$\frac{\partial \left(\delta u_i \right)}{\partial X_j} = \delta \left(\frac{\partial u_i}{\partial X_j} \right) = \delta F_{ij} \tag{320}$$

Equation (320) may be substituted into Equation (316), which can subsequently be used in Equation (315) to yield:

$$\int_{\Omega_o} \left(\delta F_{ij} P_{ji} - \delta u_i \rho_o b_i + \delta u_i \rho_o \ddot{u}_i \right) d\Omega_o - \int_{\Gamma_o^t} \delta u_i \left(t_o \right)_i d\Gamma_o^t = 0 \tag{321}$$

or, in tensor notation:

$$\int_{\Omega_o} \left(\delta \mathbf{F}^T : \mathbf{P} - \rho_o \delta \mathbf{u} \cdot \mathbf{b} + \rho_o \delta \mathbf{u} \cdot \ddot{\mathbf{u}}\right) d\Omega_o - \int_{\Gamma_o^t} \left(\delta \mathbf{u} \cdot \mathbf{i}\right) \left(\mathbf{i} \cdot \mathbf{t}_o\right) d\Gamma_o^t = 0 \quad (322)$$

The foregoing weak form is sometimes referred to as emanating from the principle of virtual work; as it is that notional mechanical interpretations may be ascribed to the individual terms of the weak form as follows:

$$\begin{aligned} \delta \mathcal{W}^{int} &= \int_{\Omega_o} \left(\delta \mathbf{F}^T : \mathbf{P}\right) d\Omega_o \\ \delta \mathcal{W}^{ext} &= \int_{\Omega_o} \left(\rho_o \delta \mathbf{u} \cdot \mathbf{b}\right) d\Omega_o + \int_{\Gamma_o^t} \left(\delta \mathbf{u} \cdot \mathbf{i}\right) \left(\mathbf{i} \cdot \mathbf{t}_o\right) d\Gamma_o^t \\ \delta \mathcal{W}^{kin} &= \int_{\Omega_o} \left(\delta \mathbf{u} \cdot \rho_o \ddot{\mathbf{u}}\right) d\Omega_o \end{aligned} \quad (323)$$

2.6.2 Updated Lagrangian (U. L.)

Within the context of an Updated Lagrangian formulation, it is sometimes the case that the strong form of the momentum conservation within the spatial domain, Ω, is expressed in a velocity form as:

$$\frac{\partial \sigma_{ji}}{\partial x_j} + \rho b_i = \rho \dot{v}_i \quad (324)$$

where the Neumann traction boundary conditions are specified on the relevant segment of the boundary, Γ^t, in the same way as in the T. L. formulation:

$$n_j \sigma_{ji} = t_i \quad (325)$$

Proceeding as before, it is possible to form a weak form of the momentum equation as:

$$\int_{\Omega} \delta v_i \left(\frac{\partial \sigma_{ji}}{\partial x_j} + \rho b_i - \rho \dot{v}_i\right) d\Omega = 0 \quad (326)$$

within which test and trial functions are once again defined; this time in terms of velocities:

$$\delta \mathbf{v}\left(\mathbf{X}\right) \in \mathcal{U}_0, \quad \mathbf{v}\left(\mathbf{X}, t\right) \in \mathcal{U} \quad (327)$$

where in this case, $\mathcal{U}$ and $\mathcal{U}_0$ are the space of kinematically admissible velocities, and velocities that satisfy the homogeneous Dirichlet conditions, respectively.

The first term within the integrand of Equation (326) may be re-expressed through integration by parts to be:

$$\int_{\Omega} \delta v_i \frac{\partial \sigma_{ji}}{\partial x_j} d\Omega = \int_{\Omega} \left(\frac{\partial}{\partial x_j}\left(\delta v_i \sigma_{ji}\right) - \frac{\partial \left(\delta v_i\right)}{\partial x_j} \sigma_{ji}\right) d\Omega \quad (328)$$

Applying Gauss' Divergence Theorem to the first term within the integrand of Equation (328) yields:

$$\int_{\Omega} \frac{\partial}{\partial x_j} \left(\delta v_i \sigma_{ji} \right) d\Omega = \int_{\Gamma} \delta v_i n_j \sigma_{ji} d\Gamma \tag{329}$$

the right hand side of which may be expanded as (using the Neumann traction condition):

$$\int_{\Omega} \frac{\partial}{\partial x_j} \left(\delta v_i \sigma_{ji} \right) d\Omega = \int_{\Gamma^t} \delta v_i t_i d\Gamma^t \tag{330}$$

The foregoing may be substituted into Equation (328) to furnish:

$$\int_{\Omega} \delta v_i \frac{\partial \sigma_{ji}}{\partial x_j} d\Omega = \int_{\Gamma^t} \delta v_i t_i d\Gamma^t - \int_{\Omega} \frac{\partial \left(\delta v_i \right)}{\partial x_j} \sigma_{ji} d\Omega \tag{331}$$

Equation (331) may subsequently be used within Equation (326) to obtain:

$$\int_{\Omega} \frac{\partial \left(\delta v_i \right)}{\partial x_j} \sigma_{ji} d\Omega - \int_{\Omega} \delta v_i \rho b_i d\Omega - \int_{\Gamma^t} \delta v_i t_i d\Gamma + \int_{\Omega} \delta v_i \rho \dot{v}_i d\Omega = 0 \tag{332}$$

where the form of Equation (332) is consistent with the form typically observed within a formulation involving the *principle of virtual power*.

It is noticed that the first term within the integrand on the right hand side of Equation (332) may be re-expressed in a more convenient form as (exploiting the symmetry in the Cauchy stress tensor):

$$\frac{\partial \left(\delta v_i \right)}{\partial x_j} \sigma_{ij} = \delta L_{ij} \sigma_{ij} = \left(\delta D_{ij} + \delta W_{ij} \right) \sigma_{ij} = \delta D_{ij} \sigma_{ij} \tag{333}$$

wherein the skew symmetry of the spin tensor, $\mathbf{W}$, has been exploited. In tensor notation, the foregoing result can be compactly expressed as:

$$\frac{\partial \left(\delta v_i \right)}{\partial x_j} \sigma_{ij} = \delta \mathbf{D} : \sigma \tag{334}$$

The suggestive name that accompany the principle of virtual power may now be assigned to each of the terms within the foregoing weak form as:

$$\begin{aligned} \delta \mathcal{P}^{int} &= \int_{\Omega} \delta \mathbf{D} : \sigma d\Omega \\ \delta \mathcal{P}^{ext} &= \int_{\Omega} \delta \mathbf{v} \cdot \rho \mathbf{b} d\Omega + \int_{\Gamma^t} \left(\delta \mathbf{v} \cdot \mathbf{i} \right) \mathbf{t} \cdot \mathbf{i} \, d\Gamma^t \\ \delta \mathcal{P}^{kin} &= \int_{\Omega} \delta \mathbf{v} \cdot \rho \dot{\mathbf{v}} d\Omega \end{aligned} \tag{335}$$

2.7 Review of stress-space plasticity

The current treatment of material nonlinear effects is limited to the case of perfect plasticity in metals (*i.e.* hardening effects are ignored), as a result of the work to come later in specializing nonlinear constitutive theories for application in stress resultant space (force space) for use with structural elements. As a point of departure for these later discussions, the current subsection reviews elementary concepts from stress-space plasticity.

Considering empirical evidence arising from work with metals possessing an underlying crystal structure that is face centered or body centered (*i.e.* FCC or BCC) in nature (*e.g.* steel, aluminum, *etc.*) it has been noticed that large changes in volume (in terms of percent difference) may be experienced, and recovered from, in an elastic manner. Indeed, it appears that FCC and BCC metals are essentially insensitive to the occurrence of hydrostatic loading when considering the activation of inelastic response. As a result, the dominant failure criteria, in applications involving metals, neglect the occurrence of the hydrostatic portion of the stress when predicting the initiation of yielding.

As a point of departure for the present discussion, consider a Newtonian fluid. A fluid differs from a typical solid in that it is unable to resist shear stresses directly, and thus shearing deformations will evolve in a given fluid domain for as long as the shear stresses are imposed. If the fluid domain is considered to constitute a thin film layer that separates two plates (one stationary, and the other moving at some constant velocity with respect to the former) then a single dimensional relationship for the stress and velocity of the plates may be given in terms of a fluid mechanical property known as viscosity:

$$\tau = \mu \frac{dv}{dx} \tag{336}$$

where v is the relative plate velocities with respect to the spatial coordinate, x; with μ being the *coefficient of viscosity*. This result may be generalized to the three dimensional case by considering the *stress deviator* on the left hand side, and the rate of deformation tensor on the right hand side:

$$\mathbf{T}' = 2\mu\mathbf{D} \tag{337}$$

the 2 being needed to cancel with the factor of $\frac{1}{2}$ present in the rate of deformation, $\mathbf{D}$. The stress deviator is straightforwardly computed as that portion of the stress tensor that remains after the hydrostatic portion of subtracted off:

$$T'_{ij} = T_{ij} - p\delta_{ij} \tag{338}$$

where p are the hydrostatic pressures that correspond to $-3Ke$; with K being the material bulk modulus and e being the mean normal strain. An analogy is realizable between the viscous flow of a Newtonian fluid (as predicted by Equation (337)) and the *plastic flow* in a yielded metal as it experiences unrecoverable deformations. However, in the latter case, with a focus on perfect

plasticity, it is not expected that there should be a very significant rate effect on the strain; and thus the viscosity term ought to be replaced by a quantity that normalizes plastic deformation in a way that will hold the salient portion of the stress tensor constant.

Such thinking enables the Levy-Mises perfectly plastic constitutive equation to be written as:

$$\mathbf{T}' = \frac{k}{\sqrt{\mathbf{II}_D}}\mathbf{D} \tag{339}$$

where $\mathbf{II}_D$ is the second invariant of the rate of deformation tensor, $\mathbf{D}$. The use of invariants is natural, as invariance to reference frame is a requirement for any plasticity formulation. The nature of the parameter, k, may be explored by squaring the terms in Equation (339):

$$\mathbf{T}'\mathbf{T}' = \frac{k^2}{\mathbf{II}_D}\mathbf{D}\mathbf{D} \tag{340}$$

If plastic incompressibility is assumed, then tr $\mathbf{D} = 0$, and thus:

$$\mathbf{II}_D = \frac{1}{2}\mathbf{D}\mathbf{D} \tag{341}$$

which implies that:

$$k^2 = \frac{1}{2}\mathbf{T}'\mathbf{T}' \tag{342}$$

It is pointed out that by neglecting the elastic deformations (a requirement since it is only the incremental strains that are in the direction of the stresses; and not the total strains), and assuming incompressibility, then the rate of deformation tensor, $\mathbf{D}$, may subsequently be thought of as the plastic strain rate of the true strains. Additionally, the right hand side of Equation (342) is recognized as the second invariant of the deviatoric stress, as:

$$\mathbf{J}_2' = \mathbf{II}_{T'} = \frac{1}{2}\mathbf{T}'\mathbf{T}' \tag{343}$$

or stated explicitly:

$$k^2 = \mathbf{J}_2' \tag{344}$$

which, may then be thought of as the *yield condition*: furnishing the state of stress whereupon plastic flow is possible.

A fundamental property of a yield condition, $f(\sigma)$ is that it is always non-positive:

$$f(\mathbf{T}) \leq 0 \tag{345}$$

with this requirement in mind, a consideration of Equation (344) leads to a statement of the *von Mises yield criterion*:

$$f(\mathbf{J}_2') \equiv \sqrt{\mathbf{J}_2'} - k = 0 \tag{346}$$

Considering the case of pure shear (*i.e.* $T_{12} = T_{21} \neq 0$, with all other components vanishing), then the second invariant of the stress deviator is given as:

$$\mathbf{J}_2' = T_{12}^2 \tag{347}$$

and so the von Mises yield condition becomes:

$$\mid T_{12} \mid -k = 0 \tag{348}$$

which indicates that the von Mises yield condition is tied to the shear stress in the differential material volume surrounding a given point of interest in a material domain. Since the invariant, $\mathbf{J}_2'$ is proportional to the strain energy causing distortion of the material volume element, the von Mises yield criterion is sometimes referred to as a *strain energy density of distortion condition.*

Another interesting example emanates from the consideration of a uniaxial state of stress: $T_{11} = Y$. In this case, the deviatoric stress tensor may be expressed in Cartesian components as:

$$T_{ij}' = T_{ij} - \sigma\delta_{ij} \tag{349}$$

where σ is the *mean normal stress*:

$$\sigma = \frac{1}{3}T_{kk} = \frac{1}{3}Y \tag{350}$$

expanding the components of Equation (349) yields:

$$\begin{bmatrix} Y & 0 & 0 \\ 0 & 0 & 0 \\ 0 & 0 & 0 \end{bmatrix} - \begin{bmatrix} \frac{Y}{3} & 0 & 0 \\ 0 & \frac{Y}{3} & 0 \\ 0 & 0 & \frac{Y}{3} \end{bmatrix} = \begin{bmatrix} \frac{2}{3}Y & 0 & 0 \\ 0 & -\frac{Y}{3} & 0 \\ 0 & 0 & -\frac{Y}{3} \end{bmatrix} = T_{ij}' \tag{351}$$

the second invariant of the devatoric strain tensor yields:

$$\begin{aligned} \mathbf{II}_{T'} &= \frac{1}{2}T_{ij}'T_{ij}' \\ &= \frac{1}{2}\left[\left(\frac{2}{3}Y\right)^2 + \left(-\frac{Y}{3}\right)^2 + \left(-\frac{Y}{3}\right)^2\right] \\ &= \frac{1}{2}\left[\frac{4}{9}Y^2 + \frac{Y^2}{9} + \frac{Y^2}{9}\right] \\ &= \frac{Y^2}{3} \end{aligned} \tag{352}$$

Since $k^2 = \mathbf{II}_{T'}$, the following is observed:

$$k = \frac{Y}{\sqrt{3}} \tag{353}$$

thus implying that the von Mises yield criterion anticipates that that yield stress in, say, unixial tension will be $\sqrt{3}$ times the yield stress in pure shear. It is instructive to explicitly state some important properties of a yield criterion, and its generated *yield surface*.

Any yield criterion may be generically stated in terms of the properties of some function of stress, $f(\mathbf{T})$, stated explicitly as follows. In the case of *elastic* material response, one of two requirements must be satisfied:

$$f(\mathbf{T}) < 0 \tag{354}$$

or that

$$f(\mathbf{T}) = 0 \quad \text{and} \quad \frac{\partial f}{\partial T_{ij}} \dot{T}_{ij} < 0 \tag{355}$$

In the case where plastic deformations become admissible, the yield function satisfies the requirements:

$$f(\mathbf{T}) = 0 \quad \text{and} \quad \frac{\partial f}{\partial T_{ij}} \dot{T}_{ij} \geq 0 \tag{356}$$

A geometric interpretation may now be ascribed to the notion of the failure surface just described: it defines a locus of points in stress space within which stress points are elastic, and to the outside of which stress points may not venture. Where it is that a stress point impinges on the *failure surface*, defined by the locus of stress points satisfying the failure criterion, a *persistency condition* must be examined. To facilitate the geometric interpretation of such conditions, a specialization of the failure criterion, $f(\mathbf{T})$, for the case of the von Mises yield surface is now considered.

As noted earlier, the von Mises condition postulates an insensitivity to hydrostatic stress in the activation of plastification of FCC and BCC metals. Additionally, it assumed that yielded material is isotropic; and thus possesses no particular directionality. With this significant (and in the case of FCC and BCC metals, empirically justified), the von Mises failure criterion may be stated as:

$$f(\mathbf{T}) = f(\sigma_1, \sigma_2, \sigma_3) \tag{357}$$

or, alternatively, in terms of stress invariants:

$$f(\mathbf{T}) = f(\mathbf{J}_1, \mathbf{J}_2, \mathbf{J}_3) \tag{358}$$

Now, more specifically, it has already been stated that the von Mises yield criterion depends on the intensity of the deviatoric component of the stress, only, and thus the yield condition may be further specialized to be:

$$\frac{1}{6}\left[(\sigma_1 - \sigma_2)^2 + (\sigma_2 - \sigma_3)^2 + (\sigma_3 - \sigma_1)^2\right] - k^2 = 0 \tag{359}$$

The geometrical interpretation of Equation (359) is that of a cylinder in principal stress space oriented such that the generator defining the cylinder major axis is aligned with the vector $(\frac{1}{\sqrt{3}}, \frac{1}{\sqrt{3}}, \frac{1}{\sqrt{3}})$. This vector orientation defines the hydrostatic stress state. The slices through the von Mises yield surface that are taken such that the hydrostatic generator is orthogonal to them, are circular in shape. These circular cross sectional slices through the yield surface are sometimes referred to as Π-*planes*, or *deviatoric planes*, and define a purely deviatoric state of stress (if the hydrostatic point is ignored - as it can since the circular radius is independent of this state of stress). The persistency condition may now be re-visited through a consideration of a 2-D specialization of the von Mises yield criterion.

In considering the specific 2-D stress state associated with plane stress condition, then it may be assumed that $\sigma_3 = 0$. In such a circumstance the geometric condition is an elliptical intersection of the von Mises cylinder with the σ_1-σ_2 plane; as can be seen from the specialization of Equation (359) for the $\sigma_3 = 0$ case:

$$\begin{aligned} \frac{1}{6}\left[(\sigma_1 - \sigma_2)^2 + \sigma_2^2 + \sigma_1^2\right] &= k^2 \\ \frac{1}{3}\left[\sigma_1^2 - \sigma_1\sigma_2 + \sigma_2^2\right] &= k^2 \end{aligned} \tag{360}$$

or, by recalling that $k = \frac{Y}{\sqrt{3}}$:

$$\sigma_1^2 - \sigma_1\sigma_2 + \sigma_2^2 = Y^2 \tag{361}$$

In such a plane stress state, the stress point of interest, $\mathbf{Q}$, may be located using a position vector emanating from the origin in principal stress space, and ending with the particular intensity. The elliptical boundary of the von Mises failure surface, demarcating the admissible stress states from the inadmissible, provides some insight into the persistency condition furnished in Equations (355) and (364). In this case, the spatial derivatives in the persistency condition may be thought of as gradients, and so the inner product with the stress rate will provide some useful physical insight. Once again considering the requirements of a failure surface, the gradients and 2-D principal stress stress components may be considered using vector dot products (the dot products are admissible when considering the principal stress components; rather than the fully populated tensor). In the case of purely elastic response, it is required that

$$f(\mathbf{Q}) < 0 \tag{362}$$

or that

$$f(\mathbf{Q}) = 0 \quad \text{and} \quad \nabla f(\mathbf{Q}) \cdot \dot{\mathbf{Q}} < 0 \tag{363}$$

In the case where plastic deformations become admissible, the yield function satisfies the requirements:

$$f(\mathbf{Q}) = 0 \quad \text{and} \quad \nabla f(\mathbf{Q}) \cdot \dot{\mathbf{Q}} \geq 0 \tag{364}$$

From a consideration of the persistency condition it is seen that time rates of change that form a positive dot product with the outward normal to the yield surface ($\nabla f(\mathbf{Q})$) occur when the included angle between the two vectors is acute; and thus the time rate of change in stress, $\dot{\mathbf{Q}}$ is also pointing in a direction that is towards the outside of the yield surface. Conversely, the negative sign associated with the dot product in the elastic case implies that the time rate of change in the stress points towards the interior of the yield surface, and thus unloading is imminent. This information concerning the stress state needed to initiate plastic flow, and the concomitant effects of this on the nature of the yield surface, are useful and important. However, what is also required is some ability to understand the nature of the plastic deformations that accompany plastic flow. *Plastic potential theory* furnishes this insight.

The basic premise of plastic potential theory is that the plastic part of the rate of deformation is proportional to the gradient of some *plastic potential*, g:

$$\dot{\mathbf{q}} = \lambda \nabla g(\mathbf{T}) \tag{365}$$

In the case of a material that is assumed to exhibit *associative flow* during plastification, the plastic potential function, g, is assumed to coincide with the failure surface, and thus:

$$\dot{\mathbf{q}} = \lambda \nabla f(\mathbf{T}) \tag{366}$$

This assumption means that the plastic deformation is occurring in a direction that is parallel to the outer normal of the failure surface. In the case of the von Mises failure surface, this implies that plastic flow is occurring within the deviatoric plane, and thus plastic incompressibility follows. As a result of this, it is realized that the plastic portion of the rate of deformation now reduces down to the rate of change in the plastic portion of the rate of natural strains:

$$\dot{\epsilon}_p = \lambda \nabla f(\mathbf{T}) \tag{367}$$

The plastic potential theory can lend important insights into plasticity problems when considering materials that satisfy Drucker's requirements:

- the plastic work done by an external agency, during the application of some additional stresses, is positive
- the net total work performed by the external agency during the cycle of adding and removing stress is non-negative

The first of these requirements may sometimes be thought of as a *stability in the small* requirements; in that increments in stress (beyond some previous loading state) bring about positive work increments:

$$\dot{\mathbf{T}} \cdot \dot{\epsilon}_p > 0 \tag{368}$$

Beyond this requirement, there is also the requirement that the total work done by the external agency in taking the stress state, from some initial value, $\mathbf{T}^*$,

to some final condition, results in non-negative work:

$$(\mathbf{T} - \mathbf{T}^*) \cdot \dot{\epsilon}_p \geq 0 \tag{369}$$

This definition of stability in a work hardening sense is somewhat phenomenological in nature: having arisen from laboratory observations related to materials such as common metals. Basically what is being conceived of is a state of stress, $\mathbf{T}^*$, that arises from some deformation, $\mathbf{u}$. This stress is then incrementally changed to a new intensity, $\mathbf{T}$, on account of an incremental deformation, $\delta\mathbf{T}$. Now in Drucker's original theory, the increment in this work had to be positive; due to Drucker's first requirement related to stability in the small. However, if perfect plasticity is considered (as in the present discussion), then the theory must be amended to admit the possibility of neutral stability in the small, and so the new requirements become:

$$\dot{\mathbf{T}} \cdot \dot{\epsilon}_p = 0 \tag{370}$$

$$(\mathbf{T} - \mathbf{T}^*) \cdot \dot{\epsilon}_p \geq 0 \tag{371}$$

The first of these requirements is intuitive since in an associated flow theory, the plastic strain increment is in the direction of the outward normal of the yield surface in stress space. Additionally, since the stress point may never exit the interior of the yield surface, then infinitesimal plastic stress increments must occur in a direction that is tangent to the yield surface. This results in an orthogonality between the plastic stress increments and strains, respectively; a condition expressed in the condition of Equation (370). Additionally, Equation (371) requires that the the vector difference between two bound vectors, beginning at the origin in principal stress space, and ending at points $\mathbf{T}$ and $\mathbf{T}^*$, respectively, form an acute angle with the plastic strain increment, $\dot{\epsilon}_p$; by virtue of the dot product. As a result, convexity in the yield surface is assured in the case of a stable material, in the sense of Drucker. Likewise, this assumption further reinforces the notion that the strain increment ought to be parallel to the outward normal to the yield surface, as it is only this condition that will assure convexity (*i.e.* a plastic potential surface other than the yield surface would be problematic in such a context.)

3 Structural elements

So-called *structural elements* afford an efficient means analyzing the mechanical response of large and complex structural systems. To treat complex structures as an assemblage of continuum elements would result in enormous number of degrees of freedom; potentially making the solution impossible, or at the very least, impractical. Structural elements take advantage of an understanding of the salient mechanical responses of individual components making up a given structural system. With this understanding in mind, engineering theories (*e.g.* Bernoulli-Eluer and Timoshenko beam theories, Kirchhoff and Mindlin-Reissner plate theory, *etc.*) may be employed in a fundamental way during the finite element formulations leading to a given type of structural element.

3.1 3D Truss

In the case where a structural system comprises, in whole or in part, a collection of two force members (one at each end; collinear with the local member axis) then the idealization of a *truss finite element* is in order. The present discussion will lead to a 3-D nonlinear, large displacement, finite strain truss element.

3.1.1 Strain-displacement relations

Recalling the general form of the Green-Lagrange strain tensor, in tensor form:

$$\mathbf{E} = \frac{1}{2}\left[\mathbf{F}^T\mathbf{F} - \mathbf{I}\right] \tag{372}$$

and in index notation:

$$E_{ij} = \frac{1}{2}\left[\frac{\partial x_k}{\partial X_i}\frac{\partial x_k}{\partial X_j} - \delta_{ij}\right] \tag{373}$$

where x_k and X_k are the coordinates for the body points in the current and reference configurations, respectively. Continuing along this line, it is recalled that the displacement, u, relates the two configurations of the body:

$$x_k = X_k + u_k; \quad u_k(X_1, X_2, X_3, t) \tag{374}$$

This leads to the a re-statement of the Green-Lagrange strain as:

$$E_{ij} = \frac{1}{2}\left[\frac{\partial\left(X_k + u_k\right)}{\partial X_i}\frac{\partial\left(X_k + u_k\right)}{\partial X_j} - \delta_{ij}\right] \tag{375}$$

Recalling from the one dimensional strain state occurring within a truss element (Equation (239)), a specialization finite Green-Lagrange strain is now possible:

$$\begin{aligned}
E_{11} &= \frac{1}{2}\left[\frac{\partial\left(X_1 + u_1\right)}{\partial X_1}\frac{\partial\left(X_1 + u_1\right)}{\partial X_1} + \frac{\partial\left(X_2 + u_2\right)}{\partial X_1}\frac{\partial\left(X_2 + u_2\right)}{\partial X_1} + \frac{\partial\left(X_3 + u_3\right)}{\partial X_1}\frac{\partial\left(X_3 + u_3\right)}{\partial X_1} - 1\right] \\
&= \frac{1}{2}\left[\left(1 + \frac{\partial u_1}{\partial X_1}\right)\left(1 + \frac{\partial u_1}{\partial X_1}\right) + \frac{\partial u_2}{\partial X_1}\frac{\partial u_2}{\partial X_1} + \frac{\partial u_3}{\partial X_1}\frac{\partial u_3}{\partial X_1} - 1\right] \\
&= \frac{1}{2}\left[1 + 2\frac{\partial u_1}{\partial X_1} + \frac{\partial u_1}{\partial X_1}\frac{\partial u_1}{\partial X_1} + \frac{\partial u_2}{\partial X_1}\frac{\partial u_2}{\partial X_1} + \frac{\partial u_3}{\partial X_1}\frac{\partial u_3}{\partial X_1} - 1\right] \\
&= \frac{\partial u_1}{\partial X_1} + \frac{1}{2}\left[\left(\frac{\partial u_1}{\partial X_1}\right)^2 + \left(\frac{\partial u_2}{\partial X_1}\right)^2 + \left(\frac{\partial u_3}{\partial X_1}\right)^2\right]
\end{aligned} \tag{376}$$

In the foregoing, the X_1, X_2, X_3 axes correspond to the X, Y, and, Z axes, respectively, depicted in Figure (12).

As in Section 1.3, a linear interpolation of the displacements and coordinates will be employed (*i.e.* a linear isoparametric formulation); with the shape functions once again taking the form:

$$h_1(\xi) = \frac{1}{2}(1 - \xi) \tag{377}$$

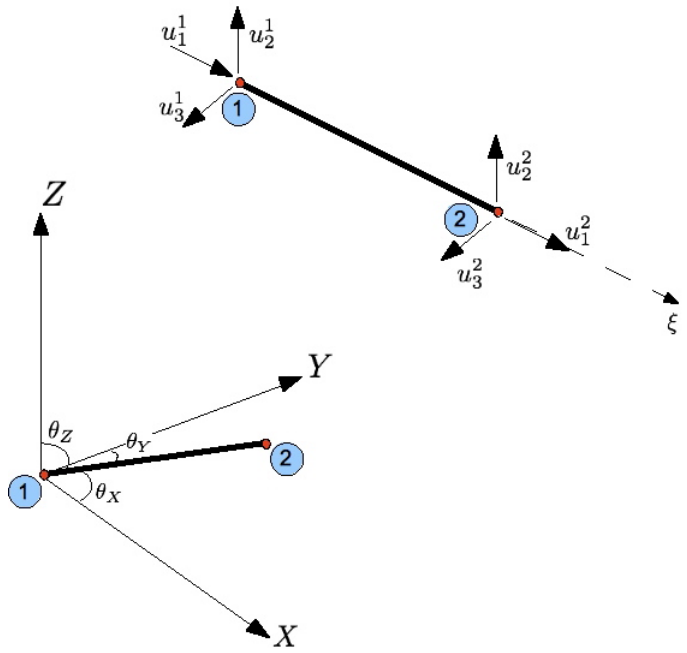

Figure 12: Parent element for nonlinear 3-D truss formulation

$$h_2(\xi) = \frac{1}{2}(1+\xi) \tag{378}$$

thus enabling the displacements and coordinates to be described in a continuous fashion, by way of discrete nodal values, as:

$$X(\xi) = \Sigma_{i=1}^{2} h_i(\xi) X_i \tag{379}$$

where X_i are the *nodal coordinates* (with respect to the coordinate of the physical system) associated with the member ends; and

$$U(\xi) = \Sigma_{i=1}^{2} h_i(\xi) U_i \tag{380}$$

where U_i are the *nodal displacements* (with respect to the coordinate of the physical system) associated with the member ends. These interpolated fields may subsequently be used in the development of a Green-Lagrange strain - displacement relationship.

Consider an application of the chain rule to the case of uniaxial Green-Lagrange strain; in reference to the case depicted in Figure (12):

$$E_{11} = \frac{\partial u_1}{\partial \xi}\frac{\partial \xi}{\partial X_1} + \frac{1}{2}\left[\left(\frac{\partial u_1}{\partial \xi}\frac{\partial \xi}{\partial X_1}\right)^2 + \left(\frac{\partial u_2}{\partial \xi}\frac{\partial \xi}{\partial X_1}\right)^2 + \left(\frac{\partial u_3}{\partial \xi}\frac{\partial \xi}{\partial X_1}\right)^2\right] \tag{381}$$

It is thus possible to use the expressions from Equations (379) and (380) to resolve the derivatives appearing in (381):

$$\frac{\partial u_k}{\partial X_1} = \sum_{i=1}^{2} \frac{\partial h_i(\xi)}{\partial \xi} \frac{\partial \xi}{\partial X_1} u_k^i \tag{382}$$

where u_k^i denotes the $k-th$ displacement component at local, parent node i. The derivatives of the shape functions follow directly from Equations (377) and (378):

$$\begin{aligned} \frac{\partial h_1(\xi)}{\partial \xi} &= -\frac{1}{2} \\ \frac{\partial h_2(\xi)}{\partial \xi} &= \frac{1}{2} \end{aligned} \tag{383}$$

and thus, the local displacement derivative becomes:

$$\begin{aligned} \frac{\partial u_k}{\partial \xi} &= \sum_{i=1}^{2} \frac{\partial h_i(\xi)}{\partial \xi} u_k^i \\ &= \frac{u_k^2 - u_k^1}{2} \end{aligned} \tag{384}$$

A similar consideration of the nodal coordinates yields:

$$\frac{\partial X_1}{\partial \xi} = \frac{X_1^2 - X_1^1}{2} = \frac{L}{2} \tag{385}$$

where L is the actual member length associated with the parent element mapped into the finite element.

The chain rule may now be applied to Equation (382), thus furnishing:

$$\frac{\partial u_k}{\partial X_1} = \frac{u_k^2 - u_k^1}{L} \tag{386}$$

This result is helpful when considering that the first term on the right hand side of Equation (381) is nothing more than the 1-1 component of linear infinitesimal strain tensor (*i.e. engineering strain*), ϵ_{11}, and thus an extension of the standard strain-siaplcement relation from Equation (241) follows as:

$$\begin{aligned} \epsilon_{11} &= \frac{\partial u_1}{\partial \xi} \frac{\partial \xi}{\partial X_1} = \frac{2}{L} \frac{\partial u_1}{\partial \xi} = \frac{2}{L} \left(\frac{u_1^2 - u_1^1}{2} \right) = \frac{1}{L} \left(u_1^2 - u_1^1 \right) \\ &= \mathbf{B}_L \mathbf{u} \end{aligned} \tag{387}$$

or in matrix form:

$$\epsilon_{11} = \frac{1}{L} \begin{bmatrix} -1 & 0 & 0 & 1 & 0 & 0 \end{bmatrix} \begin{bmatrix} u_1^1 \\ u_2^1 \\ u_3^1 \\ u_1^2 \\ u_2^2 \\ u_3^2 \end{bmatrix} \tag{388}$$

Likewise, the nonlinear strain displacement follows from a consideration of bracketed remainder of Equation (381):

$$\begin{aligned}
\eta_{11} &= \frac{1}{2}\left[\left(\frac{\partial u_1}{\partial \xi}\frac{\partial \xi}{\partial X_1}\right)^2 + \left(\frac{\partial u_2}{\partial \xi}\frac{\partial \xi}{\partial X_1}\right)^2 + \left(\frac{\partial u_3}{\partial \xi}\frac{\partial \xi}{\partial X_1}\right)^2\right] \\
&= \frac{1}{2}\left[\left(\frac{\partial u_1}{\partial \xi}\frac{2}{L}\right)^2 + \left(\frac{\partial u_2}{\partial \xi}\frac{2}{L}\right)^2 + \left(\frac{\partial u_3}{\partial \xi}\frac{2}{L}\right)^2\right] \\
&= \frac{2}{L^2}\left[\left(\frac{\partial u_1}{\partial \xi}\right)^2 + \left(\frac{\partial u_2}{\partial \xi}\right)^2 + \left(\frac{\partial u_3}{\partial \xi}\right)^2\right] \\
&= \frac{2}{L^2}\left[\left(\frac{u_1^2 - u_1^1}{2}\right)^2 + \left(\frac{u_2^2 - u_2^1}{2}\right)^2 + \left(\frac{u_3^2 - u_3^1}{2}\right)^2\right] \\
&= \frac{1}{2L^2}\left[\left(u_1^2 - u_1^1\right)^2 + \left(u_2^2 - u_2^1\right)^2 + \left(u_3^2 - u_3^1\right)^2\right] \\
&= \frac{1}{2}\mathbf{u}^T\mathbf{B}_{NL}^T\mathbf{B}_{NL}\mathbf{u}
\end{aligned} \tag{389}$$

Thus resulting in a matrix expression of the form:

$$\eta_{11} = \frac{1}{2}\frac{1}{L}\begin{bmatrix} u_1^1 & u_2^1 & u_3^1 & u_1^2 & u_2^2 & u_3^2 \end{bmatrix}\begin{bmatrix} -1 & 0 & 0 \\ 0 & -1 & 0 \\ 0 & 0 & -1 \\ 1 & 0 & 0 \\ 0 & 1 & 0 \\ 0 & 0 & 1 \end{bmatrix}\frac{1}{L}\begin{bmatrix} -1 & 0 & 0 & 1 & 0 & 0 \\ 0 & -1 & 0 & 0 & 1 & 0 \\ 0 & 0 & -1 & 0 & 0 & 1 \end{bmatrix}\begin{bmatrix} u_1^1 \\ u_2^1 \\ u_3^1 \\ u_1^2 \\ u_2^2 \\ u_3^2 \end{bmatrix} \tag{390}$$

The forgoing strain-displacement relations are useful when forming the *tangent stiffness matrix* for the 3-D nonlinear truss finite element.

3.1.2 Tangent stiffness matrix

An equivalent approach to the explicit consideration of the weak form reviewed in Section 1.2, the *principle of virtual work* is oftentimes employed in the formulation of structural elements. This principle takes as axiomatic the fact that internal virtual work will balance external virtual work. The *virtual* moniker is applied to notional (*i.e.* not real) displacements that are *kinematically admissible*; meaning that they satisfy the Dirichlet (essential) boundary conditions of the problem under consideration. The balance in virtual work may be expressed concisely as (δ denotes a virtual quantity):

$$\int_\Omega \delta\mathbf{E} : \mathbf{S}\, d\Omega = \int_\Omega \delta\mathbf{u}\cdot\mathbf{b}\, d\Omega + \int_{\partial\Omega} \delta\mathbf{u}\cdot\mathbf{f}\, d\partial\Omega \tag{391}$$

where $\mathbf{E}$ is the Green-Lagrage strain tensor, $\mathbf{S}$ is the PK2 stress tensor, $\mathbf{u}$ is the displacement vector, $\mathbf{b}$ is any body force, and $\mathbf{f}$ represents any externally

applied surface tractions. In Equation (391), the left hand integral represents the internal work (where : denotes the tensor scalar product), and the right hand side represents the external virtual work. In taking virtual work as the point of departure, the 3-D truss element tangent stiffness may be derived.

The internal work within a truss element emanates from the consideration of axial deformations as:

$$U = \int_{\Omega} \bar{U}\, d\Omega; \quad \bar{U} = \delta\mathbf{E} : \mathbf{S} \tag{392}$$

where $\bar{U}$ is known as the *strain energy density*. Using a the appropriate elasticity tensor, the strain energy may be re-expressed as:

$$\bar{U} = \delta\mathbf{E} : \mathbf{CE} \tag{393}$$

where $\mathbf{C}$ is the fourth order material tensor that relates Green-Lagrange strain and PK2 stress. This result may be simplified for the case of the 3-D truss element, wherein the *actual* internal strain energy under axial deformation may be expressed as:

$$U_T = \frac{1}{2} C E_{11}^2 \tag{394}$$

where the squared Green-Lagrange strain term may be expanded to be:

$$\begin{aligned} E_{11}^2 = \left(\frac{\partial u_1}{\partial X_1}\right)^2 + \frac{\partial u_1}{\partial X_1}\left[\left(\frac{\partial u_1}{\partial X_1}\right)^2 + \left(\frac{\partial u_2}{\partial X_1}\right)^2 + \left(\frac{\partial u_3}{\partial X_1}\right)^2\right] \\ + \frac{1}{4}\left[\left(\frac{\partial u_1}{\partial X_1}\right)^2 + \left(\frac{\partial u_2}{\partial X_1}\right)^2 + \left(\frac{\partial u_3}{\partial X_1}\right)^2\right]^2 \end{aligned} \tag{395}$$

the last term is subsequently neglected as a small quantity squared. The actual strain energy may then be expressed as an integral over the truss volume:

$$\begin{aligned} U_T &= \frac{1}{2} C \int_V \left(\frac{\partial u_1}{\partial X_1}\right)^2 dV + \frac{1}{2} C \int_V \frac{\partial u_1}{\partial X_1}\left[\left(\frac{\partial u_1}{\partial X_1}\right)^2 + \left(\frac{\partial u_2}{\partial X_1}\right)^2 + \left(\frac{\partial u_3}{\partial X_1}\right)^2\right] dV \\ &= \frac{1}{2} CA \int_X \left(\frac{\partial u_1}{\partial X_1}\right)^2 dX + \int_X \frac{1}{2} CA \frac{\partial u_1}{\partial X_1}\left[\left(\frac{\partial u_1}{\partial X_1}\right)^2 + \left(\frac{\partial u_2}{\partial X_1}\right)^2 + \left(\frac{\partial u_3}{\partial X_1}\right)^2\right] dX \\ &= \frac{1}{2} CA \int_X \left(\frac{\partial u_1}{\partial X_1}\right)^2 dX + \frac{P}{2} \int_X \left[\left(\frac{\partial u_1}{\partial X_1}\right)^2 + \left(\frac{\partial u_2}{\partial X_1}\right)^2 + \left(\frac{\partial u_3}{\partial X_1}\right)^2\right] dX \end{aligned} \tag{396}$$

where C is the relevant uniaxial component from the constitutive tensor $\mathbf{C}$, and P is the member internal force; formed by combining the linear strain term with the material constant and cross-sectional area. As it is that the actual and virtual work are related to one another through the fractional value $\frac{1}{2}$ (as well

as a splitting of the displacements into their real and virtual counterparts), the foregoing may be restated in terms of virtual internal force; along with the use of the strain-displacement relations, developed previously within this section:

$$
\begin{aligned}
U &= CA \int_X \left(\frac{\partial u_1}{\partial X_1} \right)^2 \, dX + P \int_X \left[\left(\frac{\partial u_1}{\partial X_1} \right)^2 + \left(\frac{\partial u_2}{\partial X_1} \right)^2 + \left(\frac{\partial u_3}{\partial X_1} \right)^2 \right] \, dX \\
&\Rightarrow CA \int_{-1}^{1} \mathbf{B}_L^T \mathbf{B}_L \mid J \mid d\xi + P \int_{-1}^{1} \mathbf{B}_{NL}^T \mathbf{B}_{NL} \mid J \mid d\xi \\
&= CA \int_{-1}^{1} \frac{1}{L} \begin{bmatrix} -1 \\ 0 \\ 0 \\ 1 \\ 0 \\ 0 \end{bmatrix} \frac{1}{L} \begin{bmatrix} -1 & 0 & 0 & 1 & 0 & 0 \end{bmatrix} \mid \frac{L}{2} \mid d\xi \\
&+ P \int_{-1}^{1} \frac{1}{L} \begin{bmatrix} -1 & 0 & 0 \\ 0 & -1 & 0 \\ 0 & 0 & -1 \\ 1 & 0 & 0 \\ 0 & 1 & 0 \\ 0 & 0 & 1 \end{bmatrix} \frac{1}{L} \begin{bmatrix} -1 & 0 & 0 & 1 & 0 & 0 \\ 0 & -1 & 0 & 0 & 1 & 0 \\ 0 & 0 & -1 & 0 & 0 & 1 \end{bmatrix} \mid \frac{L}{2} \mid d\xi
\end{aligned}
\tag{397}
$$

subsequently expanding to:

$$
\begin{aligned}
U = &\frac{CA}{L} \begin{bmatrix} 1 & 0 & 0 & -1 & 0 & 0 \\ 0 & 0 & 0 & 0 & 0 & 0 \\ 0 & 0 & 0 & 0 & 0 & 0 \\ -1 & 0 & 0 & 1 & 0 & 0 \\ 0 & 0 & 0 & 0 & 0 & 0 \\ 0 & 0 & 0 & 0 & 0 & 0 \end{bmatrix} \\
&+ \frac{P}{L} \begin{bmatrix} 1 & 0 & 0 & -1 & 0 & 0 \\ 0 & 1 & 0 & 0 & -1 & 0 \\ 0 & 0 & 1 & 0 & 0 & -1 \\ -1 & 0 & 0 & 1 & 0 & 0 \\ 0 & -1 & 0 & 0 & 1 & 0 \\ 0 & 0 & -1 & 0 & 0 & 1 \end{bmatrix}
\end{aligned}
\tag{398}
$$

The foregoing lead immediately to the tangent stiffness matrix:

$$
\mathbf{K}_T = \mathbf{K}_L + \mathbf{K}_{NL} \tag{399}
$$

where,

$$\mathbf{K}_L = \frac{CA}{L}\begin{bmatrix} 1 & 0 & 0 & -1 & 0 & 0 \\ 0 & 0 & 0 & 0 & 0 & 0 \\ 0 & 0 & 0 & 0 & 0 & 0 \\ -1 & 0 & 0 & 1 & 0 & 0 \\ 0 & 0 & 0 & 0 & 0 & 0 \\ 0 & 0 & 0 & 0 & 0 & 0 \end{bmatrix} \tag{400}$$

and,

$$\mathbf{K}_{NL} = \frac{P}{L}\begin{bmatrix} 1 & 0 & 0 & -1 & 0 & 0 \\ 0 & 1 & 0 & 0 & -1 & 0 \\ 0 & 0 & 1 & 0 & 0 & -1 \\ -1 & 0 & 0 & 1 & 0 & 0 \\ 0 & -1 & 0 & 0 & 1 & 0 \\ 0 & 0 & -1 & 0 & 0 & 1 \end{bmatrix} \tag{401}$$

the *linear* and *initial stress* stiffness matrices, respectively.

3.1.3 Member internal force calculation

As can be recalled from Figure (9), the tangent stiffness is used during each iteration, within a given solution increment, to propose updated displacements for use in the evolving nonlinear solution. These proposed displacement are subsequently used to arrive at the correct internal forces, $\mathbf{F}$, (*i.e.* no linearization is used, as compared with the tangent stiffness matrix; which can be viewed as a linearization of a Taylor series expansion carried out about a solution point). In the case of the current 3-D nonlinear truss finite element, the internal force calculation involves the PK2 stress, which may be obtained through an inversion of Equation (108):

$$\mathbf{S} = \frac{\rho_o}{\rho}\mathbf{F}^{-1}\,\sigma\,\mathbf{F}^{-T} \tag{402}$$

In a truss element, the deformation gradient may simply be stated as the ratio of the current length, ${}^tL$, to the initial length, ${}^0L$; and thus the PK2 stress for the truss element becomes:

$${}^t_oS_{11} = \frac{{}^o\rho}{{}^t\rho}\left(\frac{{}^oL}{{}^tL}\right)^2 {}^t\sigma_{11} \tag{403}$$

in the case of a total Lagrangian formulation. It is immediately recognized that the Cauchy stress in the current state is nothing more than the the current internal axial force, ${}^tP$, divided by the current area; this, in conjunction with the definition of the current length, results in:

$${}^t_oS_{11} = \frac{{}^o\rho}{{}^t\rho}\left(\frac{{}^oL}{{}^oL + \Delta L}\right)^2 \frac{{}^tP}{{}^tA} \tag{404}$$

from the conservation of mass, it is further recognized that:

$${}^o\rho\,{}^oL\,{}^oA = {}^t\rho\,({}^oL + \Delta L)\,{}^tA \tag{405}$$

whereupon the current area, ${}^{t}A$, is seen to be:

$$ {}^{t}A = \frac{{}^{o}\rho {}^{o}L {}^{o}A}{{}^{t}\rho \left({}^{o}L + \Delta L \right)} \tag{406} $$

Substitution of the foregoing into Equation (404) results in:

$$ {}^{t}_{o}S_{11} = \frac{{}^{o}L}{{}^{o}L + \Delta L} \frac{{}^{t}P}{{}^{o}A} \tag{407} $$

From which the current internal axial force can be solved for:

$$ {}^{t}P = {}^{t}_{o} S_{11} {}^{o}A \frac{{}^{o}L + \Delta L}{{}^{o}L} \tag{408} $$

The axial component of the PK2 stress can be obtained directly from the axial component of the Green-Lagrange strain as:

$$ {}^{t}_{o}S_{11} = C \left(\frac{\Delta L}{{}^{o}L} + \frac{1}{2} \left(\frac{\Delta L}{{}^{o}L} \right)^{2} \right) \tag{409} $$

where C is the appropriate component of the constitutive matrix. The results from Equation (409) may be used in Equation (408) to directly obtain the internal axial force for the element:

$$ {}^{t}P = {}^{o}AC \left(\frac{\Delta L}{{}^{o}L} + \frac{1}{2} \left(\frac{\Delta L}{{}^{o}L} \right)^{2} \right) \left(\frac{{}^{o}L + \Delta L}{{}^{o}L} \right) \tag{410} $$

The internal force vector $\mathbf{F}$ may be obtained directly from a coordinate transformation involving the following direction cosines (corresponding to the angles depicted in Figure (12):

- $l = \cos(\theta_x)$
- $m = \cos(\theta_y)$
- $n = \cos(\theta_z)$

These same direction cosines may be used within a coordinate transformation matrix in order to arrive at a more convenient representation of the linear stiffness matrix, $\mathbf{K}_L$:

$$ \mathbf{K}_L = \frac{CA}{L} \begin{bmatrix} l^2 & lm & ln & -l^2 & -lm & -ln \\ lm & m^2 & mn & -lm & -m^2 & -mn \\ ln & mn & n^2 & -ln & -mn & -n^2 \\ -l^2 & -lm & -ln & l^2 & lm & ln \\ -lm & -m^2 & -mn & lm & m^2 & mn \\ -ln & -mn & -n^2 & ln & mn & n^2 \end{bmatrix} \tag{411} $$

It is pointed out that the initial stress matrix, $\mathbf{K}_{NL}$, requires no such transformation.

3.2 3D Beam

The nonlinear truss element is a useful point of departure for the consideration of a doubly symmetric, prismatic nonlinear frame element. Additional responses can be layered on top of the fundamental truss behavior, so as to construct the desired frame element behavior. However, unlike the nonlinear truss, that can be formulated within either a total or updated Lagrangian reference frame, the subsequent frame element is intended for use in an updated Lagrangian reference frame only (do to certain assumptions that are discussed in the sequel).

Consider a classical Bernoulli-Euler description of flexural kinematics; along with the assumption of small strains. The flexural normal components of the strain may then be approximated as:

$$\epsilon = d_y \left(\frac{d^2 y\left(x\right)}{dx^2} \right) + d_z \left(\frac{d^2 z\left(x\right)}{dx^2} \right) \tag{412}$$

where the quantities d_y and d_z represent the perpendicular distances, measured along the y and z axes, respectively, from the relevant flexural neutral surface. Additionally, the quantities $y\left(x\right)$ and $z\left(x\right)$ denote the component of the total beam deflection measured using the y and z axes, respectively.

Adopting the notation associated with the frame parent element depicted in Figure (13), an extension of the 1-1 component of the Green-Lagrange strain,

$$E_{11} = \frac{\partial u_1}{\partial X_1} + \frac{1}{2} \left[\left(\frac{\partial u_1}{\partial X_1} \right)^2 + \left(\frac{\partial u_2}{\partial X_1} \right)^2 + \left(\frac{\partial u_3}{\partial X_1} \right)^2 \right] \tag{413}$$

may be carried out.

Neglecting any stretching and rotation of the element mid-line ξ (in this discussion it is assumed that ξ and X_1 coincide), the Bernoulli-Euler flexural normal strains may simply be added to the foregoing statement of E_{11}:

$$E_{11} = \frac{\partial u_1}{\partial X_1} + \eta \left(\frac{\partial^2 u_2}{\partial X_1^2} \right) + \zeta \left(\frac{\partial^2 u_3}{\partial X_1^2} \right) + \frac{1}{2} \left[\left(\frac{\partial u_1}{\partial X_1} \right)^2 + \left(\frac{\partial u_2}{\partial X_1} \right)^2 + \left(\frac{\partial u_3}{\partial X_1} \right)^2 \right] \tag{414}$$

Additionally, the kinematics associated with uniform torsion within an arbitrary cross-section may be given as:

$$\begin{aligned} u_2 &= -\zeta u_4 \\ u_3 &= \eta u_4 \end{aligned} \tag{415}$$

where η and ζ are the local parent element axes that are orthogonal to ξ, and coincident with the principal centroidal axes of the cross-section, X_2 and X_3, respectively (assuming a doubly symmetric, as well as prismatic, section). Taking

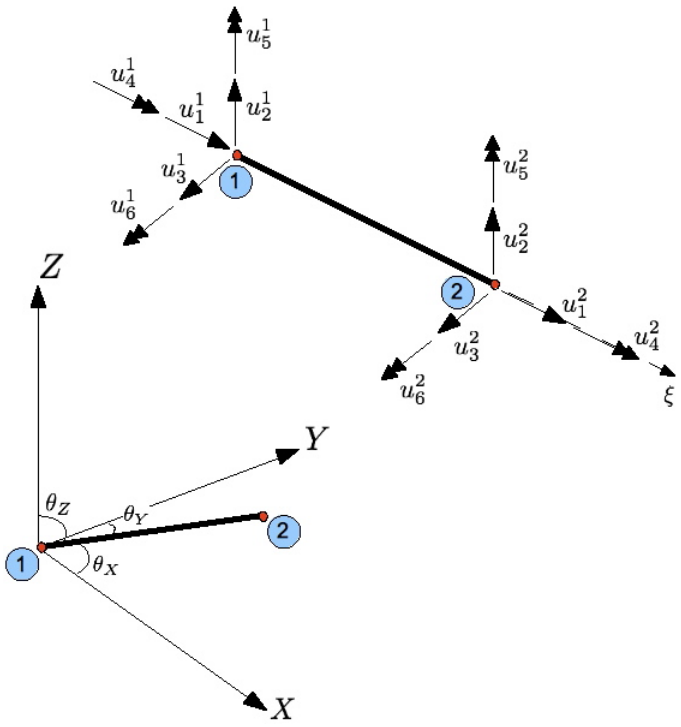

Figure 13: Parent element for nonlinear 3-D frame formulation

derivatives, the following is obtained:

$$\begin{aligned}\frac{\partial u_2}{\partial X_1} &= -\zeta \frac{\partial u_4}{\partial X_1} \\ \frac{\partial u_3}{\partial X_1} &= \eta \frac{\partial u_4}{\partial X_1}\end{aligned} \tag{416}$$

The foregoing may be added, as another quadratic term, to Equation (414); subsequently yielding:

$$\begin{aligned}E_{11} = \frac{\partial u_1}{\partial X_1} + \eta \left(\frac{\partial^2 u_2}{\partial X_1^2} \right) + \zeta \left(\frac{\partial^2 u_3}{\partial X_1^2} \right) \\ + \frac{1}{2} \left[\left(\frac{\partial u_1}{\partial X_1} \right)^2 + \left(\frac{\partial u_2}{\partial X_1} - \zeta \frac{\partial u_4}{\partial X_1} \right)^2 + \left(\frac{\partial u_3}{\partial X_1} + \eta \frac{\partial u_4}{\partial X_1} \right)^2 \right]\end{aligned} \tag{417}$$

Now that the cross-sectional normal strains have been identified for the frame element, the discussion may now switch to the selection of interpolation functions for each of the relevant displacement components.

As before in the nonlinear truss element, it will be assumed that a linear interpolation of the extensional displacements is suitable for use in the frame element (but this time expressed using the actual finite element dimensions, and not the parent element coordinates):

$$u_1(x) = \left(1 - \frac{x}{L}\right) u_1^1 + \frac{x}{L} u_1^2 \tag{418}$$

subsequently leading to the identification of the axial interpolation polynomial prototypes as:

$$\begin{aligned}h_1(x) &= \left(1 - \frac{x}{L}\right) \\ h_2(x) &= \frac{x}{L}\end{aligned} \tag{419}$$

Likewise, the twist is assumed to be distributed linearly between the nodes of the parent element as:

$$u_4(x) = \left(1 - \frac{x}{L}\right) u_4^1 + \frac{x}{L} u_4^2 \tag{420}$$

also, leading to interpolation polynomials of the same form as described in Equation (419). In the case of flexural deformations, use of the slope-deflection equations lead to a description of the transverse displacements as:

$$\begin{aligned}u_2(x) = \left[1 - 3\left(\frac{x}{L}\right)^2 + 2\left(\frac{x}{L}\right)^3\right] u_2^1 + \left[3\left(\frac{x}{L}\right)^2 - 2\left(\frac{x}{L}\right)^3\right] u_2^2 \\ + x\left(1 - \frac{x}{L}\right)^2 u_6^1 + x\left[\left(\frac{x}{L}\right)^2 - \frac{x}{L}\right] u_6^2\end{aligned} \tag{421}$$

subsequently leading to the following interpolation function prototypes (useful within either bending context):

$$
\begin{aligned}
h_1(x) &= 1 - 3\left(\frac{x}{L}\right)^2 + 2\left(\frac{x}{L}\right)^3 \\
h_2(x) &= 3\left(\frac{x}{L}\right)^2 - 2\left(\frac{x}{L}\right)^3 \\
h_3(x) &= x\left(1 - \frac{x}{L}\right)^2 \\
h_4(x) &= x\left[\left(\frac{x}{L}\right)^2 - \frac{x}{L}\right]
\end{aligned}
\tag{422}
$$

The foregoing interpolation polynomials may be employed within the framework of the principle of virtual work to arrive at the stiffness matrices for the frame element depicted in Figure (13).

Employing the principle of virtual work from elementary mechanics, in conjunction with each of the terms within Equation (417), along with their physical basis, yields:

$$
\begin{aligned}
\delta W_{int} = & \int_0^L \left(\frac{\partial u_1}{\partial X_1}\right) CA \left(\frac{\partial \delta u_1}{\partial X_1}\right) dX_1 \\
& + \int_0^L \left(\frac{\partial^2 u_2}{\partial X_1^2}\right) CI_\eta \left(\frac{\partial^2 \delta u_2}{\partial X_1^2}\right) dX_1 \\
& + \int_0^L \left(\frac{\partial^2 u_3}{\partial X_1^2}\right) CI_\zeta \left(\frac{\partial^2 \delta u_3}{\partial X_1^2}\right) dX_1 \\
& + \frac{1}{2} P \int_0^L \left[\delta\left(\frac{\partial u_1}{\partial X_1}\right)^2 + \delta\left(\frac{\partial u_2}{\partial X_1}\right)^2 + \delta\left(\frac{\partial u_3}{\partial X_1}\right)^2\right] dX_1 \\
& + \frac{1}{2} \int_0^L \int_A \sigma_{11}\, \delta\left(\frac{\partial u_4}{\partial X_1}\right)^2 \left(\eta^2 + \zeta^2\right) dA\, dX_1 \\
& - M_\eta \int_0^L \delta\left(\frac{\partial u_2}{\partial X_1}\frac{\partial u_4}{\partial X_1}\right) dX_1 + M_\zeta \int_0^L \delta\left(\frac{\partial u_3}{\partial X_1}\frac{\partial u_4}{\partial X_1}\right) dX_1
\end{aligned}
\tag{423}
$$

where C is the elastic modulus in the 1-1 direction, and with I_η and I_ζ being the second moments of the area about the X_2 and X_3 axes, respectively. The last integral term expresses the torsional work done by the projection of the applied moment onto the flexurally deformed neutral axis; while the second to last integral in Equation (423) arises out of a virtual warping strain causing the axial stress, σ_{11}, to add to the virtual work associated with the member. Additionally recognizing that the area integration of the term $\left(\eta^2 + \zeta^2\right)$ yields the St. Venant Torsion Constant, I_p, and that $\sigma_{11} = \frac{P}{A}$ (where P is the member

axial force) results in the following simplification:

$$\begin{aligned}\delta W_{int} = &\int_0^L \left(\frac{\partial u_1}{\partial X_1}\right) CA \left(\frac{\partial \delta u_1}{\partial X_1}\right) dX_1 \\ &+ \int_0^L \left(\frac{\partial^2 u_2}{\partial X_1^2}\right) CI_\eta \left(\frac{\partial^2 \delta u_2}{\partial X_1^2}\right) dX_1 \\ &+ \int_0^L \left(\frac{\partial^2 u_3}{\partial X_1^2}\right) CI_\zeta \left(\frac{\partial^2 \delta u_3}{\partial X_1^2}\right) dX_1 \\ &+ \frac{1}{2} P \int_0^L \left[\delta \left(\frac{\partial u_1}{\partial X_1}\right)^2 + \delta \left(\frac{\partial u_2}{\partial X_1}\right)^2 + \delta \left(\frac{\partial u_3}{\partial X_1}\right)^2\right] dX_1 \\ &+ \frac{PI_p}{2A} \int_0^L \delta \left(\frac{\partial u_4}{\partial X_1}\right)^2 dX_1 \\ &- M_\eta \int_0^L \delta \left(\frac{\partial u_2}{\partial X_1}\frac{\partial u_4}{\partial X_1}\right) dX_1 + M_\zeta \int_0^L \delta \left(\frac{\partial u_3}{\partial X_1}\frac{\partial u_4}{\partial X_1}\right) dX_1 \end{aligned} \tag{424}$$

Up until now, a consideration of only cross-sectional normal stresses has been adopted when forming the statement of virtual work leading to the element matrices needed for the frame element formulation. Indeed, many typical frame elements might stop at this point and make a substitution using the previously obtained interpolation polynomials, and leave it at that. Such an approach would properly account for the nonlinear coupling of axial force and flexure within the frame element, but would not correctly consider the coupling between St. Venant's torsion and flexure. To extend the present formulation to include the nonlinear coupling of uniform torsion and flexure, the nonlinear portion of the Green-Lagrange strain must be extended beyond the 1-1 component, and subsequently made to admit the presence of transverse shearing forces (and their subsequent shearing stresses - arrived at by considering equilibrium alone, as the Bernoulli-Euler theory will not admit shearing deformations, itself).

So in extending the frame element formulation to properly account for the coupling between uniform torsion and flexure, the nonlinear term from the Green-Lagrange strain, E_{nl}, must be once again examined:

$$E_{nl} = \frac{1}{2}\left(\frac{\partial u_k}{\partial X_i}\frac{\partial u_k}{\partial X_j}\right) \tag{425}$$

neglecting the axial terms (which have already been taken into consideration in Equation (424)), the following is obtained:

$$\begin{aligned} E_{nl} = &\frac{1}{2}\left[2\frac{\partial u_1}{\partial X_1}\frac{\partial u_1}{\partial X_2} + 2\frac{\partial u_2}{\partial X_1}\frac{\partial u_2}{\partial X_2} + 2\frac{\partial u_3}{\partial X_1}\frac{\partial u_3}{\partial X_2}\right] + \\ &\frac{1}{2}\left[2\frac{\partial u_1}{\partial X_1}\frac{\partial u_1}{\partial X_3} + 2\frac{\partial u_2}{\partial X_1}\frac{\partial u_2}{\partial X_3} + 2\frac{\partial u_3}{\partial X_1}\frac{\partial u_3}{\partial X_3}\right] + \\ &\frac{1}{2}\left[2\frac{\partial u_1}{\partial X_2}\frac{\partial u_1}{\partial X_3} + 2\frac{\partial u_2}{\partial X_2}\frac{\partial u_2}{\partial X_3} + 2\frac{\partial u_3}{\partial X_2}\frac{\partial u_3}{\partial X_3}\right] \end{aligned} \tag{426}$$

The forgoing may be simplified by recognizing that in-plane distortions are neglected (*i.e.* $\frac{\partial u_2}{\partial X_2} = \frac{\partial u_3}{\partial X_3} = 0$):

$$\begin{aligned} E_{nl} = & \left[\frac{\partial u_1}{\partial X_1}\frac{\partial u_1}{\partial X_2} + \frac{\partial u_3}{\partial X_1}\frac{\partial u_3}{\partial X_2}\right] + \\ & \left[\frac{\partial u_1}{\partial X_1}\frac{\partial u_1}{\partial X_3} + \frac{\partial u_2}{\partial X_1}\frac{\partial u_2}{\partial X_3}\right] + \\ & \left[\frac{\partial u_1}{\partial X_2}\frac{\partial u_1}{\partial X_3}\right] \end{aligned} \tag{427}$$

Additionally, when the virtual work expression is formulated, stresses inducing cross-sectional distortions are neglected, and thus the only required terms become:

$$\begin{aligned} E_{nl} = & \left[\frac{\partial u_1}{\partial X_1}\frac{\partial u_1}{\partial X_2} + \frac{\partial u_3}{\partial X_1}\frac{\partial u_3}{\partial X_2}\right] + \\ & \left[\frac{\partial u_1}{\partial X_1}\frac{\partial u_1}{\partial X_3} + \frac{\partial u_2}{\partial X_1}\frac{\partial u_2}{\partial X_3}\right] \end{aligned} \tag{428}$$

The foregoing results may then be used to augment Equation (424):

$$\begin{aligned} \delta W_{int} = & \int_0^L \left(\frac{\partial u_1}{\partial X_1}\right) CA \left(\frac{\partial \delta u_1}{\partial X_1}\right) dX_1 \\ & + \int_0^L \left(\frac{\partial^2 u_2}{\partial X_1^2}\right) CI_\eta \left(\frac{\partial^2 \delta u_2}{\partial X_1^2}\right) dX_1 \\ & + \int_0^L \left(\frac{\partial^2 u_3}{\partial X_1^2}\right) CI_\zeta \left(\frac{\partial^2 \delta u_3}{\partial X_1^2}\right) dX_1 \\ & + \frac{1}{2} P \int_0^L \left[\delta \left(\frac{\partial u_1}{\partial X_1}\right)^2 + \delta \left(\frac{\partial u_2}{\partial X_1}\right)^2 + \delta \left(\frac{\partial u_3}{\partial X_1}\right)^2\right] dX_1 \\ & + \frac{PI_p}{2A} \int_0^L \delta \left(\frac{\partial u_4}{\partial X_1}\right)^2 dX_1 \\ & - M_\eta \int_0^L \delta \left(\frac{\partial u_2}{\partial X_1}\frac{\partial u_4}{\partial X_1}\right) dX_1 + M_\zeta \int_0^L \delta \left(\frac{\partial u_3}{\partial X_1}\frac{\partial u_4}{\partial X_1}\right) dX_1 \\ & + \int_V \sigma_{12}\, \delta \left[\frac{\partial u_1}{\partial X_1}\frac{\partial u_1}{\partial X_2} + \frac{\partial u_3}{\partial X_1}\frac{\partial u_3}{\partial X_2}\right] dV \\ & + \int_V \sigma_{13}\, \delta \left[\frac{\partial u_1}{\partial X_1}\frac{\partial u_1}{\partial X_3} + \frac{\partial u_2}{\partial X_1}\frac{\partial u_2}{\partial X_3}\right] dV \end{aligned} \tag{429}$$

where use has been made of the fact the $\sigma_{12} = \sigma_{21}$ and $\sigma_{13} = \sigma_{31}$. It is noted that the new integrals appearing within the foregoing virtual internal work expression are furnished in terms of stress, while the remaining terms are posed in terms of stress resultants. Stress resultants are desirable from the standpoint of developing stiffness relations (*i.e.* load - deformation response)

and thus stress resultants for the area integrals involving σ_{12} and σ_{13} are now developed in terms of their physical meaning - a transverse shear force:

$$\int_A \sigma_{12}\, dA = -\frac{M_\eta^1 + M_\eta^2}{L}$$
$$\int_A \sigma_{13}\, dA = \frac{M_\zeta^1 + M_\zeta^2}{L} \tag{430}$$

subsequently leading to the consistent statement of internal virtual work, in terms of stress resultants:

$$\begin{aligned}
\delta W_{int} = & \int_0^L \left(\frac{\partial u_1}{\partial X_1}\right) CA \left(\frac{\partial \delta u_1}{\partial X_1}\right) dX_1 \\
& + \int_0^L \left(\frac{\partial^2 u_2}{\partial X_1^2}\right) CI_\eta \left(\frac{\partial^2 \delta u_2}{\partial X_1^2}\right) dX_1 \\
& + \int_0^L \left(\frac{\partial^2 u_3}{\partial X_1^2}\right) CI_\zeta \left(\frac{\partial^2 \delta u_3}{\partial X_1^2}\right) dX_1 \\
& + \frac{1}{2} P \int_0^L \left[\delta \left(\frac{\partial u_1}{\partial X_1}\right)^2 + \delta \left(\frac{\partial u_2}{\partial X_1}\right)^2 + \delta \left(\frac{\partial u_3}{\partial X_1}\right)^2\right] dX_1 \\
& + \frac{PI_p}{2A} \int_0^L \delta \left(\frac{\partial u_4}{\partial X_1}\right)^2 dX_1 \\
& - M_\eta \int_0^L \delta \left(\frac{\partial u_2}{\partial X_1}\frac{\partial u_4}{\partial X_1}\right) dX_1 + M_\zeta \int_0^L \delta \left(\frac{\partial u_3}{\partial X_1}\frac{\partial u_4}{\partial X_1}\right) dX_1 \\
& - \frac{M_\eta^1 + M_\eta^2}{L} \int_0^L \delta \left[\frac{\partial u_1}{\partial X_1}\frac{\partial u_1}{\partial X_2} + \frac{\partial u_3}{\partial X_1}\frac{\partial u_3}{\partial X_2}\right] dX_1 \\
& + \frac{M_\zeta^1 + M_\zeta^2}{L} \int_0^L \delta \left[\frac{\partial u_1}{\partial X_1}\frac{\partial u_1}{\partial X_3} + \frac{\partial u_2}{\partial X_1}\frac{\partial u_2}{\partial X_3}\right] dX_1
\end{aligned} \tag{431}$$

where M_η^1 and M_η^2 represent moments acting about the local η axis, at member ends 1 and 2, respectively. M_ζ^1 and M_ζ^2 represent similar quantities, but this time for a moment acting about the local ζ axis.

Substitution of the interpolated displacements relations appearing within Equations (418), (420), and (421) into the differentials within Equation (431) leads to the element stiffness matrices upon integration. These may be conveniently expressed in terms of the linear portion of the stiffness $\mathbf{K}_L$ and the geometrically nonlinear portion $\mathbf{K}_{NL}$.

3.2.1 Tangent stiffness matrix

As in the case of the nonlinear truss, the tangent stiffness matrix, $\mathbf{K}_T$, may be expressed as the sum of linear and geometrically nonlinear components:

$$\mathbf{K}_T = \mathbf{K}_L + \mathbf{K}_{NL} \tag{432}$$

where,

$$\mathbf{K}_L = C \begin{bmatrix} \frac{A}{L} & 0 & 0 & 0 & 0 & 0 & -\frac{A}{L} & 0 & 0 & 0 & 0 & 0 \\ 0 & \frac{12I_\zeta}{L^3} & 0 & 0 & 0 & \frac{6I_\zeta}{L^2} & 0 & -\frac{12I_\zeta}{L^3} & 0 & 0 & 0 & \frac{6I_\zeta}{L^2} \\ 0 & 0 & \frac{12I_\eta}{L^3} & 0 & -\frac{6I_\eta}{L^2} & 0 & 0 & 0 & -\frac{12I_\eta}{L^3} & 0 & -\frac{6I_\eta}{L^2} & 0 \\ 0 & 0 & 0 & \frac{I_p}{2(1+\nu)L} & 0 & 0 & 0 & 0 & 0 & -\frac{I_p}{2(1+\nu)L} & 0 & 0 \\ 0 & 0 & -\frac{6I_\eta}{L^2} & 0 & \frac{4I_\eta}{L} & 0 & 0 & 0 & \frac{6I_\eta}{L^2} & 0 & \frac{2I_\eta}{L} & 0 \\ 0 & \frac{6I_\zeta}{L^2} & 0 & 0 & 0 & \frac{4I_\zeta}{L} & 0 & -\frac{6I_\zeta}{L^2} & 0 & 0 & 0 & \frac{2I_\zeta}{L} \\ -\frac{A}{L} & 0 & 0 & 0 & 0 & 0 & \frac{A}{L} & 0 & 0 & 0 & 0 & 0 \\ 0 & -\frac{12I_\zeta}{L^3} & 0 & 0 & 0 & -\frac{6I_\zeta}{L^2} & 0 & \frac{12I_\zeta}{L^3} & 0 & 0 & 0 & -\frac{6I_\zeta}{L^2} \\ 0 & 0 & -\frac{12I_\eta}{L^3} & 0 & \frac{6I_\eta}{L^2} & 0 & 0 & 0 & \frac{12I_\eta}{L^3} & 0 & \frac{6I_\eta}{L^2} & 0 \\ 0 & 0 & 0 & -\frac{I_p}{2(1+\nu)L} & 0 & 0 & 0 & 0 & 0 & \frac{I_p}{2(1+\nu)L} & 0 & 0 \\ 0 & 0 & -\frac{6I_\eta}{L^2} & 0 & \frac{2I_\eta}{L} & 0 & 0 & 0 & \frac{6I_\eta}{L^2} & 0 & \frac{4I_\eta}{L} & 0 \\ 0 & \frac{6I_\zeta}{L^2} & 0 & 0 & 0 & \frac{2I_\zeta}{L} & 0 & -\frac{6I_\zeta}{L^2} & 0 & 0 & 0 & \frac{4I_\zeta}{L} \end{bmatrix} \tag{433}$$

and $\mathbf{K}_{NL}$ is,

$$\begin{bmatrix} \frac{P}{L} & 0 & 0 & 0 & 0 & 0 & -\frac{P}{L} & 0 & 0 & 0 & 0 & 0 \\ 0 & \frac{6P}{5L} & 0 & \frac{M_\eta^1}{L} & \frac{T}{L} & \frac{P}{10} & 0 & -\frac{6P}{5L} & 0 & \frac{M_\eta^2}{L} & -\frac{T}{L} & \frac{P}{10} \\ 0 & 0 & \frac{6P}{5L} & \frac{M_\zeta^1}{L} & -\frac{P}{10} & \frac{T}{L} & 0 & 0 & -\frac{6P}{5L} & \frac{M_\zeta^2}{L} & -\frac{P}{10} & -\frac{T}{L} \\ 0 & \frac{M_\eta^1}{L} & \frac{M_\zeta^1}{L} & \frac{PI_p}{AL} & -\frac{2M_\zeta^1-M_\zeta^2}{6} & \frac{2M_\eta^1-M_\eta^2}{6} & 0 & -\frac{M_\eta^1}{L} & -\frac{M_\zeta^1}{L} & -\frac{PI_p}{AL} & -\frac{M_\zeta^1+M_\zeta^2}{6} & \frac{M_\eta^1+M_\eta^2}{6} \\ 0 & \frac{T}{L} & -\frac{P}{10} & -\frac{2M_\zeta^1-M_\zeta^2}{6} & \frac{2PL}{15} & 0 & 0 & -\frac{T}{L} & \frac{P}{10} & -\frac{M_\zeta^1+M_\zeta^2}{6} & -\frac{PL}{30} & \frac{T}{2} \\ 0 & \frac{P}{10} & \frac{T}{L} & \frac{2M_\eta^1-M_\eta^2}{6} & 0 & \frac{2PL}{15} & 0 & -\frac{P}{10} & -\frac{T}{L} & \frac{M_\eta^1+M_\eta^2}{6} & -\frac{T}{2} & -\frac{PL}{30} \\ -\frac{P}{L} & 0 & 0 & 0 & 0 & 0 & \frac{P}{L} & 0 & 0 & 0 & 0 & 0 \\ 0 & -\frac{6P}{5L} & 0 & -\frac{M_\eta^1}{L} & -\frac{T}{L} & -\frac{P}{10} & 0 & \frac{6P}{5L} & 0 & -\frac{M_\eta^2}{L} & \frac{T}{L} & -\frac{P}{10} \\ 0 & 0 & -\frac{6P}{5L} & -\frac{M_\zeta^1}{L} & \frac{P}{10} & -\frac{T}{L} & 0 & 0 & \frac{6P}{5L} & -\frac{M_\zeta^2}{L} & \frac{P}{10} & \frac{T}{L} \\ 0 & \frac{M_\eta^2}{L} & \frac{M_\zeta^2}{L} & -\frac{PI_p}{AL} & -\frac{M_\zeta^1+M_\zeta^2}{6} & \frac{M_\eta^1+M_\eta^2}{6} & 0 & -\frac{M_\eta^2}{L} & -\frac{M_\zeta^2}{L} & \frac{PI_p}{AL} & \frac{M_\zeta^1-2M_\zeta^2}{6} & -\frac{M_\eta^1-2M_\eta^2}{6} \\ 0 & -\frac{T}{L} & -\frac{P}{10} & -\frac{M_\zeta^1+M_\zeta^2}{6} & -\frac{PL}{30} & -\frac{T}{2} & 0 & \frac{T}{L} & \frac{P}{10} & \frac{M_\zeta^1-M_\zeta^2}{6} & \frac{2PL}{15} & 0 \\ 0 & \frac{P}{10} & -\frac{T}{L} & \frac{M_\eta^1+M_\eta^2}{6} & \frac{T}{2} & -\frac{PL}{30} & 0 & -\frac{P}{10} & \frac{T}{L} & -\frac{M_\eta^1-2M_\eta^2}{6} & 0 & \frac{2PL}{15} \end{bmatrix} \tag{434}$$

with C being the uniaxial component of the constitutive tensor, P being the member axial force, T being the torques about the frame longitudinal axis, L being the member length, and I_p being the cross-sectional polar moment of inertia, taken with respect to the principle centroidal axes η and ζ.

3.2.2 Member internal force calculation

Unlike in the case of the nonlinear truss element formulation considered earlier, a rigorous determination of the frame member internal forces is frequently neglected. Instead the linearization associated with the use of the tangent stiffness matrix, $\mathbf{K}_T$, is employed within an updated Lagrangian formulation, wherein the step size is made to be small, and thus the internal force becomes:

$$^{t+\Delta t}\mathbf{F} \approx \mathbf{K}_T \Delta\mathbf{u} + {}^t\mathbf{F} \tag{435}$$

As a practical matter, this approximation is frequently not a problem, as the displacement increments must be kept small in order to allow the use of the force-space plasticity approach that will be described in the sequel.

Coordinate transformations may be handled in a manner similar to what was done for the case of the nonlinear truss finite element. Using a similar notation to that encountered during the nonlinear truss element formulation, the respective direction cosines expressing the cosines of the respective angles depicted in Figure (13) are now expressed as:

$$\begin{aligned} l_\xi &= cos\left(\theta_X\right) \\ m_\xi &= cos\left(\theta_Y\right) \\ n_\xi &= cos\left(\theta_Z\right) \end{aligned} \tag{436}$$

Similar quantities are developed for the direction cosines associated with the angles orienting the local η-axis with the global X, Y, and Z-axes, denoted respectively, as ϕ_X, ϕ_Y, and ϕ_Z:

$$\begin{aligned} l_\eta &= cos\left(\phi_X\right) \\ m_\eta &= cos\left(\phi_Y\right) \\ n_\eta &= cos\left(\phi_Z\right) \end{aligned} \tag{437}$$

and for the direction cosines associated with the angles orienting the local ζ-axis with the global X, Y, and Z-axes, denoted respectively, as α_X, α_Y, and α_Z the following proceeds:

$$\begin{aligned} l_\zeta &= cos\left(\alpha_X\right) \\ m_\zeta &= cos\left(\alpha_Y\right) \\ n_\zeta &= cos\left(\alpha_Z\right) \end{aligned} \tag{438}$$

The forgoing direction cosines may then be used to transform the global internal force vector, $\mathbf{F}$ into the local coordinate system as:

$$\left[\mathbf{F}_{local}\right] = \left[\mathbf{\Gamma}\right]\left[\mathbf{F}\right] \tag{439}$$

where

$$\left[\gamma\right] = \begin{bmatrix} l_\xi & m_\xi & n_\xi \\ l_\eta & m_\eta & n_\eta \\ l_\zeta & m_\zeta & n_\zeta \end{bmatrix} \tag{440}$$

and

$$\left[\mathbf{\Gamma}\right] = \begin{bmatrix} \left[\gamma\right] & \mathbf{0} & \mathbf{0} & \mathbf{0} \\ \mathbf{0} & \left[\gamma\right] & \mathbf{0} & \mathbf{0} \\ \mathbf{0} & \mathbf{0} & \left[\gamma\right] & \mathbf{0} \\ \mathbf{0} & \mathbf{0} & \mathbf{0} & \left[\gamma\right] \end{bmatrix} \tag{441}$$

The transformation from Equation (441) may also subsequently be used to transform the local element tangent stiffness matrix, $[\mathbf{k}_T]$, into the global version, $[\mathbf{K}_T]$, as follows:

$$\left[\mathbf{K}_T\right] = \left[\mathbf{\Gamma}\right]^T\left[\mathbf{k}_T\right]\left[\mathbf{\Gamma}\right] \tag{442}$$

3.3 Three Node DKT Shell

There are number of different ways to approach the formulation of a shell finite element. Three example approaches include: 1) the discretization of one of the particular classical shell theories; 2) the specialization of the equations of continuum mechanics to arrive at a degenerated isoparametric element formulation; and 3) superimposing of membrane effects over top of a plate bending formulation employing explicit Kirchhoff thin plate kinematics. The first approach is not suitable for application to a general purpose finite element code since no suitably general exact shell theory is known (many excellent specialized theories exist; thus enabling convenient specialized finite element formulations). Since the objective of the present discussion is the formulation of a useful general purposes nonlinear shell finite element, the second and third options become more attractive. In the case of the second formulation approach (*i.e.* degenerate isoparametric element), the issue of shear locking becomes troublesome, when thin shell behavior is of interest. While various strategies exist for treating the shear locking pathologies in degenerate isoparametric shells (*e.g.* reduced integration, selective integration, mixed interpolation, *etc.*), the present discussion will center on an alternative approach for satisfying the zero transverse shear deformation assumption that accompanies thin shell bending: the Discrete Kirchhoff theory (DKT). In such an approach, the Kirchhoff hypothesis is enforced at specific points within the shell element; subsequently resulting in satisfactory thin shell performance.

The present discussion focuses on the formulation of a three node triangular element based on the DKT. The tangent stiffness matrix of this element comprises a superposition of a plane stress membrane stiffness, $\mathbf{K}_m$, a plate bending stiffness, $\mathbf{K}_b$, and an in-plane rotational stiffness, $\mathbf{K}_\theta$:

$$\mathbf{K}_T = \mathbf{K}_m + \mathbf{K}_b + \mathbf{K}_\theta \tag{443}$$

This approach leads to an element that is suitable for large deformation analyses, but that is not suitable for consideration of finite strains (as the thickness is not updated during the solution process, and thus the Green-Lagrange strain is not treated exactly within the formulation). Additionally, as a result of the superposition of membrane and plate bending responses, since the shell is flat, coupling between the membrane and bending action is only introduced through the transformation of the nodal point forces from the local to the global coordinate system; and thus a fine mesh is required to accurately approximate the required coupling. Nonetheless, a highly efficient element formulation ensues from the consideration of the DKT within the context of a three node triangle. The sequel elucidates the DKT element formulation at issue; beginning with a consideration of the plate flexural contributions as the point of departure for the current element formulation.

3.3.1 Plate bending response

Considering a local coordinate system $(x,\, y,\, z)$ that represents a local scaling of the parent element coordinates $(\xi,\, \eta,\, \zeta)$ within a DKT triangular shell element, an initial focus on Mindlin-Reissner plate theory (*i.e.* thick plate bending theory wherein sections that were initially plane and normal to an undeformed reference surface remain plane after deformation, but not necessarily normal to the current plate middle surface) is instructive as the DKT plate kinematics are discussed. Considering the local plate displacement components coinciding with the x, y, and z directions, respectively, the following are defined:

$$\begin{aligned} u &= z\, \beta_x\, (x, y) \\ v &= z\, \beta_y\, (x, y) \\ w &= w\, (x, y) \end{aligned} \tag{444}$$

where w are the transverse (to the plane of the plate) displacements, and the subsequent edge rotations are β_x and β_y for rotations in the $x - z$ and $y - z$ planes, respectively. Taking the plate curvature to be the spatial derivative of the edge rotations, the following curvature vector is obtained:

$$\kappa = \left[\begin{array}{c} \beta_{x,x} \\ \beta_{y,y} \\ \beta_{x,y} + \beta_{y,x} \end{array} \right] \tag{445}$$

and so the strains induced by flexure are:

$$\epsilon_b = z\, \kappa \tag{446}$$

Considering next transverse shear strains, the sum of the edge rotations and spatial derivatives of the transverse displacements yield:

$$\gamma = \left[\begin{array}{c} w_{,x} + \beta_x \\ w_{,y} + \beta_y \end{array} \right] \tag{447}$$

A subsequent assumption of homogeneous, isotropic material properties within the Kirchhoff plate bending framework leads to the following definition for bending and shearing plate rigidities, respectively:

$$\mathbf{D}_b = \frac{Eh^3}{12\,(1 - \nu^2)} \left[\begin{array}{ccc} 1 & \nu & 0 \\ \nu & 1 & 0 \\ 0 & 0 & \frac{1-\nu}{2} \end{array} \right] \tag{448}$$

and

$$\mathbf{D}_s = \frac{Ehk}{2\,(1 + \nu)} \left[\begin{array}{cc} 1 & 0 \\ 0 & 1 \end{array} \right] \tag{449}$$

where h is the plate (shell) thickness, ν is Poisson's ratio, and k is the shear correction factor (usually taken as $\frac{5}{6}$). The foregoing may be used to describe

the internal strain energy within the DKT shell resulting from the consideration of plate bending:

$$U = U_b + U_s \tag{450}$$

within which

$$\begin{aligned} U_b &= \frac{1}{2}\int_\Omega \kappa^T \mathbf{D}_b \kappa dA \\ &= \frac{Eh^3}{24\left(1-\nu^2\right)}\int_\Omega \left[\beta_{x,x}^2 + \beta_{y,y}^2 + 2\nu\beta_{y,y}\beta_{x,x} + \frac{1-\nu}{2}\left(\beta_{y,x}+\beta_{x,y}\right)^2\right] d\Omega \end{aligned} \tag{451}$$

and

$$\begin{aligned} U_s &= \frac{1}{2}\int_\Omega \gamma^T \mathbf{D}_s \gamma dA \\ &= \frac{Ehk}{4\left(1+\nu\right)}\int_\Omega \left[\left(w_{,x}+\beta_x\right)^2 + \left(w_{,y}+\beta_y\right)^2\right] d\Omega \end{aligned} \tag{452}$$

and where Ω represents the spatial domain of integration coinciding with the plate middle surface. The subsequent stress resultants due to flexure appear as the following bending moment and shear force expressions, respectively:

$$\mathbf{M} = \left[\begin{array}{c} M_x \\ M_y \\ M_{xy} \end{array}\right] = \int_{-\frac{h}{2}}^{\frac{h}{2}} \sigma z \; dz = \mathbf{D}_b \kappa \tag{453}$$

and

$$\mathbf{Q} = \left[\begin{array}{c} Q_x \\ Q_y \end{array}\right] = \mathbf{k}\int_{-\frac{h}{2}}^{\frac{h}{2}} \sigma_s \; dz = \mathbf{D}_s \gamma \tag{454}$$

In the case of thin plates, the transverse shear strains is negligible in comparison with the contribution from bending. As a result, in the current DKT shell formulation, the plate bending contribution to the overall shell element strain energy will consist of only the flexural portion as:

$$U = \frac{1}{2}\int_\Omega \kappa^T \mathbf{D}_b \kappa \; d\Omega \tag{455}$$

It is immediately noticed from Equation (455) that since the only kinematical quantity appearing are the first derivatives of the edge rotations, β, then compatibility considerations between elements can be handled in a straightforward manner. However, what is more complex is how to properly admit transverse displacements, w, into the formulation (since they do not explicitly appear in Equation (455)). The required treatment of the transverse displacements is admitted within an element formulation framework that is based on nodal rotations at the three corner nodes (with components denoted as θ_x, θ_y and θ_z, depending on orientation) for a total of nine plate dofs (the U_2, θ_1, and θ_3 components depicted in Figure (14)). In order to bring the peculiarities of the

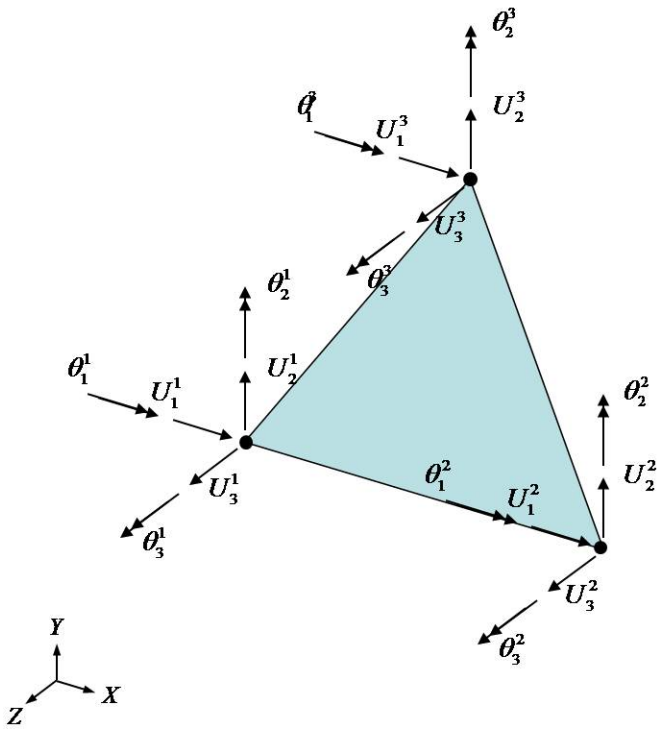

Figure 14: Parent element for nonlinear DKT shell element

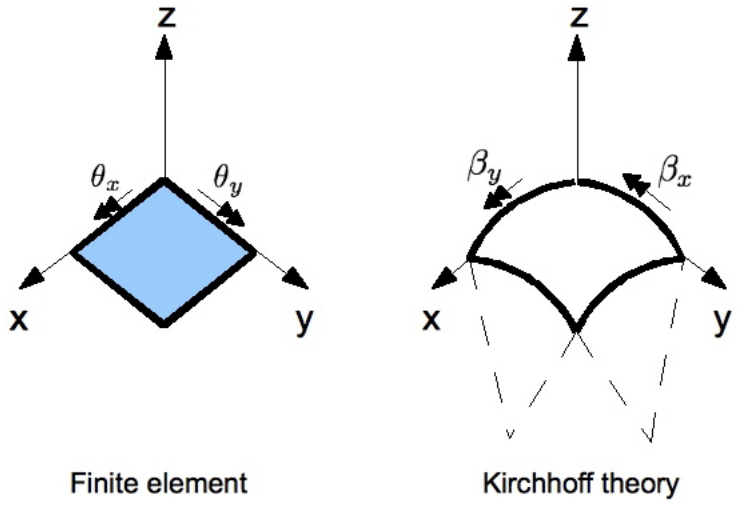

Figure 15: Positive rotational sense within the finite element (left) and Kirchhoff (right) contexts

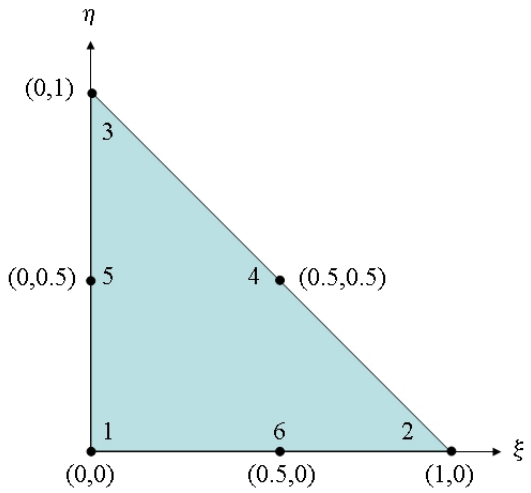

Figure 16: DKT shell: enhanced parent element

Kirchhoff plate theory's sign convention into consonance with the finite element conventions, the following forms are used to express the required mapping of sign conventions that is depicted in Figure (15), and expressed as:

$$\begin{aligned} \theta_x &= w_{,y} \\ \theta_y &= -w_{,x} \end{aligned} \tag{456}$$

While it is that the three node triangle DKT element is conceived of within the scope of thin shell structures, and thus the DKT conditions may theoretically be enforced at any location within the shell domain, Ω, care is taken to ensure that the compatibility in the edge rotations, β_x and β_y is not lost. It is pointed out that, in contrast to the edge rotations, β, the nodal rotations are denoted using θ's. As a means for ensuring that the DKT assumptions are properly enforced, the following steps are adopted within the plate bending portion of the nonlinear three node triangular DKT element at hand.

While it is that the element formulation for the plate bending component of the shell will end in a 9 dof representation, the point of departure for this discussion begins with the six parent element nodes appearing in Figure (16). It is assumed that the edge rotations, β_x and β_y vary quadratically over each of the three element sides; by employing quadratic shape functions as a means for interpolating between the six nodes adopted in the formulation, when expressing

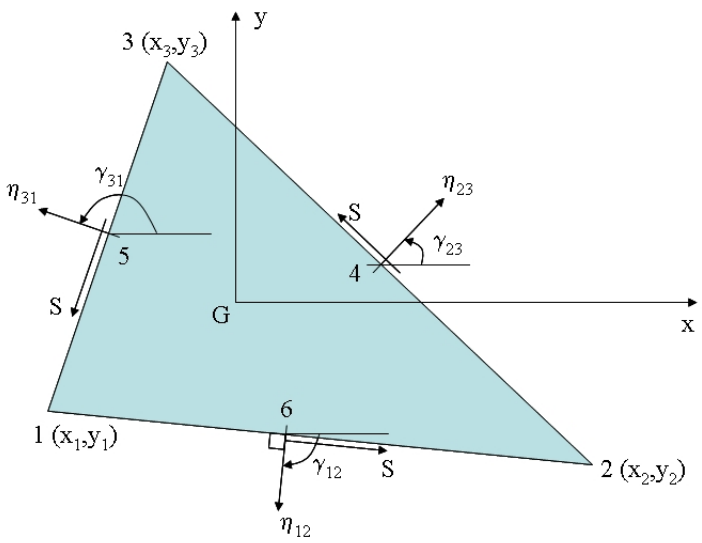

Figure 17: DKT shell element local coordinates

the Kirchhoff assumptions:

$$\begin{aligned}\beta_x &= \sum_{i=1}^{6} h_i \beta_{xi} \\ \beta_y &= \sum_{i=1}^{6} h_i \beta_{yi}\end{aligned} \tag{457}$$

where β_{xi} abd β_{yi} are the nodal values at the corner and mid-side nodes, consistent with the depiction in Figure (16). Additionally, the finite element shape functions referenced in Equation (457) appear as:

$$\begin{aligned}h_1 &= 2\left(1-\xi-\eta\right)\left(\frac{1}{2}-\xi-\eta\right) \\ h_2 &= \xi\left(2\xi-1\right) \\ h_3 &= \eta\left(2\eta-1\right) \\ h_4 &= 4\xi\eta \\ h_5 &= 4\eta\left(1-\xi-\eta\right) \\ h_6 &= 4\xi\left(1-\xi-\eta\right)\end{aligned} \tag{458}$$

where the local coordinates ξ and η are depicted in Figure (16). The DKT condition is practically enforced within the shell by ensuring that Equation (447) vanishes at specific points within the shell domain, Ω. In the case of the

current element, the locations are the corner nodes:

$$\gamma = \begin{bmatrix} \beta_x + w_{,x} \\ \beta_y + w_{,y} \end{bmatrix} = \mathbf{0} \quad \text{at nodes 1, 2, and 3} \tag{459}$$

and at the mid-side nodes:

$$\beta_{sk} + w_{,sk} = 0 \quad \text{for k = 4, 5, and 6} \tag{460}$$

Additionally, it is assumed that the cubic interpolation polynomials from Equation (422) (developed from slope-deflection equations) are imposed along the element sides (taking suitable derivatives and substituting for the mid-side node coordinates), and thus:

$$w_{,sk} = -\frac{3}{2l_{ij}} w_i - \frac{1}{4} w_{,si} + \frac{3}{2l_{ij}} w_j - \frac{1}{4} w_{,sj} \tag{461}$$

where k denoted the particular side of interest (with end points i and j); where l_{ij} denotes the length of this side. While the current DKT element formulation will not make explicit use of an interpolation polynomial on the out of plane displacements, w, the assumption of the quadratic variation in $w_{,sk}$ implies the cubic nature of w. By virtue of the DKT condition from Equation (459), involving the quadratically varying terms $w_{,s}$ and β_s that are made to agree at fixed points along the sides, the Kirchhoff hypothesis is enforced continuously along the entire problem domain $\partial\Omega$; thus a discrete imposition of the Kirchhoff condition at six points along the element perimeter leads to complete satisfaction of the Kirchhoff condition along the element boundary. In this manner, assumption of a null contribution from transverse shear strain energy in Equation (455), is supported. Figure (18) illustrates important quantities and sign conventions in support of the foregoing, as well as following formulæ. Useful additional quantities also include: the element side length is

$$l_{ij} = \sqrt{(x_{ij})^2 + (y_{ij})^2} \tag{462}$$

where

$$\begin{aligned} x_{ij} &= x_i - x_j \\ y_{ij} &= y_i - y_j \end{aligned} \tag{463}$$

and the natural coordinate along the element edge is

$$\xi = \frac{s}{l_{ij}} \tag{464}$$

thus enabling the local finite element coordinates to be expressed as

$$\begin{aligned} x &= x_i - \xi\, x_{ij} \\ y &= y_i - \xi\, y_{ij} \end{aligned} \tag{465}$$

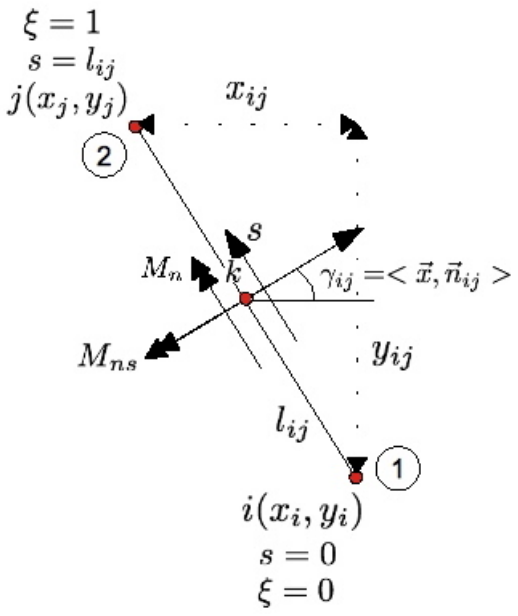

Figure 18: DKT sign conventions, angles, lengths, *etc.*

Additionally, the local coordinates of the side nodes are furnished as

$$\begin{aligned} x_k &= \frac{1}{2}(x_i + x_j) \\ y_k &= \frac{1}{2}(y_i + y_j) \end{aligned} \tag{466}$$

along with their respective direction cosines:

$$\begin{aligned} c &= cos(\gamma_{ij}) = -\frac{y_{ij}}{l_{ij}} \\ s &= sin(\gamma_{ij}) = \frac{x_{ij}}{l_{ij}} \end{aligned} \tag{467}$$

When considering the rotations occurring normal to the side of the element, β_n, a linear variation is imposed as:

$$\beta_{nk} = \frac{1}{2}(\beta_{ni} + \beta_{nj}) \tag{468}$$

where $k = 4, 5, 6$ denotes the mid side node along element edges 23, 31, and 12, respectively. To obtain β_x and β_y in terms of only nodal degrees of freedom motivates the following development.

Consider the nodal displacement vector to be given as (according to Figure (14)):

$$\mathbf{U} = \begin{bmatrix} u_2^1 \\ \theta_1^1 \\ \theta_3^1 \\ u_2^2 \\ \theta_1^2 \\ \theta_3^2 \\ u_2^3 \\ \theta_1^3 \\ \theta_3^3 \end{bmatrix} \tag{469}$$

The following development will lead to an element formulation that is based solely on these degrees of freedom (i.e. the mid-side nodes will not explicitly appear in the element matrices); in order to facilitate the elements subsequent use with other structural finite elements. In pursuit of this approach, the following geometric relations are defined for each of the element sides:

$$\begin{bmatrix} \beta_x \\ \beta_y \end{bmatrix} = \begin{bmatrix} c & -s \\ s & c \end{bmatrix} \begin{bmatrix} \beta_n \\ \beta_s \end{bmatrix} \tag{470}$$

and

$$\begin{bmatrix} w_{,s} \\ w_{,n} \end{bmatrix} = \begin{bmatrix} c & s \\ s & -c \end{bmatrix} \begin{bmatrix} \theta_x \\ \theta_y \end{bmatrix} \tag{471}$$

where c and s are defined in Equation (467). β_x and β_y can now be expressed in terms of new finite element shape functions:

$$\begin{aligned} \beta_x &= \mathbf{H}_x^T(\xi,\eta)\,\mathbf{U} \\ \beta_y &= \mathbf{H}_y^T(\xi,\eta)\,\mathbf{U} \end{aligned} \tag{472}$$

where $\mathbf{H}_x$ and $\mathbf{H}_y$ are each vectors in $\mathbb{R}^9$ defined as:

$$\begin{aligned} H_{x1} &= 1.5\,(a_6h_6 - a_5h_5) \\ H_{x2} &= b_5h_5 + b_6h_6 \\ H_{x3} &= h_1 - c_5h_5 - c_6h_6 \\ H_{x4} &= 1.5\,(a_4h_4 - a_6h_6) \\ H_{x5} &= b_6h_6 + b_4h_4 \\ H_{x6} &= h_2 - c_6h_6 - c_4h_4 \\ H_{x7} &= 1.5\,(a_5h_5 - a_4h_4) \\ H_{x8} &= b_4h_4 + b_5h_5 \\ H_{x9} &= h_3 - c_4h_4 - c_5h_5 \end{aligned} \tag{473}$$

and,

$$\begin{aligned}
H_{y1} &= 1.5\left(d_6 h_6 - d_5 h_5\right) \\
H_{y2} &= -h_1 + e_5 h_5 + e_6 h_6 \\
H_{y3} &= -b_5 h_5 - b_6 h_6 \\
H_{y4} &= 1.5\left(d_4 h_4 - d_6 h_6\right) \\
H_{y5} &= -h_2 + e_6 h_6 + e_4 h_4 \\
H_{y6} &= -b_6 h_6 - b_4 h_4 \\
H_{y7} &= 1.5\left(d_5 h_5 - d_4 h_4\right) \\
H_{y8} &= -h_3 + e_4 h_4 + e_5 h_5 \\
H_{y9} &= -b_4 h_4 - b_5 h_5
\end{aligned} \tag{474}$$

where the h_i $(i = 1 \ldots 6)$ are obtained from Equation (458), and the respective coefficients are given as:

$$\begin{aligned}
a_k &= -\frac{x_{ij}}{l_{ij}^2} \\
b_k &= \frac{3 x_{ij} y_{ij}}{4 l_{ij}^2} \\
c_k &= \frac{\left(\frac{1}{4} x_{ij}^2 - \frac{1}{2} y_{ij}^2\right)}{l_{ij}^2} \\
d_k &= -\frac{y_{ij}}{i_{ij}^2} \\
e_k &= \frac{\left(\frac{1}{4} y_{ij}^2 - \frac{1}{2} x_{ij}^2\right)}{l_{ij}^2} \\
l_{ij}^2 &= \left(x_{ij}^2 + y_{ij}^2\right)
\end{aligned} \tag{475}$$

within which $k = 4, 5, 6$ references sides $ij = 23, 31, 12$, respectively (see Figure (17)). The foregoing may be used to form a sort of transformation matrix that maps the desired finite element degrees of freedom into the a kinematical form that is useful in interfacing with the DKT that has been formulated thus far. Specifically, a strain displacement matrix relating the nodal degrees of freedom to the plate flexural curvatures may be given as:

$$\kappa = \mathbf{B}_b \mathbf{U} \tag{476}$$

where the strain displacement matrix, $\mathbf{B}_b$, takes the form:

$$\mathbf{B}_b\left(\xi, \eta\right) = \frac{1}{2A} \begin{bmatrix} y_{31}\mathbf{H}_{x,\xi}^T + y_{12}\mathbf{H}_{x,\eta}^T \\ -x_{31}\mathbf{H}_{y,\xi}^T - x_{12}\mathbf{H}_{y,\eta}^T \\ -x_{31}\mathbf{H}_{x,\xi}^T - x_{12}\mathbf{H}_{x,\eta}^T + y_{31}\mathbf{H}_{y,\xi}^T + y_{12}\mathbf{H}_{y,\eta}^T \end{bmatrix} \tag{477}$$

where $2A = x_{31}y_{12} - x_{12}y_{31}$ and the derivatives of $\mathbf{H}_x$ and $\mathbf{H}_y$ with respect to ξ and η being given as:

$$\mathbf{H}_{x,\xi} = \begin{bmatrix} P_6\,(1-2\xi) + (P_5 - P_6)\,\eta \\ q_6\,(1-2\xi) - (q_5 + q_6)\,\eta \\ -4 + 6\,(\xi+\eta) + r_6\,(1-2\xi) - \eta\,(r_5 + r_6) \\ -P_6\,(1-2\xi) + \eta\,(P_4 + P_6) \\ q_6\,(1-2\xi) - \eta\,(q_6 - q_4) \\ -2 + 6\xi + r_6\,(1-2\xi) + \eta\,(r_4 - r_6) \\ -\eta\,(P_5 + P_4) \\ \eta\,(q_4 - q_5) \\ -\eta\,(r_5 - r_4) \end{bmatrix} \tag{478}$$

$$\mathbf{H}_{y,\xi} = \begin{bmatrix} t_6\,(1-2\xi) + \eta\,(t_5 - t_6) \\ 1 + r_6\,(1-2\xi) - \eta\,(r_5 + r_6) \\ -q_6\,(1-2\xi) + \eta\,(q_5 + q_6) \\ -t_6\,(1-2\xi) + \eta\,(t_4 + t_6) \\ -1 + r_6\,(1-2\xi) + \eta\,(r_4 - r_6) \\ -q_6\,(1-2\xi) - \eta\,(q_4 - q_6) \\ -\eta\,(t_4 + t_5) \\ \eta\,(r_4 - r_5) \\ -\eta\,(q_4 - q_5) \end{bmatrix} \tag{479}$$

$$\mathbf{H}_{x,\eta} = \begin{bmatrix} -P_5\,(1-2\eta) - \xi\,(P_6 - P_5) \\ q_5\,(1-2\eta) - \xi\,(q_5 + q_6) \\ -4 + 6\,(\xi+\eta) + r_5\,(1-2\eta) - \eta\,(r_5 + r_6) \\ \xi\,(P_4 + P_6) \\ \xi\,(q_4 - q_6) \\ -\xi\,(r_6 - r_4) \\ P_5\,(1-2\eta) - \xi\,(P_4 + P_5) \\ q_5\,(1-2\eta) + \xi\,(q_4 - q_5) \\ -2 + 6\eta + r_5\,(1-2\eta) + \xi\,(r_4 - r_5) \end{bmatrix} \tag{480}$$

$$\mathbf{H}_{y,\eta} = \begin{bmatrix} -t_5\,(1-2\eta) - \xi\,(t_6 - t_5) \\ 1 + r_5\,(1-2\eta) - \xi\,(r_5 + r_6) \\ -q_5\,(1-2\eta) + \xi\,(q_5 + q_6) \\ \xi\,(t_4 + t_6) \\ \xi\,(r_4 + r_6) \\ -\xi\,(q_4 - q_6) \\ t_5\,(1-2\eta) - \xi\,(t_4 + t_5) \\ -1 + r_5\,(1-2\eta) + \xi\,(r_4 - r_5) \\ -q_5\,(1-2\eta) - \xi\,(q_4 - q_5) \end{bmatrix} \tag{481}$$

where,

$$
\begin{aligned}
P_k &= \frac{-6x_{ij}}{l_{ij}^2} = 6a_k \\
q_k &= \frac{3x_{ij}y_{ij}}{l_{ij}^2} = 4b_k \\
t_k &= \frac{-6y_{ij}}{l_{ij}^2} = 6d_k \\
r_k &= \frac{3y_{ij}^2}{l_{ij}^2}
\end{aligned} \tag{482}
$$

for $k = 4, 5, 6$ associated with $ij = 23, 31, 12$, respectively. Using the strain displacement from Equation (477), the plate bending stiffness matrix may be arrived at.

The plate bending stiffness matrix is obtained most efficiently through the use of numerical integration for the evaluation of:

$$
\mathbf{K}_{DKT} = 2A \int_0^{-1} \int_0^{1-\eta} \mathbf{B}_b^T \mathbf{D}_b \mathbf{B}_b \, d\xi \, d\eta \tag{483}
$$

Equation (483) may be integrated using a Gauss quadrature rule wherein the sampling points, g_i, coincide with the mid-side nodes and the weights, W_i, are specified as $\frac{1}{3}$:

$$
\begin{aligned}
\mathbf{K}_{DKT} &= 2A \int_0^{-1} \int_0^{1-\eta} \mathbf{B}_b^T \mathbf{D}_b \mathbf{B}_b \, d\xi \, d\eta \\
&= \sum_i^{numpts} W_i \mathbf{B}_b \left(g_i\right)^T \mathbf{D}_b \mathbf{B}_b \left(g_i\right) \\
&= \sum_i^{numpts} \frac{1}{3} \mathbf{B}_b \left(g_i\right)^T \mathbf{D}_b \mathbf{B}_b \left(g_i\right)
\end{aligned} \tag{484}
$$

The subsequent element local internal forces are computed as in in linear analysis: by assuming that $\mathbf{F} = \mathbf{KU}$.

3.3.2 Membrane response

In handling the membrane behavior of the DKT shell, it is merely assumed that the standard plane stress assumptions may be applied to the membrane deformations as follows in the sequel. Beginning in this way, natural coordinates are defined.

Consider a triangular domain with three nodes at the vertices (as depicted in Figure (19)). Natural coordinates may be considered as area fractions associated

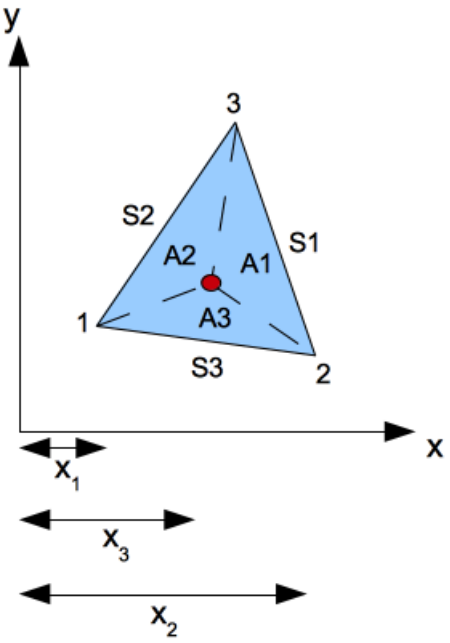

Figure 19: Natural coordinates for DKT membrane formulation

with parsing, into three subsequent triangular sub-areas, of the original domain in response to the occurrence of an arbitrarily positioned point, P (as depicted in Figure (19)). Natural coordinates are subsequently identified as:

$$\xi_1 = \frac{A_1}{A}, \quad \xi_2 = \frac{A_2}{A}, \quad \xi_3 = \frac{A_3}{A} \tag{485}$$

The obvious requirement that:

$$A = A_1 + A_2 + A_3 \tag{486}$$

yields the following result:

$$\begin{aligned} \frac{A_1}{A_1 + A_2 + A_3} + \frac{A_2}{A_1 + A_2 + A_3} + \frac{A_3}{A_1 + A_2 + A_3} &= \frac{1}{A_1 + A_2 + A_3}(A_1 + A_2 + A_3) \\ &= 1 \\ \implies \xi_1 + \xi_2 + \xi_3 &= 1 \end{aligned} \tag{487}$$

The last result from Equation (487) constitutes a constraint equation for the interpolation within natural coordinates.

In consideration of an arbitrarily located point, P, the partition of unity properties associated with interpolation demand that in the case of the spatial

x-coordinate of any given point:

$$x = \sum_i \xi_i x_i = \xi_1 x_1 + \xi_2 x_2 + \xi_3 x_3 \tag{488}$$

and similarly for the y-direction:

$$y = \sum_i \xi_i y_1 \tag{489}$$

and all subject to Equation (487). These results may be restated more compactly as:

$$\begin{bmatrix} 1 \\ x \\ y \end{bmatrix} = [A] \begin{bmatrix} \xi_1 \\ \xi_2 \\ \xi_3 \end{bmatrix} \tag{490}$$

where,

$$[A] = \begin{bmatrix} 1 & 1 & 1 \\ x_1 & x_2 & x_3 \\ y_1 & y_2 & y_3 \end{bmatrix} \tag{491}$$

and inversely,

$$\begin{bmatrix} \xi_1 \\ \xi_2 \\ \xi_3 \end{bmatrix} = [A]^{-1} \begin{bmatrix} 1 \\ x \\ y \end{bmatrix} \tag{492}$$

with,

$$[A]^{-1} = \frac{1}{2A} \begin{bmatrix} x_2 y_3 - x_3 y_2 & y_{23} & x_{23} \\ x_3 y_1 - x_1 y_3 & y_{31} & x_{13} \\ x_1 y_2 - x_2 y_1 & y_{12} & x_{21} \end{bmatrix} \tag{493}$$

where, again, such quantities as y_{12}, are equal to $y_1 - y_2$. An additional result can be found from the definition of the determinant, applied in a clever manner (with some patience):

$$2A = \mid \mathbf{A} \mid = x_{21} y_{31} - x_{31} y_{21} \tag{494}$$

where $2A$ represents twice the area of the triangular element.

In developing the portion of the DKT shell element formulation dealing with membrane effects, it will be necessary to compute Cartesian derivatives of the shape functions, h_i, that appear in terms of area (natural) coordinates. This can be accomplished through an application of the chain rule:

$$\begin{aligned} \frac{\partial h}{\partial x} &= \frac{\partial h}{\partial \xi_1}\frac{\partial \xi_1}{\partial x} + \frac{\partial h}{\partial \xi_2}\frac{\partial \xi_2}{\partial x} + \frac{\partial h}{\partial \xi_3}\frac{\partial \xi_3}{\partial x} \\ \frac{\partial h}{\partial y} &= \frac{\partial h}{\partial \xi_1}\frac{\partial \xi_1}{\partial y} + \frac{\partial h}{\partial \xi_2}\frac{\partial \xi_2}{\partial y} + \frac{\partial h}{\partial \xi_3}\frac{\partial \xi_3}{\partial y} \end{aligned} \tag{495}$$

where the definition of the inverse, as the adjoint (transpose of the matrix of cofactors - in this case one value) divided by the determinant, may be used to obtain:

$$\begin{aligned}
\frac{\partial \xi_1}{\partial x} &= \frac{y_{23}}{2A} \\
\frac{\partial \xi_2}{\partial x} &= \frac{y_{31}}{2A} \\
\frac{\partial \xi_3}{\partial x} &= \frac{y_{12}}{2A} \\
\frac{\partial \xi_1}{\partial y} &= \frac{x_{32}}{2A} \\
\frac{\partial \xi_2}{\partial y} &= \frac{x_{13}}{2A} \\
\frac{\partial \xi_3}{\partial y} &= \frac{x_{21}}{2A}
\end{aligned} \tag{496}$$

The membrane strains may now be treated as:

$$\epsilon = \begin{bmatrix} \epsilon_{11} \\ \epsilon_{22} \\ \epsilon_{12} \end{bmatrix} = \begin{bmatrix} \frac{\partial u_1}{\partial x} \\ \frac{\partial u_2}{\partial y} \\ \frac{\partial u_1}{\partial y} + \frac{\partial u_2}{\partial x} \end{bmatrix} = \frac{1}{2A} \begin{bmatrix} y_{32} & 0 & -y_{31} & 0 & y_{21} & 0 \\ 0 & -x_{32} & 0 & x_{31} & 0 & -x_{21} \\ -x_{32} & y_{32} & x_{31} & -y_{31} & x_{21} & y_{21} \end{bmatrix} \begin{bmatrix} u_1^1 \\ u_2^1 \\ u_1^2 \\ u_2^2 \\ u_1^3 \\ u_2^3 \end{bmatrix} \tag{497}$$

and thus the membrane strain-diaplcement relation, $\mathbf{B}_m$, may be expressed as:

$$\mathbf{B}_m = \frac{1}{2A} \begin{bmatrix} y_{32} & 0 & -y_{31} & 0 & y_{21} & 0 \\ 0 & -x_{32} & 0 & x_{31} & 0 & -x_{21} \\ -x_{32} & y_{32} & x_{31} & -y_{31} & x_{21} & y_{21} \end{bmatrix} \tag{498}$$

The foregoing results may be used to construct the finite element matrices required for the implementation of the formulation.

In the case of the membrane local internal force contribution, a simple linear formulation is assumed, and an subsequent coupling with regard to bending effects is handled via coordinate transformations:

$$\mathbf{F} = \int_\Omega \mathbf{B}_m^T \mathbf{N} d\Omega \tag{499}$$

where the membrane edge loading, $\mathbf{N}$, is furnished as:

$$\mathbf{N} = h\mathbf{C}\mathbf{B}_m\mathbf{U} \tag{500}$$

with $\mathbf{C}$ being the usual plane stress constitutive matrix.

Unlike the plate bending response, the tangent stiffness matrix for the membrane effects does include nonlinear effects and thus the usual, two-part, formulation is adopted:

$$\mathbf{K}_T = \mathbf{K}_{Lm} + \mathbf{K}_{NLm} \tag{501}$$

where the linear matrix appears as:

$$\mathbf{K}_{Lm} = \int_\Omega \mathbf{B}_m^T \mathbf{C} \mathbf{B}_m d\Omega \tag{502}$$

and the nonlinear matrix as:

$$\mathbf{K}_{NLm} = \int_\Omega \mathbf{B}_{NLm}^T \hat{\mathbf{N}} \mathbf{B}_{NLm} d\Omega \tag{503}$$

where:

$$\hat{\mathbf{N}} = \begin{bmatrix} \bar{\mathbf{N}} & & \\ & \bar{\mathbf{N}} & \\ & & \bar{\mathbf{N}} \end{bmatrix} \tag{504}$$

and

$$\bar{\mathbf{N}} = \begin{bmatrix} N_{11} & N_{12} \\ N_{12} & N_{22} \end{bmatrix} \tag{505}$$

Additionally,

$$\mathbf{B}_{NL} = \frac{1}{2A} \begin{bmatrix} -y_3 & 0 & 0 & y_3 & 0 & 0 & 0 & 0 & 0 \\ x_{32} & 0 & 0 & -x_3 & 0 & 0 & x_2 & 0 & 0 \\ 0 & -y_3 & 0 & 0 & y_3 & 0 & 0 & 0 & 0 \\ 0 & x_{32} & 0 & 0 & -x_3 & 0 & 0 & x_2 & 0 \\ 0 & 0 & -y_3 & 0 & 0 & y_3 & 0 & 0 & 0 \\ 0 & 0 & x_{32} & 0 & 0 & -x^3 & 0 & 0 & x_2 \end{bmatrix} \tag{506}$$

3.3.3 In-plane rotational response

A useful and simple approach may be adopted in assigning a stiffness to the in-plane rotational degree of freedom. This approach involves the assignment of 10^{-14} times the smallest bending stiffness value in the stiffness matrix; so as to coincide with the so-called *drilling degree of freedom* within the shell.

3.4 Inelastic material response

As it is that the foregoing structural elements deal directly in displacements and stress resultants, it would be cumbersome to attempt to reapply the stress-space plasticity theories, reviewed earlier, to the case of structural elements. Instead, an approach wherein a failure surface is postulated to exist in a force-space derived from element stress resultants, is adopted. It turns out that such a force-space approach to predicting plastification within structural elements will lead to significant savings in computation times accompanying the solution of finite element models comprising large numbers of structural elements.

3.4.1 Force-space plasticity

The point of departure surrounding the force-space approach for identifying the onset of plastification within a structural element begins with the notion of a failure surface. For illustrative purposes, the current discussion will begin with a force-space formulation that is appropriate for use with the previously developed frame finite element. Thus, rather than formulating a failure surface within the three space accompanying a three dimensional principal stress condition, stress resultants are instead associated with the coordinate axes used to describe loading points within the three dimensional force space considered: axial force, P, strong axis moment, M_x, and weak axis moment, M_y. Where the designation of *strong* and *weak axes* pertains to the sense of the bending moment occurring about the major and minor principal centroidal axes, respectively. The given failure surface, so defined in force space, encloses a region within which elastic member response is maintained. Force points that impinge on the failure surface are then assumed to coincide with the physical condition wherein full plastic hinging is activated. This assumed behavior is very much consistent with the notion of elastic-perfectly plastic material response that was maintained in the earlier discussion pertaining to stress space plasticity. It is further assumed that the case of constrained plasticity is the rule, and thus it is expected that the force point will persist on the failure surface unless unloading is explicitly called for during the analysis. Finally, an assumption consistent with associated flow plasticity of a stable (in the sense of Drucker) plastic material in stress space will be adopted in the force space formulation, and thus the plastic displacement is assumed to be additive to the elastic displacement increment, and to coincide with the direction of the outward normal to the failure surface; while the force increment coinciding with this point is assumed to maintain tangency to this surface. Before describing how to arrive at such a surface, the discussion will focus on what to do with the foregoing assumptions in order to place the force space plasticity approach into a context that is convenient for finite element implementation.

The present discussion begins with a normalization of the force axes used to describe the failure surface. In the case of axial loading, the axial load, P, is divided by the *squash load*, $A\sigma_y$: the member cross-sectional area multiplied by the uniaxial yield stress. Similarly, the moments, M, are normalized by their respective fully yielded capacities, $Z\sigma_y$: the corresponding plastic section modulus multiplied by the uniaxial yield stress. The subsequently normalized axial force and moment quantities can be labeled as p, m_x, and m_y, to describe the axial force, strong moment, and weak moment coordinates, respectively, of an given force point of interest. In a generic sense, the failure surface may be expressed as a function of these normalized force quantities:

$$\Phi\left(p, m_x, m_y\right) \tag{507}$$

This failure surface would then be applicable in describing the material condition occurring at each end of a given frame finite element. Considering the

normality condition accompanying an associative flow hypothesis, the plastic force increment at the *a-end* of the frame element may be given as:

$$d\mathbf{u}_p^a = \lambda^a \mathbf{G}^a \tag{508}$$

where $\mathbf{G}^a$ is the gradient to the force space failure surface at the loading point coinciding with the force state at the *a-end* of the given member:

$$\mathbf{G}^a = \begin{bmatrix} \frac{\partial \Phi}{\partial p^a} \\ \frac{\partial \Phi}{\partial m_x^a} \\ \frac{\partial \Phi}{\partial m_y^a} \end{bmatrix} \tag{509}$$

and λ^a is the magnitude of the plastic displacement increment, in a constrained plasticity context. A straightforward extension of the foregoing, to admit the possibility of plasticity at both ends of the frame element, appears as:

$$d\mathbf{u}_p = \begin{bmatrix} d\mathbf{u}_p^a \\ d\mathbf{u}_p^b \end{bmatrix} = \begin{bmatrix} \mathbf{G}^a & \mathbf{0} \\ \mathbf{0} & \mathbf{G}^b \end{bmatrix} \begin{bmatrix} \lambda^a \\ \lambda^b \end{bmatrix} = \mathbf{G}\lambda \tag{510}$$

As it is that the total deformation increment is assumed to satisfy the additive decomposition given as:

$$d\mathbf{u} = d\mathbf{u}_e + d\mathbf{u}_p \tag{511}$$

the role of the matrix, $\mathbf{G}$, is to reduce the extensional and rotational resistances at plastified member ends, and to constrain the elastic displacement increment to be tangent to the failure surface: yielding the admissible (in the sense of Drucker) force increment of the form:

$$d\mathbf{F} = \mathbf{K}_L d\mathbf{u}_e \tag{512}$$

where $\mathbf{K}_L$ is the usual linear elastic stiffness matrix. Based on the orthogonality of the plastic displacement increment and the tangent force increment, the following relationship follows immediately:

$$d\mathbf{u}_p \cdot d\mathbf{F} = \lambda \mathbf{G}^T d\mathbf{F} = 0 \tag{513}$$

which, on account of the arbitrariness in λ, leads to:

$$\mathbf{G}^T d\mathbf{F} = 0 \tag{514}$$

From Equations (514) and (512) it is noticed that:

$$\mathbf{G}^T \mathbf{K}_L d\mathbf{u}_e = 0 \tag{515}$$

and thus an application of Equation (511) results in:

$$\mathbf{G}^T \mathbf{K}_L \left(d\mathbf{u} - d\mathbf{u}_p \right) = 0 \tag{516}$$

An application of Equation (510) within the foregoing yields:

$$\mathbf{G}^T \mathbf{K}_L \left(d\mathbf{u} - \lambda \mathbf{G} \right) = 0 \tag{517}$$

and thus,

$$\mathbf{G}^T\mathbf{K}_L d\mathbf{u} = \lambda \mathbf{G}^T\mathbf{K}_L\mathbf{G} \tag{518}$$

and so

$$\lambda = \frac{\mathbf{G}^T\mathbf{K}_L}{\mathbf{G}^T\mathbf{K}_L\mathbf{G}} d\mathbf{u} \tag{519}$$

Additionally, from Equations (512) and (511) it is observed that:

$$d\mathbf{F} = \mathbf{K}_L \left(d\mathbf{u} - d\mathbf{u}_p \right) \tag{520}$$

and so from an application of Equation (510) it is observed that:

$$d\mathbf{F} = \mathbf{K}_L \left(d\mathbf{u} - \mathbf{G}\lambda \right) \tag{521}$$

and then applying Equation (519), and distributing, results in:

$$d\mathbf{F} = \left(\mathbf{K}_L - \frac{\mathbf{G}^T\mathbf{K}_L}{\mathbf{G}^T\mathbf{K}_L\mathbf{G}} \mathbf{K}_L\mathbf{G} \right) d\mathbf{u} \tag{522}$$

or, by defining a new stiffness quantity as:

$$\mathbf{K}_M = -\mathbf{K}_L\mathbf{G} \frac{\mathbf{G}^T\mathbf{K}_L}{\mathbf{G}^T\mathbf{K}_L\mathbf{G}} \tag{523}$$

and so then the force increment is expressible as:

$$d\mathbf{F} = \left(\mathbf{K}_L + \mathbf{K}_M \right) d\mathbf{u} \tag{524}$$

It is pointed out that the possibility for elastic unloading at the member end is indicated when a negative sign appears within one, or more, or the entries in Equation (519). This indicates that the given solution increment should be restarted with the the corresponding entries in $\mathbf{G}$ zeroed out.

4 Stability analysis

4.1 Linearized eigenvalue buckling analysis

There is an increasing availability of commercial finite element software that permits the consideration of the effects of geometric nonlinearity in structural analysis. Oftentimes these software systems will have the capability to treat stability problems through eigenvalue extraction routines applied to the global system stiffness matrix; an approach referred to, alternately, as *buckling*, *eigenvalue buckling*, or *linearized eigenvalue buckling* analysis.

This type of a stability analysis is attractive from the standpoint that it is computationally inexpensive. As compared with a more general incremental analysis that traces the entire nonlinear equilibrium path of the structural system, the eigenvalue buckling approach concerns itself with only one or two

points on the equilibrium path. In addition, results obtained from eigenvalue buckling analyses, when applied to stability problems exhibiting bifurcation instability, are usually quite accurate [7]; and this accuracy is obtained without much concern on the part of the software user. However, care must be taken when applying this technique to problem types exhibiting other manifestations of instability (*e.g.* limit point instability).

In practice, situations may arise in the design office where the application of eigenvalue buckling may seem attractive for problems involving elastic beam buckling (*e.g.* lateral torsional buckling of a beam or planar truss) or elastic snap-through buckling (*e.g.* lattice dome, arch, or shallow truss assembly). In the domain of stability research, too, linearized eigenvlaue buckling is oftentimes attractive as a means for identifying a *seed imperfection* for application in a more detailed incremental nonlinear finite element analysis of a beam or framework, for instance. In all of the foregoing, there are finite structural deformations prior to the onset of instability that are additive to the governing buckling mode (as compared to a bifurcation instability where the pre- and post-buckling deformations may be thought of as being orthogonal to one another). This fact creates an inconsistency with regard to assumptions made in the formulation of the linearized eigenvalue buckling procedure itself.

The present discussion examines the underlying assumptions within the formulation of the eigenvalue buckling method in order to highlight the problem types that most readily lend themselves to solution by this method. In addition, problems presenting responses that violate these fundamental assumptions are also examined. In this latter case, it becomes very important to understand the nature of the implementation of eigenvalue buckling in the given software system (example problems, variously solved with *MASTAN2*, *ADINA*, *ANSYS*, and *ABAQUS*, are included in this discussion); certain implementations will make application of eigenvalue buckling, to other than bifurcation problems, extremely problematic. The present discussion related to the various finite element buckling formulations employs a single, standardized notation to allow for a transparent comparison of underlying assumptions.

4.2 Overview of dominant finite element buckling analysis approaches

The literature adopts the term *buckling analysis* when referring to a family of finite element techniques applied to structural systems for the identification of critical load levels through the solution of an *eigen-problem* arising out of assumptions made relative to changes in structural stiffness; and concomitant applied loadings. While the technique is applicable to structures that exhibit critical responses arising from *limit point* as a well as *bifurcation of equilibrium*, the term *buckling* is nonetheless universally applied. While this may seem inconsistent, since buckling is normally associated with the condition of bifurcation

in the equilibrium path only, the nomenclature is defensible nonetheless, as a result of the fact that the eigen-problem posed within the finite element context resembles the case where the vanishing of the determinant of the stiffness matrix is associated with a form of the *Sturm-Liouville problem* [12] [3]. All formulations within the present discussion will be presented in a standardized notation (to facilitate comparison) that is defined subsequently.

Since the analyses considered here are strictly static, time will be used to signify an equilibrium point within the configuration space of a given structure; corresponding to certain load level. Definitions for several left subscripts are now introduced to facilitate subsequent discussions. A generic place holder term, Ω, will be used to show the relative locations of the subscripts:

- ${}_o\Omega \equiv$ generic quantity, Ω, evaluated at the equilibrium configuration associated with the trivial case of no external actions.
- ${}_t\Omega \equiv$ generic quantity, Ω, evaluated at an intermediate equilibrium configuration occurring between the unloaded and critical configurations.
- ${}_{\Delta t}\Omega \equiv$ denotes the change in a generic quantity, Ω, occurring as a result of movement from location t to $t + \Delta t$ on the equilibrium path.
- ${}_{t+\Delta t}\Omega \equiv$ generic quantity, Ω, evaluated at an intermediate equilibrium configuration occurring between the unloaded and critical configurations; that is arbitrarily close to ${}_t\Omega$.

In subsequent discussions, it will also be helpful to define three applied loading conditions that are used to reckon an assumed characteristic change in the system stiffness. In general, the applied loading will be denoted with P.

- $\{P_{baseline}\} \equiv$ loading condition used to bring the structure to a point in configuration space associated with the left subscript t.
- $\{P_{characteristic}\} \equiv$ loading condition used to bring the structure to a point in configuration space associated with the left subscript $t + \Delta t$.
- $\{P_{cr}\} \equiv$ the critical load associated with the equilibrium configuration at incipient instability.

Structural stiffness will be denoted by the usual quantity $[K]$, amplified as follows:

- $[{}_oK_o] \equiv$ linear elastic stiffness matrix whose elements are independent of the current structural configuration
- $[{}_\tau K_\sigma] \equiv$ *initial stress matrix* dependent on the state of stress at an arbitrary time, τ. This matrix is populated with terms that include both linear and quadratic dependencies on the current displacement field.

The sum of the foregoing two stiffness matrices is typically what is referred to as the *tangent stiffness matrix*, associated with a specific equilibrium point in configuration space. Some readers may be more familiar with the notion of the tangent stiffness being associated with the linear terms of a Taylor series expansion of the internal force vector about the current configuration during the solution, while others may recognize it as emanating from the stationarity of the total potential functional whose internal energy term includes the influence of finite strains. While other options exist for the population of the tangent stiffness matrix [13] [9] [5] the former definition has emerged as the most dominant to date. Other stiffness quantities associated with structural state under consideration may be characterized using tangent stiffness measures defined according to the following:

- $[K_{baseline}] \equiv$ the instantaneous stiffness of the structure arrived at by retaining only the linear terms in a Taylor series expansion of the load-deflection response of the structure about the point in configuration space corresponding with the the applied loading $\{P_{baseline}\}$
- $[K_{characteristic}] \equiv$ the instantaneous stiffness of the structure arrived at by retaining only the linear terms in a Taylor series expansion of the load-deflection response of the structure about the point in configuration space corresponding with the applied loading $\{P_{characteristic}\}$

4.2.1 Classical formulation

The initial treatment of the finite element buckling analysis appeared in the literature prior to the formal naming of the finite element method [8]; this earliest reference identified the approach as being based on the *discrete element procedure*. In light of the foregoing, and based on a survey of the literature, it appears that in the most commonly held definition of the classical formulation for finite element buckling analysis, the following problem is solved [6] [9] [5] [4]

$$det\left([{}_oK_o] + \lambda[{}_tK_\sigma]\right) = 0 \tag{525}$$

It is frequently assumed in the literature that the equilibrium point at time t is very close to the initial configuration at time 0, but this is not a strict requirement. The subsequent buckling load is computed as:

$$\{P_{cr}\} = \lambda\{P_{baseline}\} \tag{526}$$

4.2.2 Secant formulation

The present discussion adopts the name *secant formulation* to describe the variation of the finite element buckling problem that is referred to variously as the *secant formulation* [2] [1] and the *linear and nonlinear analysis* [9]. This problem is posed as:

$$det\left([K_{baseline}] + \lambda\left([K_{characteristic}] - [K_{baseline}]\right)\right) = 0 \tag{527}$$

and the subsequent buckling load is computed as:

$$\{P_{cr}\} = \{P_{baseline}\} + \lambda\left(\{P_{characteristic}\} - \{P_{baseline}\}\right) \tag{528}$$

4.3 Example problems

In the following examples, comparisons of results from the two approaches to finite element buckling analyses are considered (i.e. those involving software packages employing buckling approaches characterized by Equations (525) and (526), and (527) and (528), respectively). In some instances the results from closed form solutions are also presented. In addition, some cases also include results from manual implementation of the finite element buckling approaches as encapsulated in equations (525) and (526).

This discussion begins by distinguishing between bifurcation and limit point instability in a formal way. Consider the classical form of the finite element statement of the incremental equilibrium equations:

$$\left([{}_oK_o] + [{}_tK_\sigma]\right)\{{}_{t+\Delta t}\Delta u\} = \{{}_{t+\Delta t}R\} \tag{529}$$

where $\{\Delta u\}$ are the incremental nodal displacements, and $\{R\}$ is the *residual force vector* representing the imbalance between the internal forces at time t, and the desired load levels associated with some set of external forces, $\{P\}$.

We may use the standard form of the eigenvalue problem to compute eigenvalues, ω_i, and eigenvectors, $\{\phi\}_i$ for the tangent stiffness matrix according to:

$$\left([{}_oK_o] + [{}_tK_\sigma]\right)\{\phi\}_i = \omega_i\{\phi\}_i \tag{530}$$

This leads to the *spectral representation* of the tangent stiffness matrix:

$$[K_T] = \sum_i \omega_i\{\phi\}_i\{\phi\}_i^T \tag{531}$$

These same eigenvectors may also be used to define a projection operator that takes the original displacement and load vectors and projects them onto a new vector space, spanned by the eigenvectors, $\{\phi\}_i$, such that

$$\{{}_{t+\Delta t}\Delta u\} = \sum_i \alpha_i\{\phi\}_i; \qquad \{{}_{t+\Delta t}P\} = \sum_i \rho_i\{\phi\}_i \tag{532}$$

where $\{P\}$ is the externally applied load vector on the structure and $\rho_i = \{\phi\}_i^T\{P\}$. The transformations embodied in Equations (531) and (532) effectively diagonalize Equation (530) and result in the following transformation [11]:

$$\omega_i\alpha_i = \lambda\rho_i \tag{533}$$

In an elastic structure, the first critical point occurs when the equilibrium equations become singular, or in other words, when the tangent stiffness matrix is

no longer positive definite. Well ordered eigenpairs result from this being one case of the *Sturm-Liouville problem*, and thus it can be recognized that loss of positive definiteness of the stiffness occurs when $\omega_1 = 0$; at which point the condition $\lambda\rho_1 = 0$ occurs. Based on this fact, it can be recognized that a distinction between bifurcation and limit point instability exists [11]. If $\rho_1 \neq 0$, then it is clear that the eigenvector is not orthogonal to the externally applied loading vector $\{P\}$, and thus λ will have to be zero in order for $\lambda\rho_1 = 0$ to be true. In this case, a limit point instability condition exists (this point will become more clear subsequently). Conversely, $\rho_1 = 0$, when the loading is orthogonal to the eigenmode, and buckling is occurring. This may be summarized as follows:

- Limit point instability: $\omega_1 = 0$, and $\{\phi\}_1^T\{P\} \neq 0$;
- Bifurcation instability: $\omega_1 = 0$, and $\{\phi\}_1^T\{P\} = 0$

These results lead to the following interpretation. In the neighborhood of limit points on the equilibrium path in configuration space, there is no increasing load, and the eigenvector is not orthogonal to the external load vector. Conversely, if an increase in loading is possible in the neighborhood of the critical point, and the eigenvector is orthogonal to the load vector, then bifurcation instability is present.

4.3.1 Bifurcation instability

Two classical examples of bifurcation instability are considered next. In these problems, pre-buckling deformations are small, and thus the assumptions in this regard, that underlie the linearized eigenvalue buckling approach, are preserved. The first problem considers a one dimensional structural idealization of a three dimensional problem, while the second example treats a two dimensional idealization of a three dimensional case.

A classical *Euler column* example is depicted in Figure 20. This figure displays the problem geometry, along with boundary condition, cross-section, and material response information. The well known solution of the example problem is given below as:

$$P_{cr} = \frac{\pi^2 EI}{L^2} \tag{534}$$

and ultimately leading to an exact answer of $P_{cr} = 238 kips$ for the example problem shown in Figure 20. Clearly this agrees well with both linear eigenvalue buckling solutions (also shown in Figure 20), irrespective of baseline loading, $P_{baseline}$.

The second bifurcation instability example is given in Figure 21. This plate buckling problem, also, has a well known solution:

$$\sigma_{cr} = k\frac{\pi^2 E\sqrt{\eta}}{12\left(1-\nu^2\right)\left(\frac{b}{t}\right)^2} \tag{535}$$

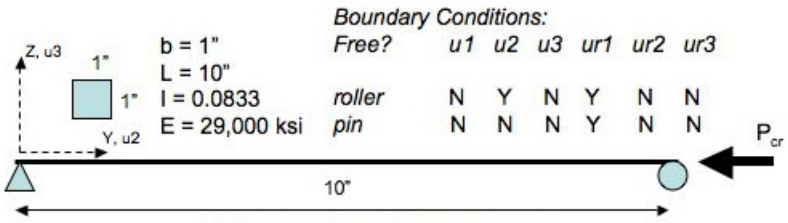

Boundary Conditions:

Free?	u1	u2	u3	ur1	ur2	ur3
roller	N	Y	N	Y	N	N
pin	N	N	N	Y	N	N

Linearized Eigenvalue Buckling Results:
(5 ADINA Hermitian beam elements)

$P_{imposed}$	P_{cr}	Method
200k	*235*	*Classical*
100k	*235.8*	*Classical*
10k	*236.5*	*Classical*
1k	*236.6*	*Classical*
200k	*235*	*Secant*
100k	*235.8*	*Secant*
10k	*236.5*	*Secant*
1k	*236.6*	*Secant*

Figure 20: Euler column example

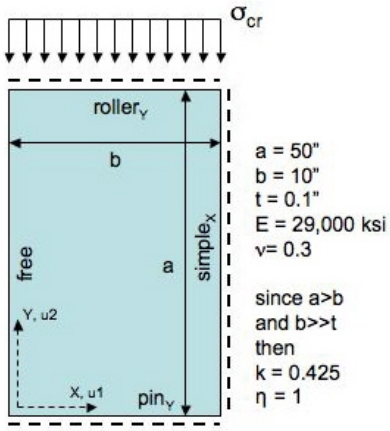

a = 50"
b = 10"
t = 0.1"
E = 29,000 ksi
ν= 0.3

since a>b
and b>>t
then
k = 0.425
η = 1

Linearized Eigenvalue Buckling Results:
(10 ADINA MITC4 four node shell elements across width)

$P_{imposed}$	σ_{cr}	Method
0.001 k/in	*1.222 ksi*	*Classical*
0.01 k/in	*1.217 ksi*	*Classical*
0.04 k/in	*1.217 ksi*	*Classical*
0.05 k/in	*1.217 ksi*	*Classical*
0.12 k/in	*NA*	*Classical*
0.001 k/in	*NA*	*Secant*
0.01 k/in	*1.217 ksi*	*Secant*
0.04 k/in	*1.217 ksi*	*Secant*
0.05 k/in	*1.217 ksi*	*Secant*
0.12 k/in	*NA*	*Secant*

Boundary Conditions:

Free?	u1	u2	u3	ur1	ur2	ur3
roller_Y	Y	Y	N	Y	N	N
pin_Y	Y	N	N	Y	N	N
simple_X	N	Y	N	N	Y	N
free	Y	Y	Y	Y	Y	N

Figure 21: Plate buckling example

Substitution of the problem parameters described in Figure 21 yields a critical stress of 1.114 ksi. As might be expected, this is in close agreement with finite element buckling results presented in the same figure; for both finite element buckling approaches under discussion.

Based on the two simple bifurcation buckling examples presented, it may seem as though linearized eigenvalue buckling approaches satisfactorily predict critical loads in this type of problem. However this is not always the case [7] and the reader is cautioned against merely accepting the buckling loads from finite element software; even under the favorable conditions of bifurcation buckling. For example, it is noted here that in the case of the ADINA two-point buckling formulation (known as the *secant formulation* in the ADINA literature), it is not possible to know what the load level of $P_{characteristic}$ is since the information contained in the output file and porthole file are incomplete in this regard. This is considered to be a critical shortcoming in ADINA in terms of reliance on the so-called secant formulation for finite element buckling analysis. As will be seen subsequently, it is not possible to employ the secant method intelligently when using ADINA, since insufficient information regarding the underlying solution process is available to the user, and thus critical judgment related to the specification of $P_{baseline}$, or even simply the interpretation of results, is severely compromised.

4.3.2 Limit point instability

The remaining cases for discussion all exhibit *limit point* (*snap-through*) instability, and thus pre-buckling deformations tend to be finite. Strictly speaking, this may be viewed as a violation of the underlying assumptions used in the formulations of Equations (525) and (527). Thus, it might be reasonably concluded that finite element buckling analyses are, technically, not applicable to such instances. However, the fact remains that engineers do employ this type of approach to cases that are not strictly in consonance with the underlying assumptions of the formulation; and thus it is important to consider this class of problems within the present discussion. In addition, it is not possible to escape the fact that, under certain circumstances, very good answers are obtained when comparing finite element buckling results with the results of more exact methods of analysis.

In the subsequent discussion, it will be useful to refer to a class of diagrams known as *eigenvalue plots* [4] [9]. Such a plot depicts a graph of $P_{critical}$ versus $P_{baseline}$ (both normalized by dividing by the exact critical load). An example of such a plot appears in Figure 22. The depiction of the eigenvlaue plot in Figure 22 is useful to consider in the case of limit point instabilities, since it highlights the dependence of the finite element buckling solution on the selection of a reasonable baseline loading, $P_{baseline}$. The predicted critical loading from the finite element buckling solution is arrived at by multiplying the eigenvalues by the baseline loads, as described in Equations (526) and (528), respectively,

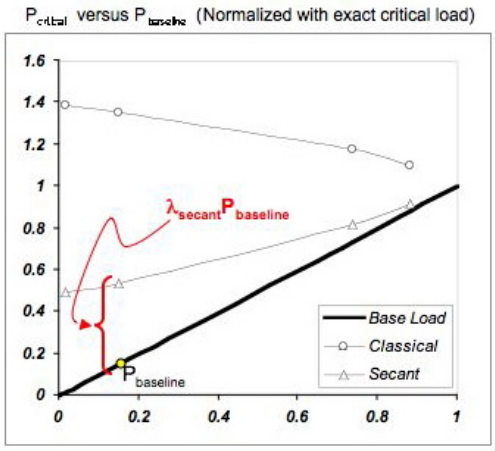

Figure 22: Representative *eigenvalue plot*

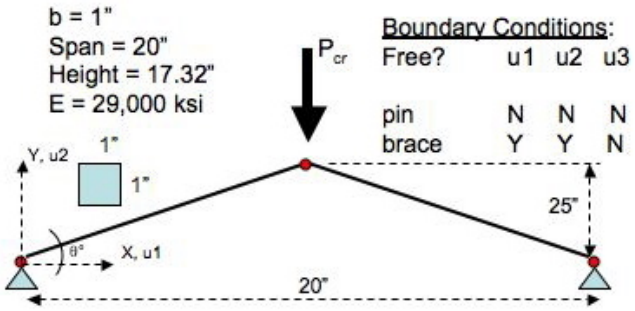

Figure 23: Truss-arch example

for the classical and secant approaches. The results presented in Figure are consistent with what is expected, from the standpoint that the approximate finite element buckling loads improve in accuracy as the magnitude of the baseline load increases.

Considering now the case of a truss arch, we may study instances involving various height-to-span ratios. In all of the following examples, the span length is held constant at 20 inches, and the height is varied from 2 to 17 inches (see Figure 23.) The truss arch is a particularly useful example, since it affords the opportunity to easily obtain results using hand calculations. In the case of the truss arch from Figure 23, with a height of 2 inches (*i.e.* shallow case), an energy formulation involving the *stationarity* of the *total potential* yields a critical load of 85.4 kips. For this particular truss arch geometry, finite element buckling results were obtained using MASTAN2, ANSYS and ADINA. In the case of the

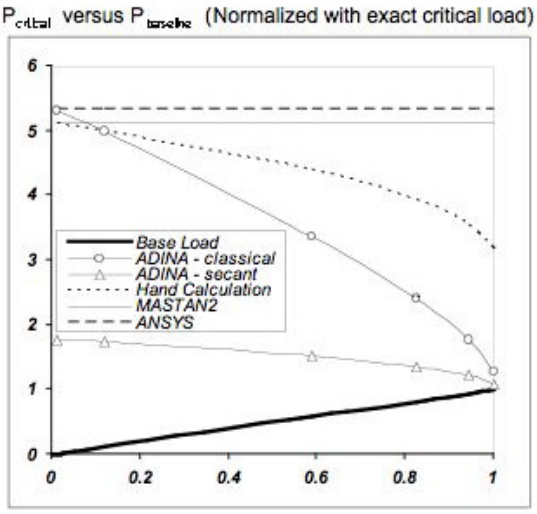

Figure 24: Truss-arch example results for shallow case

first two software packages, only a very small axial force is considered in the formulation of the tangent stiffness matrix used in the classical approach from Equation (525). These results, along with a hand calculation meant to parallel the classical formulation, as presented in Equations (525) and (527), appear in Figure 24. From Figure 24 it is clear that MASTAN2, ADINA, ANSYS, and the hand calculation all agree reasonably well for small values of $P_{baseline}$. However, as $P_{baseline}$ grows, MASTAN2 and ANSYS remain constant in their predictions, since their implementation of the classical method does not admit the possibility of a varying $P_{baseline}$. In addition, while the hand calculations, and ADINA, both permit a variation in $P_{baseline}$, the agreement at high levels is less favorable than at low values of $P_{baseline}$. This may be as a result of subtle differences in the way the classical formulation is implemented in ADINA; but as an unfortunate byproduct of a lack of inclusion (within the .out files of ADINA) of intermediate values in the solution process, it very difficult to test any theories aimed at understanding the nature of the observed differences.

In the case of the 17 inches high truss arch (*i.e.* deep case), we see a difference in the trending of the response observed in the eigenvalue plots appearing in Figure 25. While the MASTAN2 and hand calculations agree well with each other at low loads, and produce a reasonable estimate for the critical load, the same is not true for the ADINA results. The ADINA secant results are clearly diverging from the correct solution (13,000 kips; obtained from a incremental nonlinear finite element analysis) while the ADINA classical result begin at a point inexplicably far away from the other two classical implementations.

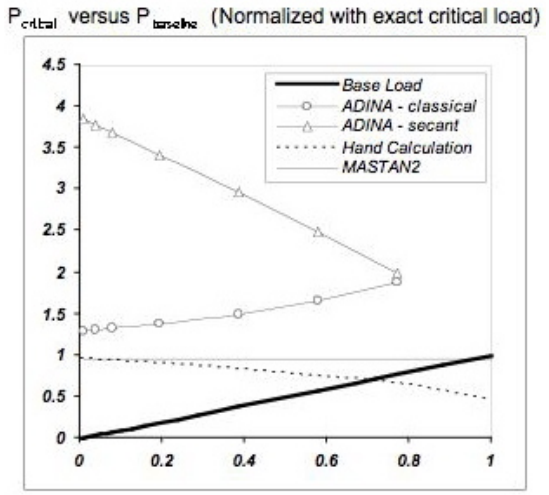

Figure 25: Truss-arch example results for deep case

4.4 Linearized eigenvalue buckling for imperfection seeding in incremental nonlinear finite element analysis

Linearized eigenvalue buckling analysis techniques are sometimes employed as a means for obtaining a *seed imperfection*, in order to enable the execution of a realistic incremental nonlinear finite element analysis (*e.g.* so as to facilitate equilibrium branch switching in the study of a bifurcation problem). In such an approach, it is the eigenvector values at each node that are scaled to define an initial displacement field that is assigned (as a perturbation) to the ideal nodal geometries of a mesh employed in an incremental nonlinear analysis. Such an approach is predicated on the notion of repeatability across commercial codes (*i.e.* commercial codes should all yield similar mode shapes from models possessing identical parameters). However, it has been clearly illustrated that each of the dominant formulations for eigenvalue analysis solves a slightly different eigenproblem; as seen in equations (525) through (527), and thus uniformity in predictions across commercial codes is unlikely. In order to further analyze the significance of this variation in formulation, eigenvector results are quantified to facilitate comparison.

The eigenvectors computed with the secant and classical formulations for a given model may be very similar, or, unfortunately, drastically different. This difference, or similarity, in results can accompany minor changes in geometry and/or loading conditions, as well as changes in eigenproblem formulation. Finite element post-processing software most often scales any reported eigenvectors, in order to facilitate visualization of the mode shape in post processing facilities. This scaling can cause problems when comparing results from differ-

TABLE 1. Nominal dimensions of example beams

Measure	Case 1	Case 2
Length, L	250" (6,350 mm)	29" (736 mm)
Depth, d	19.00" (483 mm)	8.25" (210 mm)
Flange Width, b_f	6" (152.4 mm)	4" (101.6 mm)
Web Thickness, t_w	1.00" (25.4 mm)	0.20" (5.1 mm)
Flange Thickness, t_f	1.00" (25.4 mm)	0.25" (6.4 mm)

ent commercial programs. In order to more precisely compare the eigenvectors from different formulations (applied to models with identical geometries and material paramters), a sampling of eigenvector values along the centerline of two example beams, (depicted in Figure 10), is taken. A discrete Fourier analysis is then conducted with these data; using the position along the beam as the independent variable.

Case 1 is a steel I-beam that is loaded with a uniformly distributed pressure on the top flange. Twist is prevented at the ends of the beam by guiding the rectangular stiffener plates to resist out-of-plane deformation. Nominal dimensions for the two cases depicted in Figure 26 are presented in Table 1. The two beam cases are modeled in both ADINA and ABAQUS using shell elements. The shell element formulations are not the same for ADINA and ABAQUS; however any differences in formulation are not critical in this comparison since the observed behavior is never outside the elastic, small strain response region (all element meshes were of equivalent density using linear, 4 node shells; the meshes were also seen to be convergent). In ADINA the analysis was run twice: once using the classical formulation, and once with the secant formulation; ABAQUS only allows for a classical type of analysis (although it is possible to use the 'restart' option to approximate a secant buckling analysis.) Figure 27 shows that the resulting Case 1 mode shapes look very similar for both programs.

The eigenvectors obtained from ADINA and ABAQUS post-processing are normalized, to enable comparison, using the relation:

$$\|\phi_i\| = \frac{\phi_i}{\phi_{max}} \tag{536}$$

where ϕ represents the eigenvector in question, with the subscripts corresponding to the discrete nodal contributions to the vector.

When using eigenvector data corresponding to the weak-axis displacement component, from the nodes along the centerline of the web, it becomes apparent that (see Figure 28) the mode 1 eigenvectors are slightly different for this problem; depending on the formulation used. This difference in mode shape becomes more conspicuous once a discrete Fourier transform of the weak-direction eigenvector displacement data is carried out. Figure 28 displays the results from this approach, highlighting that the mode 1 shape resulting from the ADINA

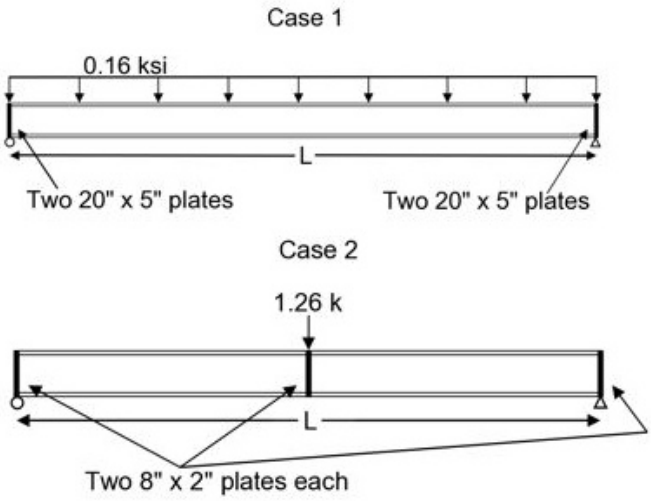

Figure 26: Beam imperfection example cases

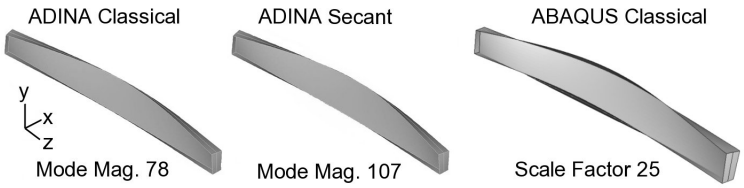

Figure 27: Case 1 buckling mode predictions

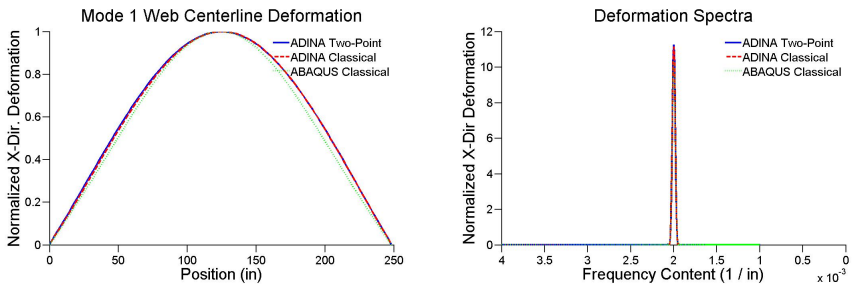

Figure 28: Case 1 eigenvector plots along the web centerline (left). Discrete Fourier transformation of these eigenvectors (right)

Figure 29: Case 2 buckling mode predictions

classical formulation, the ADINA secant formulation, and ABAQUS' formulation are related. They are obviously all harmonic, and their peaks occur at the same frequency. The frequency of the Fourier transform in Figure 28 corresponds to the number of cycles of the harmonic function which describes the deformation per length of the member. The peak amplitude of the ABAQUS Fourier ananlysis is 8% less than the peak amplitude of both ADINA secant formulation Fourier analysis results. This difference in peak frequency is only 1% between the ADINA classical and secant formulation results. In mode 2 the difference in Fourier peaks between ABAQUS and ADINA results is 30%.

The Case 2 example problem incorporates an extra stiffener plate at the center of the I-beam, with loading distributed linearly along the upper edge of the center stiffener plates (see Figure 26). The nominal dimensions of this steel beam are, once again, listed in Table 1. Visualization results for this model, obtained using ADINA and ABAQUS, are shown in Figure 29. The results vary to such an extent that the discrepancies are clearly not an artifact of magnification or scaling. Eigenvector values along the centerline nodes are plotted in Figure 30. The discrete Fourier transform of the weak-axis component of the eigenvector data (also presented in Figure 30) shows that there is not only a difference in the peak height of the results, but that the peaks are also located at different points along the member longitudinal axis. The secant formulation solution has a much more pronounced harmonic displacement field, as compared to the classical formulation. In this case the ABAQUS results are nearly equivalent to those of the ADINA classical formulation. ADINA classical and secant formulation differ significantly, in that the major peaks do not coincide in height or location.

4.5 Observations on linearized eigenvalue buckling

Finite element buckling analysis results should be interpreted with great care. The results of ostensibly identical formulations (as described in theory manuals, etc.) within various software packages frequently lead to estimates of critical loads that vary significantly for identical structural configurations.

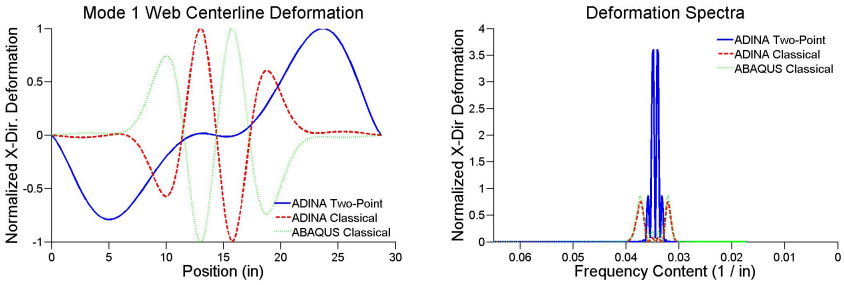

Figure 30: Case 2 eigenvector plots along the web centerline (left). Discrete Fourier transformation of these eigenvectors (right)

It seems reasonable to avoid using such finite element buckling approaches for all but the simplest cases of bifurcation buckling; but even then care must be taken when considering the validity of the results.

It also appears that the approach of using eignenmodes, obtained from linearized eignevalue buckling analyses, as an imperfection seed within a more general incremental nonlinear finite element analysis, should be approached with caution; as models with identical geometries and materials properties may result in very different imperfection fields, depending on the commercial software that is used, and with what formulation options the analysis is carried out.

4.6 Incremental nonlinear stability analysis

4.6.1 Influence of imperfections: geometric, material, and boundary conditions

5 Transient dynamic analysis

The standard *equations of motion (EOM)* in a problem from solid mechanics take the familiar form emanating from the use of *D'Alebert's Principle*, and a subsequent consideration of an equivalent "statical equilibrium":

$$\mathbf{M}\ddot{\mathbf{U}} + \mathbf{C}\dot{\mathbf{U}} + \mathbf{K}\mathbf{U} = \mathbf{R} \tag{537}$$

where $\mathbf{M}$ is the *mass matrix*, $\mathbf{C}$ is the *damping matrix*, and $\mathbf{K}$ is the *stiffness matrix*. Additionally, The vectors $\mathbf{U}$ and $\mathbf{R}$ represent the displacement and applied loads, respectively. When solving the time discrete equations of Equation (537), it is common to adopt a *finite difference* approach for the temporal discretization (as compared with the application of a weak form for the finite element spatial discretization). Specifically, in the present discussion a focus on the *central difference method* (also sometimes referred to as the *Crank - Nicolson scheme*) is adopted.

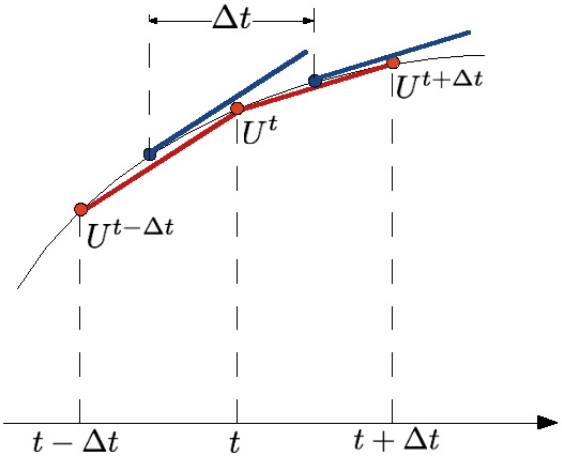

Figure 31: Single degree of freedom response example

In the central difference method, the discrete representation of the displacement derivatives are furnished through a consideration of the displacements themselves; as illustrated in Figure (31) and Equations (538) and (539)

$$\dot{U} = \frac{1}{2}\left(\frac{U^t - U^{t-\Delta t}}{\Delta t} + \frac{U^{t+\Delta t} - U^t}{\Delta t}\right) = \frac{1}{2\Delta t}\left(U^{t+\Delta t} - U^{t-\Delta t}\right) \tag{538}$$

$$\ddot{U} = \frac{\frac{U^{t+\Delta t}-U^t}{\Delta t} - \frac{U^t-U^{t-\Delta t}}{\Delta t}}{\Delta t} = \frac{1}{\Delta t^2}\left(U^{t+\Delta t} - 2U^t + U^{t-\Delta t}\right) \tag{539}$$

Using the foregoing, the following re-expression of the the EOM is possible:

$$\begin{aligned}
&\mathbf{M}\ddot{\mathbf{U}} + \mathbf{C}\dot{\mathbf{U}} + \mathbf{K}\mathbf{U} = \mathbf{R} \\
&\frac{\mathbf{M}}{\Delta t^2}\left(\mathbf{U}^{t+\Delta t} - 2\mathbf{U}^t + \mathbf{U}^{t-\Delta t}\right) + \frac{\mathbf{C}}{2\Delta t}\left(\mathbf{U}^{t+\Delta t} - \mathbf{U}^{t-\Delta t}\right) + \mathbf{K}\mathbf{U}^t = \mathbf{R}^t \\
&\mathbf{R}^t - \left(\mathbf{K} - \frac{2\mathbf{M}}{\Delta t^2}\right)\mathbf{U}^t - \left(\frac{\mathbf{M}}{\Delta t^2} - \frac{\mathbf{C}}{2\Delta t}\right)\mathbf{U}^{t-\Delta t} = \left(\frac{\mathbf{M}}{\Delta t^2} + \frac{\mathbf{C}}{2\Delta t}\right)\mathbf{U}^{t+\Delta t}
\end{aligned} \tag{540}$$

Based on the form of Equation (540), it is apparent that centered differencing yields an *explicit integration* of the EOM in time; that is a form wherein the solution at time $t + \Delta t$ is obtained directly from the results of previously solved time steps (*i.e.* at times t and $t - \Delta t$).

Strictly speaking, the form of the mass matrix should take a form that is consistent with the spatial discretization by the finite element method:

$$\mathbf{M}_{ij} = \rho \int_\Omega N_i\left(\mathbf{x}\right) N_j\left(\mathbf{x}\right) d\Omega \tag{541}$$

where ρ is the mass density of the medium being discretized. The for the mass matrix furnished in Equation (541) is known as the *consistent mass matrix*. This matrix (along with the damping matrix $\mathbf{C}$) frequently is dense; thus precipitating the need for a factorization of the coefficients acting on $\mathbf{U}^{t+\Delta t}$ within the left hand side of Equation (540). It is frequently possible to increase the efficiency of the central difference method by:

- neglecting damping
- *lumping* the mass matrix

Various schemes exist for the lumping of the mass matrix, but the two most common techniques are the *row sum* and *nodal point integration*. In the former case, the rows of the consistent mass matrix are summed and assigned to the diagonal location for the particular row:

$$M_{ij} = \sum_{j=1}^{ndof} M_{ij}, \quad i = 1, 2 \dots ndof \tag{542}$$

The nodal point integration method is more intuitive when applied to structural elements, and thus can be efficiently illustrated through an example involving the previously introduced 12 degree of freedom beam element:

$$\mathbf{M} = \begin{bmatrix} m & 0 & 0 & 0 & 0 & 0 & 0 & 0 & 0 & 0 & 0 & 0 \\ 0 & m & 0 & 0 & 0 & 0 & 0 & 0 & 0 & 0 & 0 & 0 \\ 0 & 0 & m & 0 & 0 & 0 & 0 & 0 & 0 & 0 & 0 & 0 \\ 0 & 0 & 0 & M & 0 & 0 & 0 & 0 & 0 & 0 & 0 & 0 \\ 0 & 0 & 0 & 0 & M & 0 & 0 & 0 & 0 & 0 & 0 & 0 \\ 0 & 0 & 0 & 0 & 0 & M & 0 & 0 & 0 & 0 & 0 & 0 \\ 0 & 0 & 0 & 0 & 0 & 0 & m & 0 & 0 & 0 & 0 & 0 \\ 0 & 0 & 0 & 0 & 0 & 0 & 0 & m & 0 & 0 & 0 & 0 \\ 0 & 0 & 0 & 0 & 0 & 0 & 0 & 0 & m & 0 & 0 & 0 \\ 0 & 0 & 0 & 0 & 0 & 0 & 0 & 0 & 0 & M & 0 & 0 \\ 0 & 0 & 0 & 0 & 0 & 0 & 0 & 0 & 0 & 0 & M & 0 \\ 0 & 0 & 0 & 0 & 0 & 0 & 0 & 0 & 0 & 0 & 0 & M \end{bmatrix} \tag{543}$$

where $m = \frac{\bar{m}L}{2}$ and $M = \frac{3\bar{m}LI_m}{2A}$; with $\bar{m}$ being the mass per unit length, L being the beam length, A being the cross-sectional area, and I_m denoting the maximum bending moment of inertia for the beam cross-section. These lumped quantities are somewhat *ad-hoc*; with the foregoing conforming to the recommendations outlined in the ADINA Theory Manual [1].

When performing a nonlinear analysis, the central difference method permits a significant simplification of the incremental solution that was introduced in earlier discussions on the Newton-Raphson and modified spherical arc length methods. Indeed, if mass lumping is assumed, and damping is neglected, then the EOM from Equation (537) may be re-expressed as:

$$\mathbf{M}\ddot{\mathbf{U}}^t + \mathbf{F}^t = \mathbf{R}^t \tag{544}$$

where $\mathbf{F}^t = \mathbf{K}\mathbf{U}^t$. In an incremental nonlinear analysis, $\mathbf{F}^t$ is recognized as the internal force in the structure; associated with the previously converged load increment. The difference between this internal force, $\mathbf{F}^t$, and the newly applied external action, $\mathbf{R}^t$, represents a residual force imbalance that leads to an acceleration:

$$\begin{aligned} \mathbf{M}\ddot{\mathbf{U}}^t &= \mathbf{R}^t - \mathbf{F}^t \\ \frac{\mathbf{M}}{\Delta t^2}\left(U^{t+\Delta t} - 2U^t + U^{t-\Delta t}\right) &= \mathbf{R}^t - \mathbf{F}^t \end{aligned} \tag{545}$$

thus leading to:

$$\mathbf{U}^{t+\Delta t} = \frac{\Delta t^2}{\mathbf{M}}\left(\mathbf{R}^t - \mathbf{F}^t\right) + 2\mathbf{U}^t - \mathbf{U}^{t-\Delta t} \tag{546}$$

whereupon each displacement step is arrived at through a simple application of Newton's Second Law. It is pointed out that there is no need to deal with the tangent stiffness matrix and the usual solution of the system of linear equations associated with the system stiffness matrix. Rather, as a result of the diagonal mass matrix, the new displaced configuration is obtained through a series of matrix multiplications (*i.e.* no factorization is required). Of course this convenience comes with a price: the explicit central difference method is only conditionally stable, and thus a restriction exists on the size of the time increments.

For our particular case of explicit time integration within the wave equation, we seek to have a *Courant number* of unity, defined as follows:

$$C = \gamma\frac{\Delta t}{h} \tag{547}$$

where γ is the speed of sound in the mesh, and h is the smallest distance between any two nodes in the mesh. The critical time step can then be found from satisfying the condition were $C = 1$. An equivalent, alternate framing has:

$$\Delta t_{cr} = \frac{T_n}{\pi} \tag{548}$$

where T_n is the smallest period that is resolvable within the given mesh.

References

[1] ADINA. *Theory Manual.* ADINA R and D, Inc., 2007.

[2] K. J. Bathe and E. N. Dvorkin. On the automatic solution of nonlinear finite element equations. *Computers and Structures*, 17(5-6):871–879, 1983.

[3] W. E. Boyce and R. R. DiPrima. *Elementary Differential Equations and Boundary Value Problems, fourth edition.* John Wiley and Sons, Inc., 1986.

[4] B. Brendel and E. Ramm. Linear and nonlinear stability analysis of cylindrical shells. *Computers and Structures*, 12:549–558, 1980.

[5] S. C. Chang and J. J. Chen. Effectiveness of linear bifurcation analysis for predicting the nonlinear stability limits of structures. *International Journal for Numerical Methods in Enginering*, 23:831–846, 1986.

[6] R. D. Cook, D. S. Malkus, M. E. Plesha, and R. J. Witt. *Concepts and Applications of Finite Element Analysis, Fourth Edition*. John Wiley and Sons, Inc., 2002.

[7] C. J. Earls. Observations on eigenvalue buckling analysis within a finite element context. In *Proceedings of the Structural Stability Research Council, Annual Stability Conference*, New Orleans, LA, USA, 2007.

[8] R. H. Gallagher, R. A. Gellatly, J. Padlog, and R. H. Mallett. A discrete element procedure for thin-shell instability analysis. *AIAA Journal*, 5(1):138–145, 1967.

[9] S. M. Holzer, J. F. Davalos, and C. Y. Huang. A review of finite element stability investigations of spatial wood structures. *Bulletin of the International Association for Shell and Spatial Structures*, 31(2):161–171, 1990.

[10] L. E. Malvern. *Introduction to the Mechanics of a Continuous Medium*. Prentice-Hall, 1969.

[11] D. A. Pecknold, J. Ghaboussi, and T. J. Healey. Snap-through and bifurcation in a simple structure. *Journal of Engineering Mechanics*, 111(7):909–922, 1985.

[12] B. D. Reddy. *Introductory Functional Analysis*. Springer, 1998.

[13] R. D. Wood and B. Schrefler. Geometrically non-linear analysis - a correlation of finite element notations. *International Journal for Numerical Methods in Engineering*, 12:635–642, 1978.